Study of Formation and Analysis of Structures Induced in Polymeric and Amorphous Materials by Irradiation of Near-Infrared Femtosecond Laser Pulse.

「近赤外フェムト秒パルスレーザー照射による高分子・アモルファス材料中の誘起構造形成ならびに構造解析に関する研究」

July 2003

Shigeru　Katayama

（片山　茂）

京都工芸繊維大学　大学院　工芸科学研究科　博士後期課程

機能科学専攻　高分子機能科学講座　高分子機能制御研究室

Contents

Chapter 4: Grating structures induced by irradiation of NIR femtosecond laser pulse in polymeric materials and diffraction measurement of those structures

4-1 Introduction
4-2 Experimental
4-3 Results and Discussion
4-4 Conclusion
References and notes

Chapter 5: Grating structures induced by irradiation of NIR femtosecond laser pulse in dyed polymeric materials and diffraction measurement of those structures

5-1 Introduction
5-2 Experimental
5-3 Results and Discussion
5-4 Conclusion
References and notes

Chapter 6: Upheaval structures on the surface induced by irradiation of NIR femtosecond laser pulse in polymeric materials and application for micro-lens of those structures

6-A Laser molding in polymeric materials using NIR femtosecond laser pulse and replication via electroforming

6-A-1 Introduction
6-A-2 Experimental
6-A-3 Results and Discussion
6-A-4 Conclusion
References and notes

6-B Periodic bell-shaped upheaval structure on surface of polycarbonate by irradiation of femtosecond laser pulse

Chapter 1: General Introduction

1-1 Introduction

Polymer materials have been widely used in various fields such as industrial products, household articles, medical products, clothes so forth. Polymer materials have superior properties to other materials, such as metal, inorganic materials; lightness, easy processing, wide functional variation and low cost so forth. Polymer material components can be widely changed, that is, the type of polymer chain backbone, such as linear, branch, and star, the composition and molecular weight, etc. These wide variations in components of polymer materials are a basis of wide usage in various fields of polymer materials. Many polymer materials are amorphous and transparent not having significant absorption in the wavelength of the visible region. They are used optical products, recording media, electrical products, commodities so forth due to its transparent property. Especially, optical products, such as polarizing film, touch panel sensor, and optical fiber, have been key components in the field of display and communication which sustain our modern life.

Polymer material has intrinsic property different from inorganic material. Inorganic material is composed with covalent-bond isotropically but polymer material has long chain structure in backbone with an-isotropical covalent-bond. Intra-chain and inter-chain overlapping forms 'entanglement' and 'entanglement' is the origin of intrinsic property of polymer material in particular of amorphous polymer material. Polymer material has lower glass transition temperature (T_g) and lower thermal conductivity than inorganic material due to 'an-isotropical covalent-bond'. Another intrinsic property of amorphous polymer material is 'viscoelastic property'. Amorphous polymer materials possess glassy, rubbery, and liquid states depending on temperature. The elasticity of amorphous polymer material shows drastic changes according to the change of states; high elasticity in glassy state, low elasticity in rubbery state, and viscous elasticity in liquid state. These 'viscoelastic properties' are significantly related to the thermal behavior of polymer materials.

Since the 1970's, many investigations have shown that the effects in inorganic materials and polymer materials by irradiation of short wavelength light and/or laser in the ultraviolet (UV) and visible region induced ablation of the surface and produced refractive index changes.[1-3] Poly (methyl methacrylate) (PMMA) shows easy photo-degradation and photo-crosslinking by irradiation of UV light.[3] In contrast, induced phenomena by laser irradiation of long wavelength in the infrared (IR) and visible region had received little attention owing to the low photon energy at these

1

wavelengths. With the development of a near-infrared (NIR) ultra-short pulse laser with high peak power, it has come possible to induce ablation and structures via multi-photon photochemical reaction. Many studies have been carried out in this field in transparent inorganic materials.[4-12] However, only a few studies have been reported for polymer materials.

1-2 Feature of femtosecond laser pulse with high peak power

In recent year, the development of small size and high performance ultra-short laser pulse with high peak power has progressed rapidly. More recently, femto (10^{-15}) second laser pulses with pulse width of sub-ten (<10) femtosecond and peak power of terawatt (10^{12} W) have been developed. Femtosecond also corresponds to the time constant of lattice vibration motion. Femtosecond laser pulse has high peak power, even if low maximum pulse energy (<1 µJ/ pulse) and average power, in addition to the ordinal feature of laser, such as spatio-temporal coherency, high directional property. Irradiation of focused femtosecond laser pulses in materials gives intense electric-field (for example 100 terawatt/cm^2) and this intense electric-field is high enough to produce non-linear optical effect, multi-photon absorption, and re-orientation of dipole and to generate plasma and/or coherent phonon in various materials. Femtosecond laser pulse has been usually used as a measuring tool in ultra-short time range and as a communication source in ultra-fast optical communication such as optical time division multiplexing (OTDM). Recently, it has been also used as a manufacturing tool in production of micro-structure induced by irradiation. It has been reported that 'non-thermal diffusion processing' becomes possible for manufacturing of metal, and inorganic materials by means of femtosecond laser pulse.

Figure. 1 shows relationship between damage fluence and pulse width for fused silica and CaF$_2$ at 1053 nm for pulse duration (pulse width) τ ranging 270 fs to 1ns. A deviation from the $\tau^{1/2}$ plot at approximately 20 ps indicates that damage results from plasma and ablation for $\tau \leqq 10$ ps and from conventional melting and boiling for $\tau > 100$ ps.[10]

Figure. 2 shows scanning electron microscope (SEM) micrographs of front surface damage of fused silica produced by 1053 nm pulses of duration 900 ps (a) and 500 fs (b), respectively. At the pulse duration of 500 fs, obtained morphology showed ablation and fracture in contrast to melting at the pulse duration of 900 ps.[10]
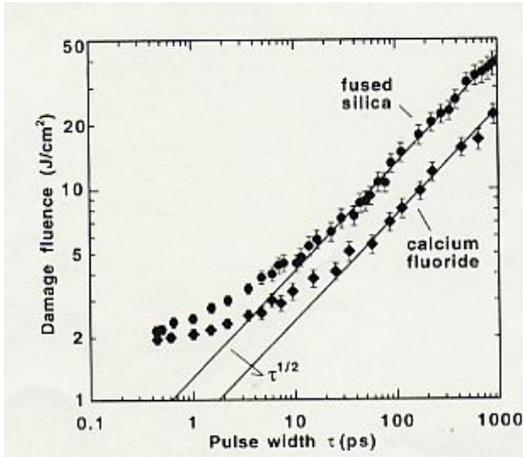
Fig. 1 Observed value of damage threshold at 1053 nm for fused silica (●) and CaF$_2$(◆). Solid line are $\tau^{1/2}$ fits to long pulse results. Estimated uncertainty in the absolute fluence is ±15%.
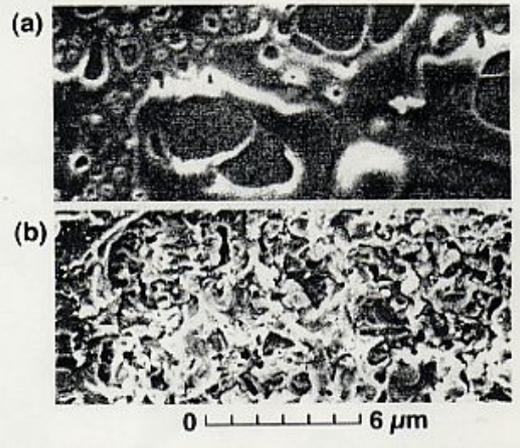
Fig. 2 Scanning electron micrograph of front surface damage of fused silica produced by 1053 nm pulse of duration 900 ps (a) and 500 fs (b).

Figure.3 also shows SEM photographs of after-irradiation on the surface of TiO$_2$ under same irradiation energy and same number of shots by Ti-sapphire femtosecond laser pulse with pulse width of 120 fs (a) and KrF nanosecond laser pulse with pulse width of 30 nm (b), respectively. Irradiation by femtosecond laser pulse produces clear structure with no melt-phase as shown in (a) but irradiation by nanosecond laser pulse shows melt-phase structure (b).[13]
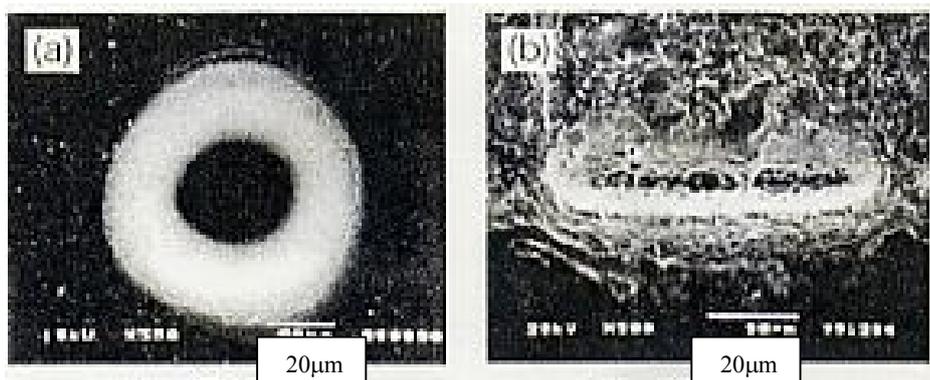
Fig. 3 SEM photographs of after-irradiation on the surface of TiO$_2$ by Ti-sapphire femtosecond laser pulse with pulse width of 120 fs (a) and KrF nanosecond laser pulse with pulse width of 30 nm (b). irradiated energy, 0.15mJ; number of shots, 3000.

1-3 Multi-photon absorption process

Another feature of femtosecond laser pulse with high peak power is multi-photon absorption. Two-photon absorption and three-photon absorption occur according to square and cubic of irradiated energy, respectively. The emergence of NIR femtosecond laser pulse with high peak power has realized application of multi-photon absorption in photo-chemical reaction, manufacturing, spectroscopy, and microscope so forth. Especially, laser manufacturing using multi-photon absorption has advantage of localized, selective processing at a desired position. NIR femtosecond laser pulses have wavelength of approximately 800 nm, therefore, incident beam of laser pulses to materials which is transparent at 800 nm transmits to focused point without any influence in the optical pass and multi-photon absorption can be occurred around the focused point.

(a)   (b)
One-photon absorption   Multi-photon absorption

Objective lens

Focused point
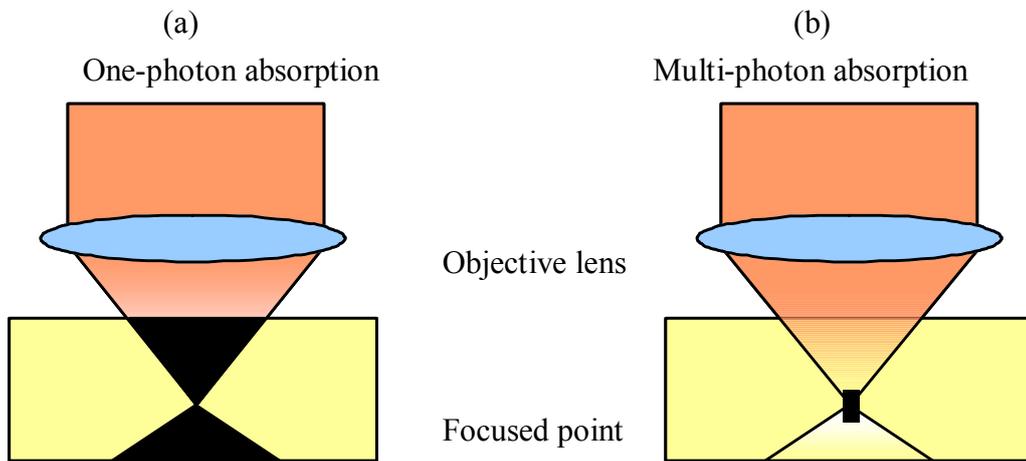
Fig. 4 Schematic of absorption regions for one-photon absorption (a) and for multi-photon absorption (b).

Figure. 4 shows schematic of absorption regions for one-photon absorption (a) and for multi-photon absorption (b), respectively. In the case of multi-photon absorption, absorption region is localized around the focused point because, for example, two-photon absorption occurs in proportion to square of photon density (optical intensity). The localized absorption leads photo-chemical reaction in the sample to localized one and resultantly precise localized manufacturing.

The other important point of multi-photon absorption is that 'selection rule' of multi-photon absorption is different from that of one-photon absorption. If a molecule has a high symmetry, the molecule is able to be excited to another excitation level different from one-photon excitation level according to the selection rule. For example, poly (di-hexyl silane) with high molecular symmetry has higher excitation level by

two-photon absorption than that by one-photon absorption as shown in Fig. 5.[14-16]
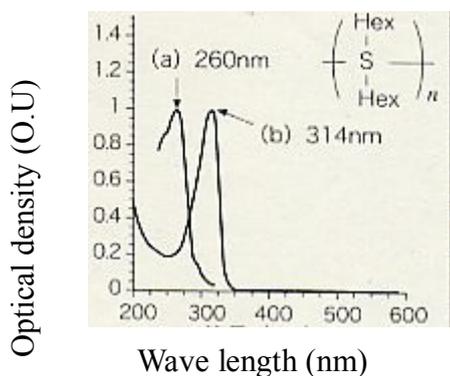
Fig. 5 Absorption spectra of poly (di-hexyl silane).
(a) two-photon absorption
(b) one-photon absorption

To the contrary, poly (methyl phenyl silane) with molecular asymmetry has same excitation level of two-photon absorption as that of one-photon absorption. The selective multi-photon absorption of symmetric molecules is expected for applications in the control of photo-reactions and photo-responsible functions.

Figure. 6 shows relationships between power (photon) density, probability of two-photon absorption, probability of three-photon absorption and distance from a focused point (z).
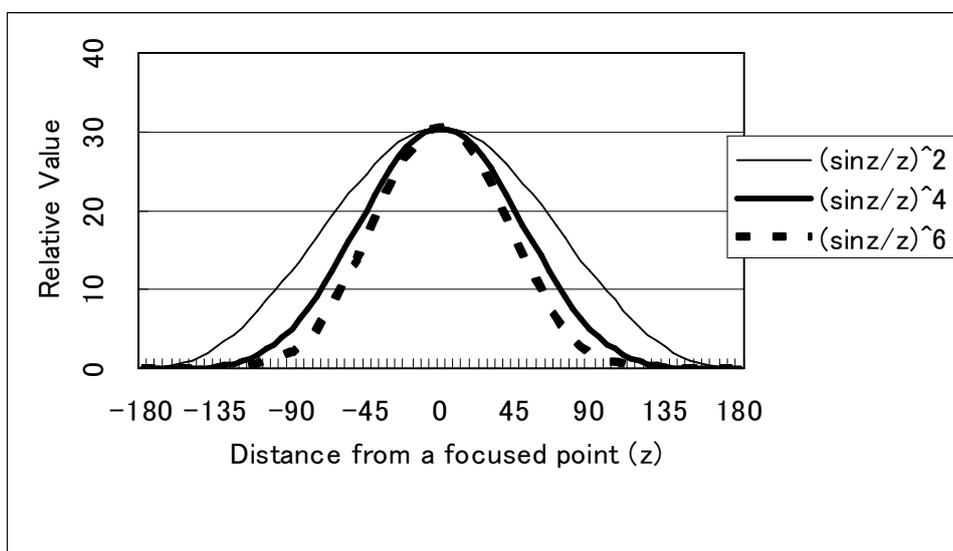
Fig. 6 Relationship between power density, probability of two-photon absorption, probability of three-photon absorption and distance from a. focused point (z)

Power density (PD) of incident laser beam is generally given by $PD=(\sin(cz)/cz)^2$. In this equation, c is a constant which is determined by wavelength of incident beam

and the numerical aperture (NA) of the objective lens and z is the distance from the focused point along the Z direction (z=0 at the focused point). The probabilities of the two photon absorption and three-photon absorption are in proportion to square and cubic of the power density (photon density), respectively , therefore （sin（cz）/cz)^4 and （sin（cz）/cz)^6, respectively. Figure 6 shows functional shapes of (sin(cz)/cz)^2 and (sin(cz)/cz)^4, (sin(cz)/cz)^6, which are normalized at each peak value. The two-photon absorption and three-photon absorption occur symmetrically according to (sin(cz)/cz)^4 and (sin(cz)/cz)^6 along the incident path and the absorbed energy was maximum at the focused point. Focused irradiation using objective lens with smaller numerical aperture shows wider distribution in the relation power density, probability of multi-photon absorption and distance from the focused point (z). This means that there is a considerable influence at points far from the focused point in the case of irradiation using objective lens with small NA.

Self focusing phenomenon of femtosecond laser pulse with high peak power has been observed in the case of irradiation in optical fiber[17,18] and/or in the case of irradiation in transparent materials using objective lens with small NA.[4,18-23]
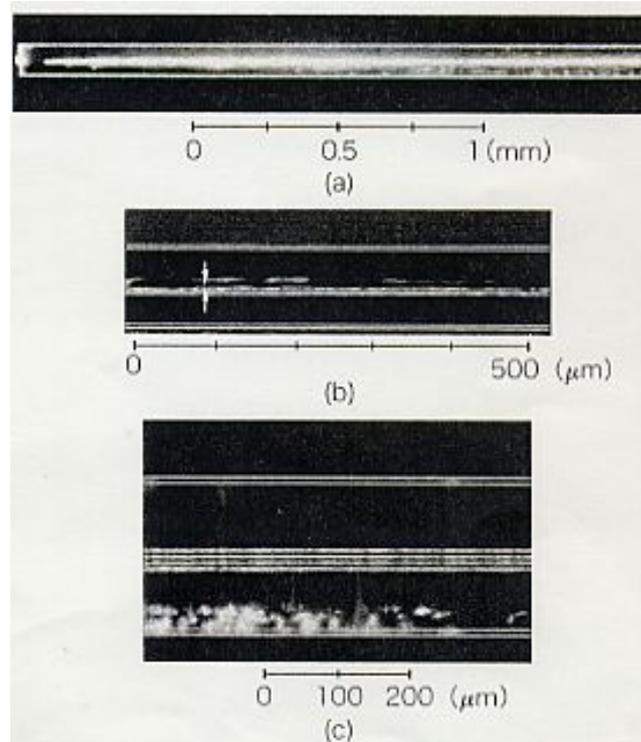
Fig. 7 Formation of plasma channeling in optical fiber by incident beam of femtosecond laser pulse (a) and formed waveguide in optical fiber (b), (c).

Figure. 7 shows photograph of formation of plasma channeling in quartz optical fiber by incident beam of Ti-Sapphire femtosecond laser pulse (pulse width, 110 fs; repetition rate, 1 kHz) (a) and formed waveguide in optical fiber; single waveguide (b), four waveguides (c).[17,18] When irradiation energy of laser pulse comes over the threshold value, laser pulse propagates with keeping a constant spot-size in optical fiber. This phenomenon is called 'channeling' and considereds to occur under the balance of beam propagation between self-focusing caused by the optical Kerr effect and self-divergence owing to ionization.[17,18]

Related phenomenon to 'channeling' is formation of filaments by irradiation of femtosecond laser pulse in transparent inorganic materials using objective lens with small NA (NA<0.3).[4,18-24] The length of formed filament becomes longer with decrease of NA. In the case of focusing a laser beam on the entrance surface, the modification starts at the end farthest from the entrance surface and grows towards this surface with the observed length increasing linearly with the number of laser shots as shown in Fig.8.[24] This formation of filaments is also attributed to the balance between self-focusing caused by the optical Kerr effect and self-defocusing due to diffraction from the generated plasma. The formed filaments in inorganic glass have higher refractive index than un-irradiated bulk and have a function to be waveguide and diffraction grating as shown in Fig. 9 and 10, respectively.[21]
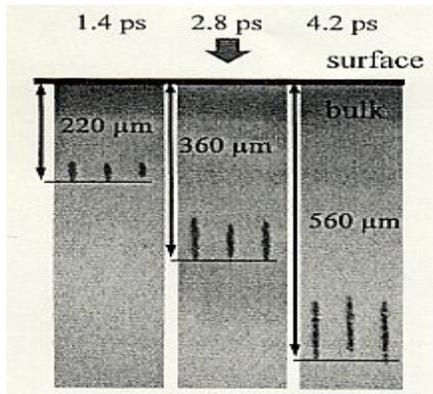
Fig.8 Microscopic sideview of bulk modifications in a-SiO_2 after 100 laser shots, with the laser beam focused at the entrance surface, for three different pulse duration. The energy per pulse was 20 μJ, focus diameter 920 μm^2, and λ=790 nm.
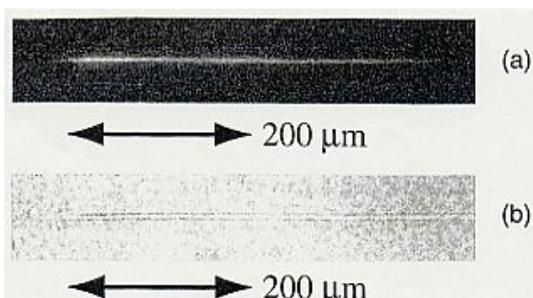
Fig.9 Relationship between a filament and the region of refractive index change:
(a) Optical images of the filament
(b) The region of refractive index change
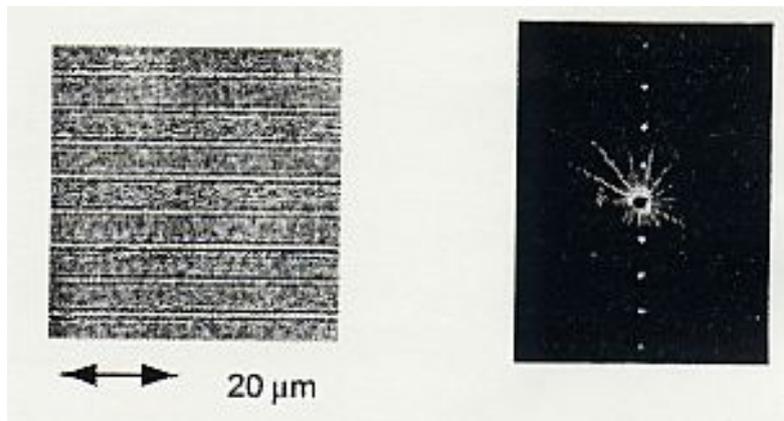
Fig. 10 Diffraction grating formed by ensemble of filament (a) and obtained diffraction pattern.

1-4 Structures induced in inorganic materials by irradiation of near-infrared (NIR) femtosecond laser pulse

Structures induced in inorganic materials by irradiation of NIR femtosecond laser pulse have been investigated by many researchers. K. Hirao's group of 'Hirao active glass project' (ERATO project of JST) has vigorously investigated in this field and reported many interesting induced structures. Some of these interesting induced structures reported by Hirao *et al* are shown as follows.

1) Photo-written optical waveguide in various glasses:[4, 11, 25)]

In these papers, they have investigated the optical waveguide formed by translating the sample either parallel or perpendicular to the axis of the femtosecond laser pulse beam. They demonstrated that permanent optical waveguide with refractive index changes of $10^{-2} - 10^{-3}$ could be successfully formed in various glasses, such as high silica, borate, and soda-lime-silicate. They also showed a mechanism of forming the induced structure in Ge-doped silica glass and they suggested that the refractive index increases by irradiation of femtosecond laser pulse are contributed by two factors. The first one is the formation of Ge E' centers which is probably brought by multi-photon process, and the other one is densification and strain in the irradiated material.

2) Photo-induced reduction of noble ion and crystallization:[7)]

In this paper, they have investigated photo-induced reduction and crystallization in Ag^+ doped glass, and they reported that photo-reaction of $Ag^+ + e^- \rightarrow Ag^o$ is

8

induced only at the focal points. Investigation in various glasses with different composition showed NaF crystallites are precipitated using Ag colloids as nuclei. They also reported that induced crystal length is significantly related to the length of filamentation (self-trapping).

Hirao *et al* have reported also the methods of measurement and analysis for structures induced by irradiation of NIR laser pulse, for example, spectroscopy with pump-probe and photon echo methods,[26] determination of local arrangement of induced structures by X-ray Absorption Fine Structure (XAFS),[27,28] femtosecond time-resolved spectroscopy and Raman scattering[29,30] and so forth.

With respect to the application of induced structures, Hirao *et al* demonstrated several functional devices, such as micro-sphere laser,[31] UV and blue up-conversion laser,[32] waveguide multiplexed optical memory,[33,34] photo-induced dye-sensitized solar cell,[35] Faraday effect glasses,[36,37] long-period fiber grating,[38] ultrafast optical Kerr switching[39-41] and so forth.

1-5 Studies on structure induced in polymer and organic materials by irradiation of NIR femtosecond laser pulse

There have not been many papers of studies on structure induced in polymer materials by irradiation of NIR femtosecond laser pulse.

Y. Kawata's group reported ultra high density optical memory with multi-layer composing photosensitive urethane-urea resin and poly-vinyl alcohol (PVA) using femtosecond laser pulse as incident beam.[42,43]

The other examples of studies on application of photosensitive resin for formation of structures induced by NIR femtosecond laser pulse are fabrication of photonic crystals by H. Misawa's group[44-47] as shown in Fig.11, functional micro-devices by S. Kawata's group as shown in Fig. 12.[48]
Both groups applied two-photon photo-polymerization for fabrication of precise structures induced by irradiation of NIR femtosecond laser in photosensitive acrylic resins.

T. Watanabe et al reported photo-responsive hydrogel microstructure fabricated by two-photon initiated polymerization with NIR femtosecond laser. They showed that the hydrogel microstructure acts as a micro-cantilever by irradiation of UV light as shown in Fig. 13.[49]
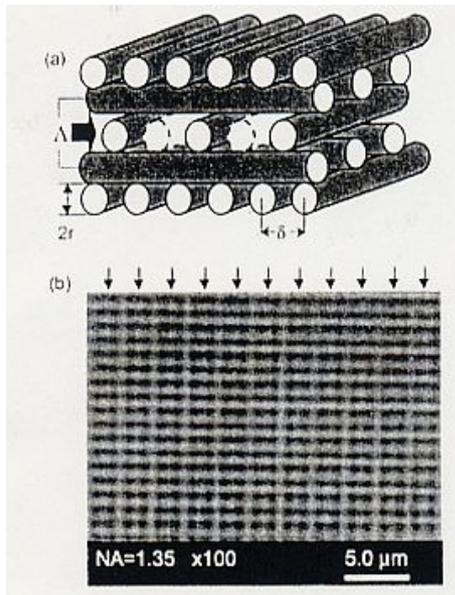
Fig. 11 Schematic of the log-pile structure (a) and optical micrograph of the layer with the defect (top view) in the log pile photonic crystals.
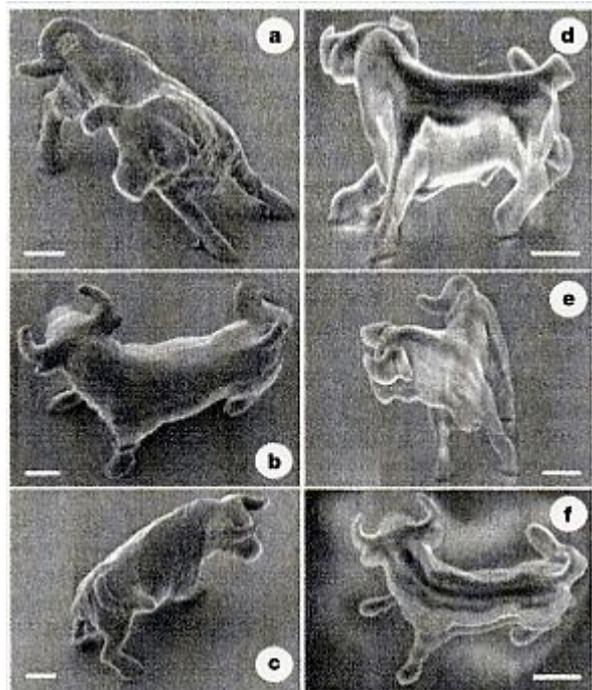
Fig. 12 Micro-fabrication by irradiation of Ti-sapphire laser pulse (780 nm wavelength, 150 fs, 76 MHz). (a)-(f) are photographs of bull sculpture formed by irradiation of (NIR) laser pulse.(scale bars represent 2 μm)
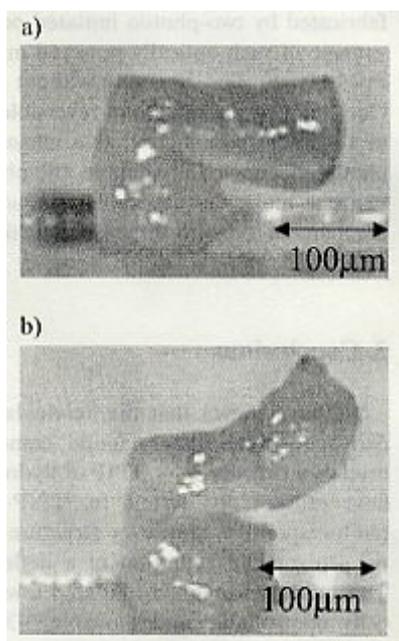
Fig. 13. (a) Optical microscopy image of a micro-cantilever in water prior to UV irradiation. The micro-cantilever was fabricated on a fused silica substrate.

(b) Optical microscopy image of the micro-cantilever in water after UV irradiation. The micro- cantilever was irradiated with UV light through the fused silica substrate.
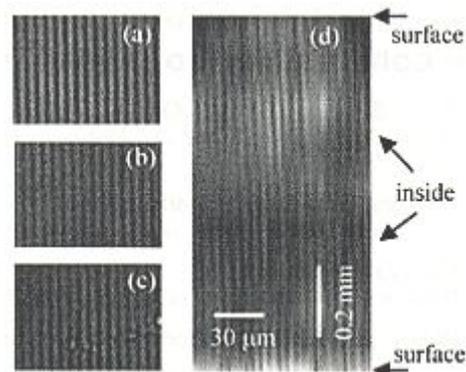
Fig. 14. Optical microscopic photos (a-c) of the photo-induced grating on the top surface (a), in the inner that is 0.4 mm from the top surface (b), and on the bottom surface of the sample (c). The photo on the right (d) is an orthogonal section image of the grating observed using a confocal laser scanning microscope. The horizontal and vertical scale bars represent 30 μm and 0.2 mm, respectively.
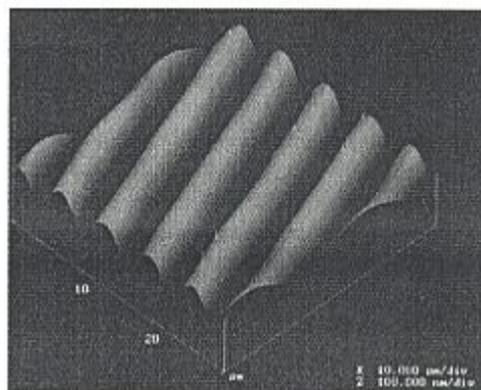
Fig. 15. AFM scans of the photo-induced gratings. The surface modulation of the surface relief gratings is about 50 nm

J. Si and K. Hirao *et al* reported photo-induced permanent gratings inside bulk azodye-doped polymers by the coherent field of a NIR femtosecond laser as shown in Fig. 14, Fig.15.[50]

H. Masuhara et al reported laser ablation of a substituted Cu-phthalocyanine by irradiation of NIR laser pulse[51] and laser ablation of liquid benzyl chloride by irradiation of femtosecond KrF laser.[52]

1-6 Objectives of the present work

Study on structure induced by irradiation of NIR femtosecond laser pulse in polymer material has not been done enough yet and it remains to be investigated in detail how and what structures are induced by NIR femtosecond laser pulse. In order to study on structures induced by irradiation of NIR femtosecond laser in polymer materials, it may be necessary that systematic approach noticing intrinsic properties of polymer material and utilizing of model compound is carried out. It may be also necessary to pay attention for applicability of obtained structures induced by irradiation of NIR femtosecond laser.

In this thesis, the author studies on the formation and analysis of structures induced in polymeric and amorphous materials by irradiation of NIR laser pulse.

First, the author carries out irradiation of NIR laser pulse in various polymer materials having different T_g's and investigates relationship between induced structures and T_g's of polymer materials.

Second, the author investigates the difference in induced structures between polymer materials and inorganic materials and analyzes the fundamental factors which bring the difference in polymer materials.

Third, the author investigates specific structures induced in polymer materials and optimization and application of these structures.

Fourth, the author investigates and makes clear the feature of femtosecond laser pulse to the formation of induced structures in polymeric and amorphous materials, especially multi-photon absorption and self-focusing.

Additionally, the author investigates methodology of analysis and evaluation of minute induced structures and methodology of measurement of properties emerged from the induced structures and investigates also application of those induced structures for various devices.

1-7 Outline of this thesis

This thesis is composed of 8 Chapters.

Chapter 1 deals with general introduction of this thesis including explanation of the feature of femtosecond laser pulse with high peak power and multi-photon absorption process and introduction of related studies on induced structures in inorganic materials and polymer materials.

In Chapter 2, experimental procedures are summarized. It contains explanation of outline of used NIR laser pulse, irradiation of NIR laser pulse, sample preparation, observation and identification of induced structures by irradiation of NIR femtosecond

laser pulse, diffraction measurement and evaluation of micro-lens effect.

Chapter 3 describes structures induced by irradiation of NIR femtosecond laser pulse in polymeric materials having various glass transition temperature (T_g's). Relationship between induced structures and T_g's of polymers is investigated.

Chapter 4 describes grating structures induced by irradiation of NIR femtosecond laser pulse in p-(MMA/EA-BA) block copolymers and diffraction measurement of those structures. Optimization to obtain Bragg type diffraction grating is investigated.

Chapter 5 describes grating structures induced by irradiation of NIR femtosecond laser pulse in dyed polymeric materials and diffraction measurement of those structures. Relationship between induced structures and absorption and fluorescence properties of doped dyes is investigated.

Chapter 6 describes upheaval structures on the surface induced by irradiation on NIR femtosecond laser pulse in polymeric materials and application for micro-lens of those structures. Chapter 6 is composed of two sub-Chapters 6-A and 6-B. Chapter 6-A describes laser molding in polymeric materials using NIR femtosecond laser pulse and replication via electroforming. Micro-lens effect of periodic bell-shaped upheaval structures is investigated. Chapter 6-B describes mechanism of the formation of periodic bell-shaped upheaval structures on surface of polycarbonate by irradiation of NIR femtosecond laser pulse. The mechanism is investigated on the basis of observation of the periodic bell-shaped upheaval structures using various microscopes.

Chapter 7 describes structures induced by irradiation of NIR femtosecond laser pulse in amorphous materials. Chapter 7 is composed of two sub-Chapters 7-A and 7-B. Chapter 7-A describes crystallization and permanent relief grating structures induced by irradiation of NIR femtosecond laser pulse in amorphous inorganic (In_2O_3＋1wt% TiO_2) films. Relationship between induced permanent relief grating structures and irradiation condition is investigated. Chapter 7-B describes structures induced by irradiation of NIR femtosecond laser pulse in polysilane and polysilane layer coated polymer film. Photo-sensitive effect of polysilane layer coated on polymer bulk is investigated.

Chapter 8 describes summary of this thesis. In Chapter 8, each conclusion from Chapter 1 to Chapter 7 and features of structures induced by NIR femtosecond laser pulse in polymer materials comparing with those of inorganic glasses are described.

References

(1) K.O. Hill, Y. F. Fujii, D. C. Johnson, and B. S. Kawasaki: Appl. Phys. Lett. **32** (1978) 647.

(2) W. J. Tomlinson, I. P. kaminov, E. A. Chandross, R. L. Fork and W. T. Silfvast: Appl. Phys. Lett. **16** (1970) 486.

(3) J. P. Allison: J. Polym. Sci. Part A, **4** (1966) 1209.

(4) K. Miura, J. Qiu, H. Inoue, T. Mitsuyu, K. Hirao: Appl. Phys. Lett. **71** (1997) 3329.

(5) Y. Kondo, J. Qiu, T. Miura, K. Hirao, T. Yoko: Jpn. J. Appl. Phys. **38** (1999) L1146.

(6) T. Toma, Y. Furuya, W. Watanabe, K. Ito, J. Nishii, K. Hayashi: Opt. Rev. **7** (2000) 14.

(7) Y. Kondo, T. Suzuki, H. Inoue, K. Miura, K. Hirao: Jpn. J. Appl. Phys. **37** (1998) 94.

(8) K. Hirao, K. Miura: Jpn. J. Appl. Phys. **37** (1998) 2263.

(9) K. Miura, H. Inoue, J. Qiu, K. Hirao: Nuclear Instruments and Methods in Physics Research. **B141** (1998) 726.

(10) B. C. Stuart, M. D. Feit, A. M. Rubenchik, B. W. Sore, M. D. Perry: Phys. Rev. Lett. **74** (1995) 2248.

(11) K. M. Davis, K. Miura, N. Sugimoto, K. Hirao: Opt. Lett. **21** (1996) 1729.

(12) E. N. Glezer, M. Milosavljevic, L. Huang, R. J. Finlay, T. H. Her, J. P. Callan, E. Mazur: Opt. Lett. **21** (1996) 2023.

(13) K. Takahashi, K. Furusawa. M. Obara: CLEO/Pacific Rim'99, TUK7, Seol, Sep, 1999.

(14) J. R. G. Thorne, Y. Ohsako, J. M. Zeigler, R. M. Hochstrasser: Chem. Phys. Lett. **162** (1989) 455.

(15) H. Tachibana, Y. Kawabata, S. Koshihara, Y. Tokura: Solid. State. Commun.**75** (1990) 5.

(16) T. Miyazaki, T. Saeki, C. Liu, M. Kita: J. Am. Chem. Soc. **120** (1998) 1084.

(17) S. H. Cho, H. Kumagai, I. Yokota, K. Midorikawa, M. Obara: Jpn. J. Appl. Phys. **37** (1998) 1737.

(18) S. H. Cho, H. Kumagai, K. Midorikawa, M. Obara: Opt. Comm. **168** (to be published)

(19) D. Homoelle, W. Wielandy, A. L. Gaeta, E. F. Borrelli, C. Smith: Opt. Lett. **24** (1999) 1311.

(20) Y. Sikorski, A. A. Said, P. Bado, M. Mayanard, C. Florea, K. A. Winick: Electron.

Lett. **36** (2000) 226.

(21) K. Yamada, W. Watanabe, T. Toma, K. Ito, J. Nishii: Opt. Lett. **26** (2001) 19.

(22) C. B. Schaffer, A. Brodeur, J. F. Garca, E. Mazur: Opt. Lett. **26** (2001) 93.

(23) M. Will, S. Nolte, B. N. Chichkov, A. Tunnermann: Appl. Opt. **41** (2002) 4360.

(24) D. Ashkenasi, H. Varel, A. Rosenfeld, S. Henz, J. Hermann, E. E. B. Cambell: Appl. Phys. Lett. **72** (1998) 1442.

(25) K. Hirao, K. Miura: J. Appl. Phys. **37** (1998) 49.

(26) R. Yano, M. Mitsunaga, N. Uesugi: Phys. Rev. **B 50** (1994) 9031.

(27) K. Hirao, S. Todoroki, D. H. Cho, N. Soga: Opt. Lett. **18** (1993) 1586.

(28) D. H. Cho, K. Hirao, N. Soga: J. Non-Cryst. Solids. **189** (1995) 181.

(29) R. Eichberger , F. Willig: Chem. Phys. **141** (1990) 159.

(30) K. Iwata et al: Rev. Sci. Instrum. **64** (1993) 2140.

(31) K. Miura et al: J. Mat. Sci. Lett. **15** (1996) 1854.

(32) K. Hirao, S. Tanabe, S. Kishimoto, K. Tamai, N. Soga: J. Non-Cryst. Solids. **135** (1991) 90.

(33) M. Mitsunaga, N. Uesugi, H. Sasaki, K. Karaki: Opt. Lett. **19** (1994) 752.

(34) H. Sasaki, K. Karaki, M. Mitsunaga, N. Uesugi: J. Lumin. **64** (1995) 273.

(35) B. O'regan, M. Gratzel: Nature. **353** (1991) 737.

(36) J. Qiu, Y. Kawamoto, K. Hirao: Jpn. J. Appl. Phys. **36** (1997) 1091.

(37) J. Qiu, J. B. Qiu, H. Higuchi, Y. Kawamoto, K. Hirao: J. Appl. Phys. **80** (1996) 5297.

(38) Y. Kondo, K. Nouchi, T. Mitsuyu, M. Watanabe, P. G. Kazansky, K. Hirao: Opt. Lett. **24** (1999) 646.

(39) N. Sugimoto, H. Kambara, S. Fujiwara, K. Tanaka, K. Hirao: Opt. Lett. **21** (1996) 1637.

(40) H. Kambara, N. Sugimoto, S. Fujiwara, K. Hirao: Opt. Commun **148** (1998) 101.

(41) K. Hirao, H. Kambara, S. Fujiwara, K. Tanaka, N. Sugimoto: J. Ceram. Soc. Japan. **105** (1997) 1115.

(42) S. Kawata, Y. Kawata: Chem. Rev. **100** (2000) 1777.

(43) Y. Kawata: Proc. SPIE. **4081** (2001) 76.

(44) H. B. Sun, S. Matsuo, H. Misawa: Appl. Phys. Lett. **74** (1999) 786.

(45) H. Misawa, S. Juodkazis, H. B. Sun, S. Matsuo, J. Nishii: Proc. SPIE **4088** (2000) 29.

(46) H. B. Sun, V. Mizeikis, Y. Xu, S. Juodkazis, J. T. Ye, S. Matsuo, H. Misawa: Appl. Phys. Lett. **79** (2001) 1.

(47) T. Komdo, S. Matsuo, S. Juodkazis, H. Misawa: Appl. Phys. Lett. **79** (2001) 725.

(48) S. Kawata, H. B. Sun, T. Tanaka, K. Takada: Nature. **412** (2001) 697.

(49) T. Watanabe, M. Akiyama, K. Totani, S. M. Kuebler, F. Stellacci, W. Wenseleers, K. Braun, S. R. Marder, J. W. Perry: Adv. Funct. Mater. **12** (2002) 611.

(50) J. Si, J. Qiu, J. Zhai, Y. Shen, K. Hirao: Appl. Phys. Lett. **80** (2002) 359.

(51) Y. Hosokawa, M. Yashiro, T. Asahi, H. Fukumura, H. Masuhara: Appl. Sur. Sci. **154-155** (2000) 192.

(52) K. Hatanaka, T. Ito, T. Asahi, N. Ichinose, S. Kawanishi, T. Sasuga, H. Fukumura, H. Masuhara: Chem. Phys. Lett. **300** (1999) 727.

Chapter 2: Experimental Section

2-1 Outline of used NIR laser pulse

   We used a re-generatively amplified Ti-sapphire mode-locked laser system (800 nm wavelength) with 150 fs pulse duration, 4 μJ pulse energy, and 200 kHz repeating rate, as an irradiation source. Schematic diagram of experimental setup for femtosecond pulse laser irradiation system is shown in Fig. 1.
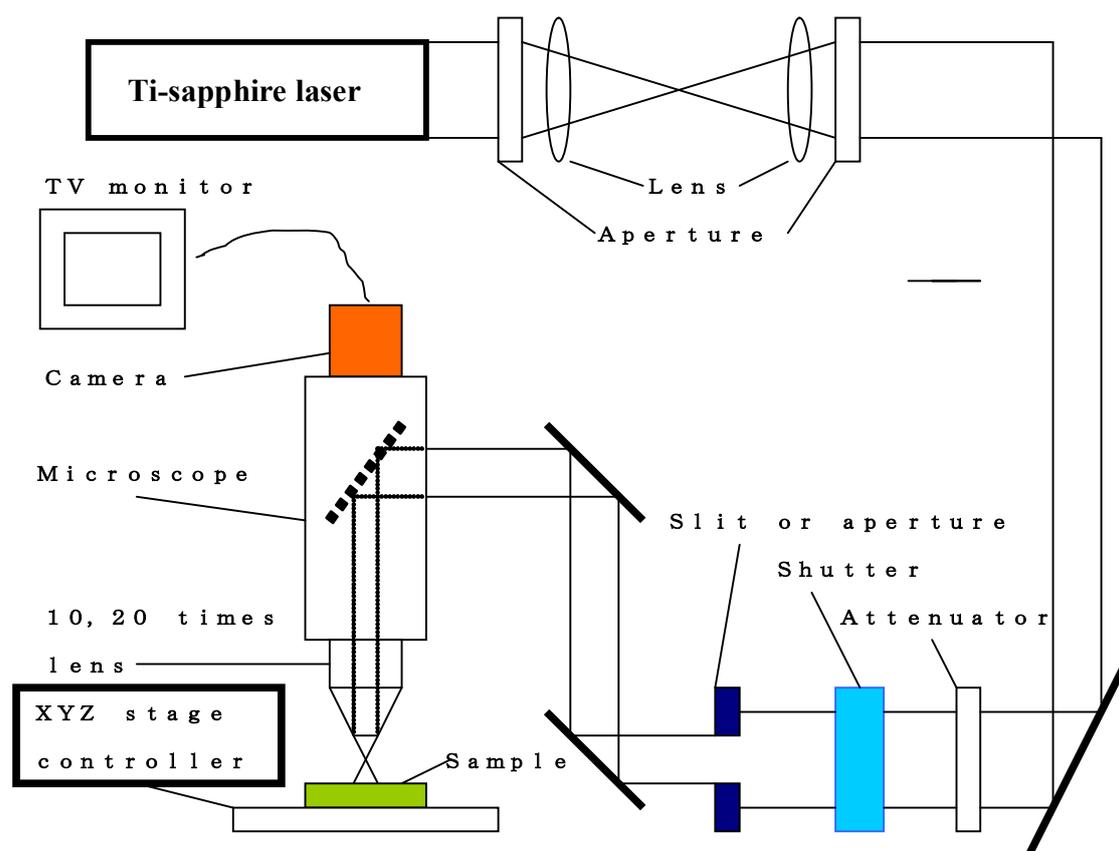
Fig. 1 Schematic diagram of irradiation system using a femtosecond pulse laser.

   The beam diameter of 8 mm in Gaussian mode produced by a re-generatively amplified Ti-sapphire laser was widen to diameter of ca. 20 mm in order to get uniform pulse irradiation strength, and the center of beam was passed through slit or aperture selectively. The pulse energy was controlled using an attenuator or neutral density (ND) filters and irradiation time was controlled by opening period of shutter. Controlled irradiation beam was guided into a microscope and focused by a 10X or a 20X objective lens selectively (for 10X and 20X objective lens, numerical aperture NA is 0.30 and 0.46, respectively) and injected into the given depth of the polymer sample. We

observed the polymer sample *in situ* during the focused irradiation of femtosecond pulses using a charge-coupled device (CCD) camera mounted on the microscope. The beam diameter before focusing through the objective lens was 2.5 mm.

2-2 Irradiation of NIR laser pulse

The polymer sample was scanned by a computer-controlled XYZ-stage at a given scan rate. As show in Fig. 2, laser beam was focused into the given depth (Z axis) and sample was scanned along the direction (X axis) at a given rate under shutter opened (line irradiation). Therefore, irradiation conditions are irradiated energy (nJ/pulse), used objective lens (10X or 20X), target depth (μm) and scanning rate (μm/s) to a given sample in the line irradiation.
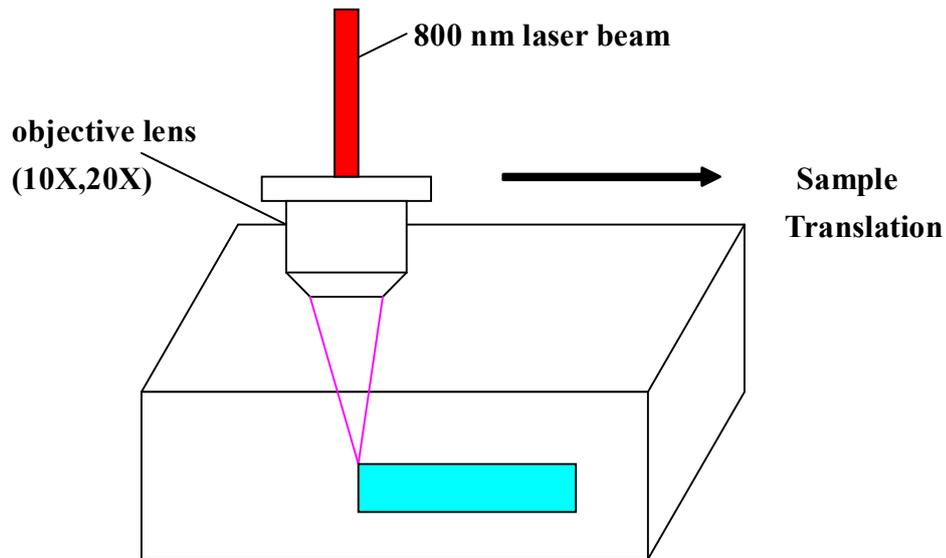
Fig. 2 Line irradiation method. The sample was scanned along the direction perpendicular to the incident laser beam.

The diffraction grating structures with grating thickness of L in Z axis and grating pitch (equal interval) of Λ in Y axis and ensemble of bell-shaped upheaval for micro-lens array were fabricated by repeating this line irradiation with equal interval as shown in Fig. 3. Multiple line irradiation method was carried by superimposing line irradiation on the structure already fabricated. In this case, the pitch of irradiation line (Λ) is an additional irradiation condition
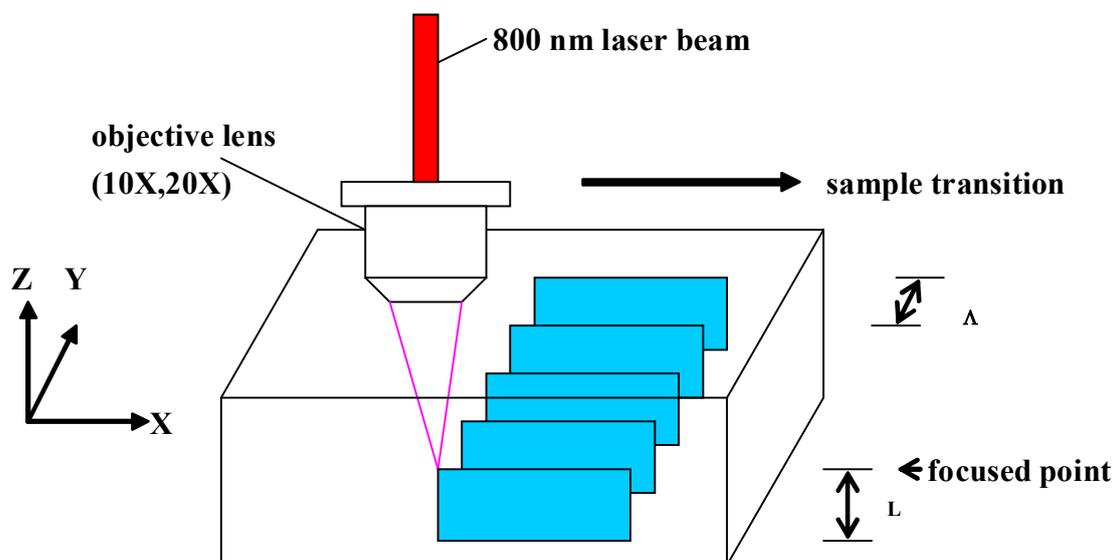
Fig. 3 Line irradiation method in the case of forming a diffraction grating structure.

2-3 Sample preparation

Commercially available sheet sample of polymer materials and powder of dyes were used without any treatment. Commercially available powder and/or block of polymer materials were dissolved in solvent and cast the solution onto a glass substrate to prepare a film with approximately 500 μm thickness.

The copolymer of methyl-methacrylate (MMA) and ethyl-acrylate-butyl-acrylate (EA-BA) (p-(MMA/EA-BA) copolymer) is prepared by living-radical polymerization in the laboratory of Nitto Denko Corporation; First, random copolymer of EA and BA was prepared from EA and BA monomers with equivalent molar ratio using a living–radical polymerization with 1-buromo-ethyl-iso-butylate as an initiator, copper bromide as an catalyst and 2,2-bipyridine derivative as a co-catalyst. Second, MMA monomer was added to the living (EA-BA random) copolymer and living polymer chain of (EA-BA random) copolymer was propagated by the same living-radical polymerization of MMA and PMMA block chain was added to the prepared block (EA-BA random) chain. After purification of these copolymers through filters or ion-exchange resins, we added 1 weight part triazine as photo-crosslinker (maximum absorption wavelength of triazine is ca. 360 nm) to 100 weight parts copolymer, then dissolved mixture of purified copolymer and cross-linker in ethyl acetate and made ca. 30 wt% solution. We made approximately 500 μm thick films by casting the 30 wt% solution onto a glass substrate.

The deposition methods to form amorphous ITO (In_2O_3+10 wt%SnO_2) and (In_2O_3+1

wt%TiO_2) thin films were DC magnetron sputtering with Ar, O_2, H_2O mixture (0.4Pa, Ar:O_2:H_2O=95:3:2) using a sintered oxide ceramic (In_2O_3+10 wt%SnO_2 and In_2O_3+1 wt%TiO_2) target at room temperature. Water vapor was taken from a water-filled bottle and its quantity was controlled by a needle pressure valve on the bottle. The target had a 6 inch diameter and the applied sputtering power was 2 W/cm^2. The substrate was rotated during sputtering to obtain a uniform layer on it. The thickness obtained was controlled by the sputtering time.

Replication method using electroforming and molding (pseudo-LIGA process) was conducted as follows;

First, a non-electrolytic plating of Ni was carried out to obtain pre-coated samples with approximately 1 μm in thickness and then an electrolytic plating of Ni using pre-coated samples as negative electrode and Ni plate as positive electrode in nickel sulfamic acid plating bath. Finally, coated samples with Ni of approximately 36 μm in thickness was formed as an electroformed mother mold. Molding was carried out by potting a polymer dissolved solution (approximately 30 wt%) into the electroformed mother mold and then evaporating the solvent. Replicated sample was removed from the electroformed mother mold.

2-4 Observation and identification of induced structures by irradiation of NIR femtosecond laser pulse

The structures on the surface of the polymer materials induced by the pulsed laser irradiation were observed by an optical interference microscope. To measure the cross-section of the irradiated region of the sample film, the sample film was cut by a microtome. The cross sectional and transmission image by an optical microscope were observed and we obtained an information of transmission property of irradiated and un-irradiated region. We obtained an information of refractive index property of irradiated and un-irradiated region by differential interference contrast images of laser scanning microscope (wavelength of laser, 488nm; observation mode, transmitted mode; optically sliced thickness, 5 μm; number of stacked layers, approximate 30 layers). We also observed the morphology of the cross section by a scanning electron microscope (SEM) and an atomic force microscope (AFM).

The characterization of the change in chemical structure and crystallinity induced by irradiation were investigated by microspectrophotometry (FT-IR ATR) and by X-ray diffraction analysis, respectively. Molecular weight of block p-(MMA/EA-BA) co-polymers were measured using Gel Permeation Chromatography (GPC) and composition of block p-(MMA/EA-BA) co-polymer are presented by weight percentage

(wt%) of PMMA in the total weight of p-(MMA/EA-BA) copolymer; the ratio of Mw of PMMA block chain to the total Mw of p-(MMA/EA-BA) copolymer. Absorption and fluorescence properties of dye-doped and un-dye-doped polymer films removed from a glass substrate were measured UV-Visible absorptiometry and Visible-Near-infrared fluorometry, respectively. T_g's of polymers prepared in the laboratory of Nitto Denko Corporation were measured by dynamic viscoelastic measurement method.

2-5 Diffraction measurement

The incident beam employed for diffraction experiment was an He - Ne laser beam (wave length; 632.8nm, maximum power; 10mW). Schematic diagram of diffraction system with the He - Ne laser is shown in Fig. 4. Diffraction experiment was carried out as follows; first, sample sandwiched between two glass-plates was set on the sample holder. Second, incident laser beam was irradiated to the sample and diffracted beam patterns were projected on a black screen which was placed at 300 mm far from the sample.
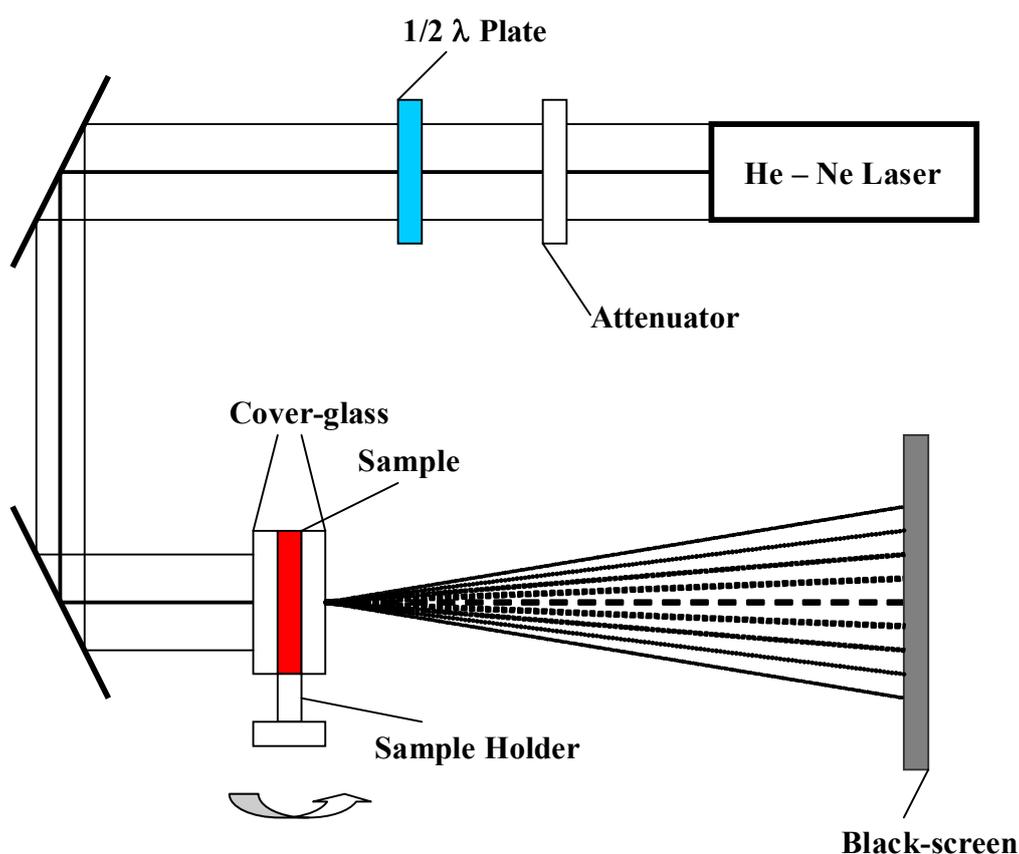
Fig. 4 Schematic diagram of diffraction experiment system.

2-6 Evaluation of micro-lens effect

The micro-lens effect of the upheaval structure was checked by an He-Ne laser beam irradiation from the backside of the upheaval structures and the observation of focused beam as shown in Fig. 5.

Focused position   Unfocused position
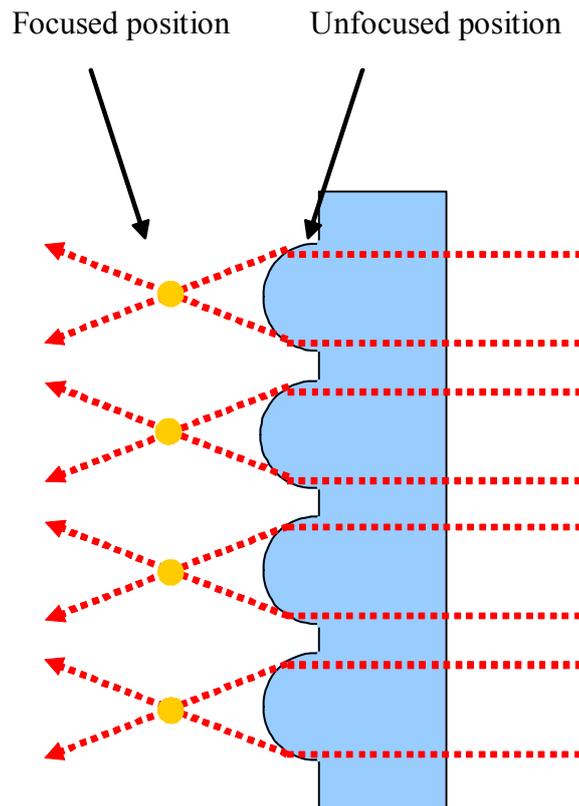
Fig. 5 Schematic of evaluation of micro-lens effect

Chapter 3: Structures induced by irradiation of NIR femtosecond laser pulse in polymeric materials

3-1 Introduction

In this Chapter, we investigate structures induced by irradiation of NIR femtosecond laser pulse in various polymer materials; olefin gel, acrylic adhesive as low glass transition temperature (T_g) polymers; poly-ether-sulphone (PES), poly-methyl-methacrylate (PMMA), poly-carbonate (PC) as high T_g polymers; and block copolymers of methyl-methacrylate and ethyl-acrylate-butyl-acrylate { p-(MMA/EA-BA) block copolymer} as having both low and high T_g polymers. Line irradiation is carried out for polymers mentioned above and we investigate relationship between T_g's of polymers and structures induced by irradiation of NIR femtosecond laser pulse. For unique induced structures of polymer, we investigate in detail relationship between irradiation conditions and changes of induced structures.

3-2 Experimental

Irradiation system and methods of measurement and observation were same as described in Chapter 2. The main polymer samples used for laser irradiation are summarized in Table 1. The polymers, olefin gel, acrylic adhesive, poly-ether-sulphone (PES), poly-methyl-methacrylate (PMMA), and poly-carbonate (PC) are commercially available. The copolymer of methyl-methacrylate (MMA) and ethyl-acrylate-butyl-acrylate (EA-BA) (p-(MMA/EA-BA) copolymer) is a block one prepared by living-radical polymerization in the laboratory of Nitto Denko Corporation. Acrylic adhesive is also prepared in laboratory of Nitto Denko Corporation. T_g's of polymers are cited from catalogs of provider except for p-(MMA/EA-BA) copolymer and Acrylic adhesive which were measured by dynamic viscoelastic method.

Table 1. Polymer materials used for laser irradiation

Sample Name	Main Component	Thickness(mm)	Tg(℃)
(a) Acrylic adhesive	Iso-nonyl-acrylate, Acrylic acid	2.0	25
(b)Olefin gel	Poly-olefin resin, Paraffin,Naphtene	5.0	－36
(c)PES	Poly-ether-sulphone	0.2	220
(d)PMMA	Poly-methyl-methacrylate	3.0	105
(e)PC	Poly-carbonate	0.5	160
(f)P-(MMA/EA・BA) copolymer	Poly-(methyl-methacrylate/ ethyl-acrylate・butyl-acrylate) copolymer	0.5	－30,100

(a),(f);Nitto Denko Corporation
(b);Nihon Denshi Seiki Co.,Ltd.
(c);Sumitomo Bakelite Co., Ltd.
(d);Mitsubishi Rayon Co.,Ltd.
(e);Teijin Chemicals Ltd.

3-3 Results and Discussion

First, we carried out line irradiation in polymer materials with different glass transition temperature (T_g), by focusing laser beam (37.6 nJ/pulse) into 30 μm depth of the samples using 10X objective lens and scanning the focused spot at a rate of 25 μm/s as shown in Chap.2. Figures 1 and 2 show optical interference micrographs of olefin gel (T_g ; -36 °C) and acrylic adhesive (T_g ; 25 °C) with low T_g's and those of PES (T_g ; 220 °C) and PMMA (T_g ; 105 °C) with high T_g's after laser irradiation, respectively.
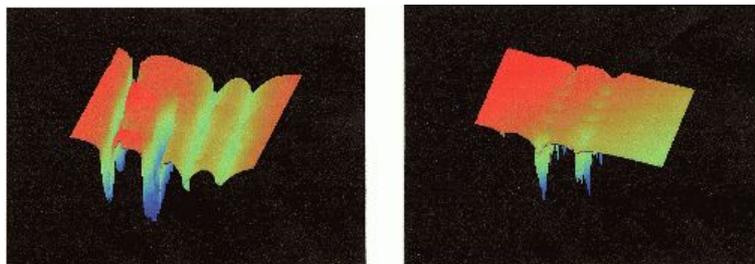
Fig.1 Optical interference micrograph of caves and channels on the surface induced by laser irradiation for lower T_g polymer:(a) olefine gel and (b) acrylic adhesive.
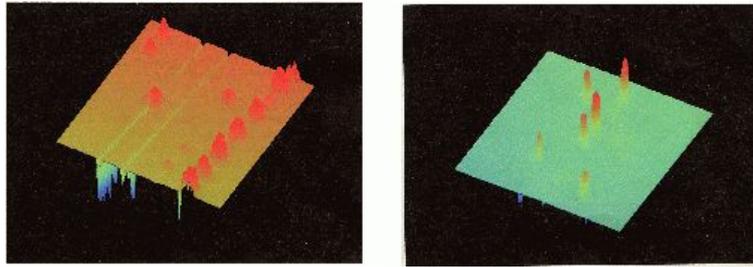
Fig. 2 Optical interfaerence micrograph of volcano-like upheaval on the surface Induced by laser irradiation for higher T_g polymers : (a) PES and (b) PMMA.

As shown in Figs. 1 (a) and (b), caves or channels was formed on the surface of the irradiated areas for olefin gel and acrylic adhesive with low T_g. On the other hand, PES and PMMA with high T_g had volcano-like upheaval on the surface of the irradiated area, as shown in Figs. 2 (a) and (b).

Second, we carried out line irradiation for PC (T_g ; 160 °C) to make clear the depth effect on formed structures for high T_g polymers. With using 10X objective lens and focusing laser beam of 75 nJ/pulse into different depth, those were 30 μm, 90 μm and 150 μm, from the surface and moving the samples perpendicular to the incident laser beam at a rate of 500 μm/s. Figure 3 shows SEM micrograph of surface and cross-section of irradiated region by laser focused to 30 μm depth (target depth). Figure 6 also shows that to 90 μm depth (target depth).

Surface

Bulk

100μm

Surface

Bulk

60μm

Volcano-like upheaval

Surface

Bulk

Void

20μm
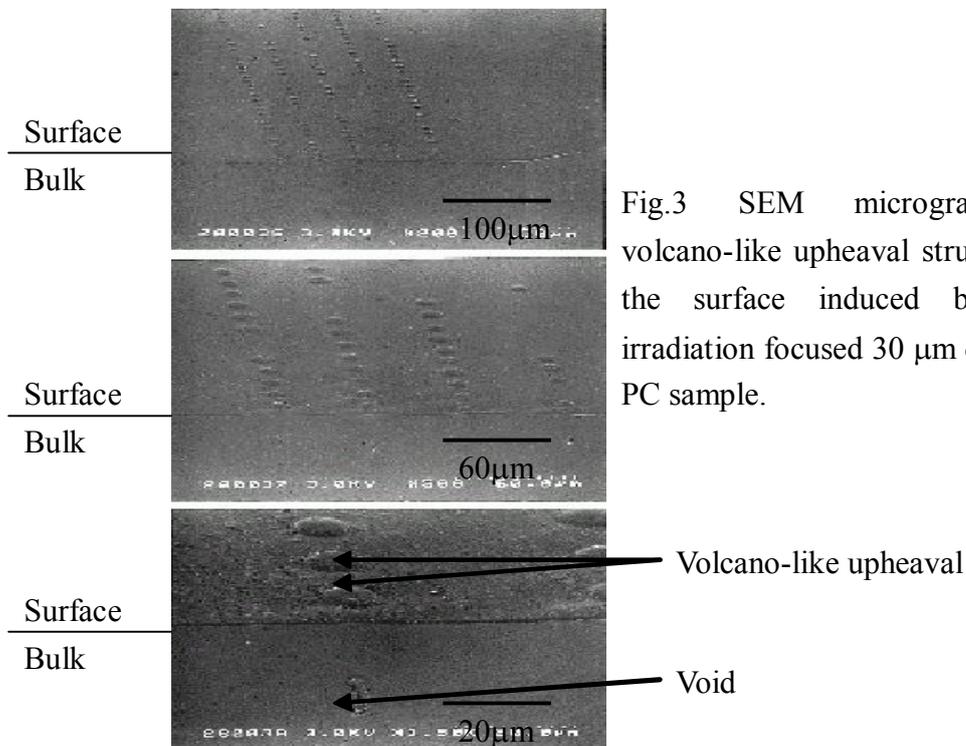
Fig.3 SEM micrograph of volcano-like upheaval structure on the surface induced by laser irradiation focused 30 μm depth. in PC sample.

25

For 30 μm depth irradiation, as shown in Fig. 3, volcano-like upheaval structures were observed as the case of PES and PMMA in the same depth irradiation as shown in Fig. 2 and there seemed voids around the irradiated depth. For 90 μm depth irradiation, any structures were not formed on the surface but voids were created on the irradiated spot, from which the cracks were grown down to the direction of laser propagation as shown in Fig. 4. No structure was formed both on the surface and in the bulk of the samples for 150 μm depth irradiation.
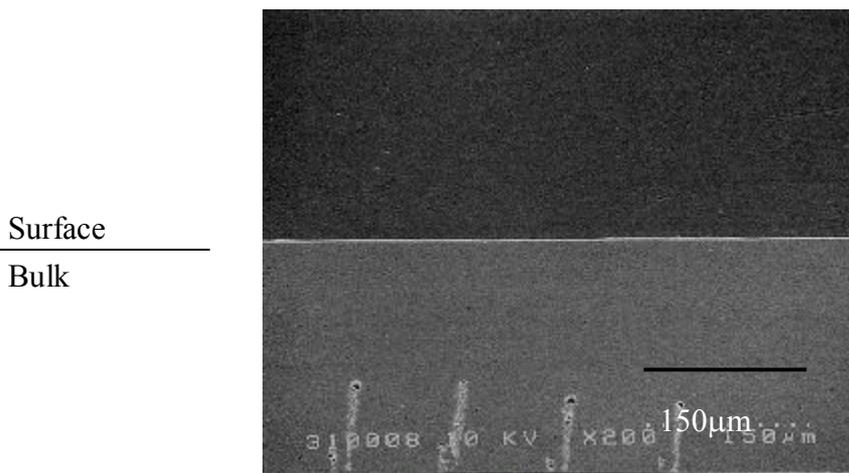
Fig. 4 SEM micrograph of induced voids and cracks by 90 μm depth (depth is target depth) laser irradiation in PC sample.

Third, we carried out line irradiation for p-(MMA/EA-BA) block co-polymer (PMMA block content; 70 wt%, Mw; 83,000) sample. We set up two kinds of experiments. The common irradiation condition for both experiments was the following: The sample scanning rate; 500 μm/s, objective lens; 10X. The selective irradiation conditions for respective experiment were as follows:

Experiment 1: The irradiated depth; 30 μm (target depth). The pulse energy were changed from 185 nJ/pulse, 300 nJ/pulse, to 400 nJ/pulse.

Experiment 2: The pulse energy; 125 nJ/pulse. The irradiated depth (target depth) was changed from 30 μm, 50 μm, to 80 μm.

Figure 5 shows the optical micrograph of cross-sectional copolymer sample after laser irradiation with various conditions described above. In both experiments, no significant change in structure was observed on the surface of the irradiated samples but in the samples the aggregation of sub-micron scale deposit was developed from the focused point to the direction of laser propagation, which can be observed as a stripe structure. The length of the stripe structure developed was ca.100 μm and the width ware 3 – 5 μm. Induced structures supposedly had different optical properties from un-irradiated region (or pre-irradiated polymer materials).
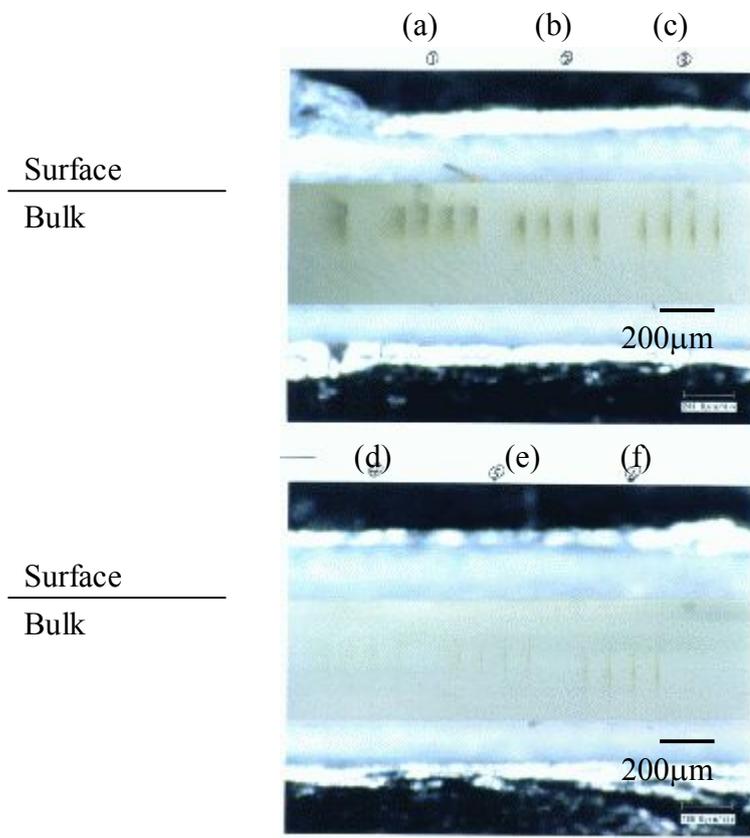
Fig. 5 Optical micrograph of stripe-like structure induced by laser irradiation for PMMA/EA-BA copolymer.　(a) 30 μm 400 nJ/pulse (b)30 μm 300 nJ/pulse　(c) 30 μm 185 nJ/pulse　(d) 30 μm 125 nJ/pulse (e) 50 μm 125 nJ/pulse　(f) 80 μm 125 nJ/pulse. (depths are target depths)
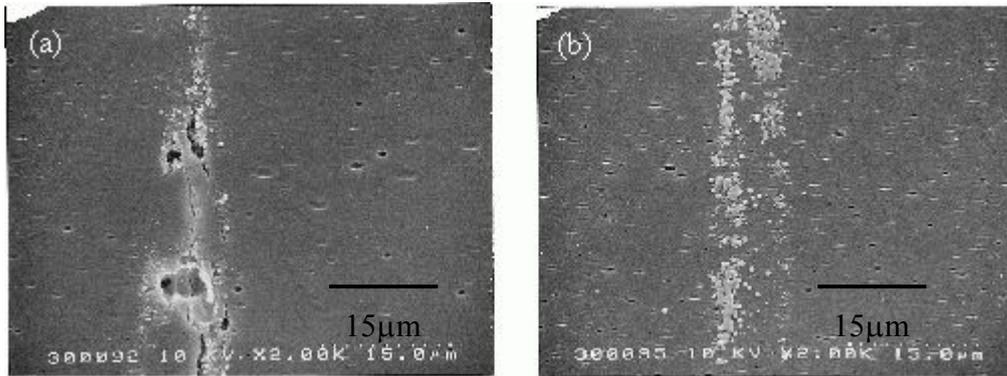
Fig. 6 SEM micrograph of aggregated stripe-like structure induced by laser irradiation for PMMA/EA-BA copolymer (PMMA, 70 wt%): (a) 185 nJ/pulse, 30 μm depth and (b) 125 nJ/pulse, 80 μm depth (depths are target depths)

Further observation of the cross-section of the samples by SEM, as shown in Fig 6, revealed that the strong pulse irradiation with 185 nJ/pulse leads to the cracks among the aggregations, but the moderate pulse energy irradiation with 125 nJ/pulse does not cause any cracks. These aggregation forms quite different structure compared with that for PES, PMMA and PC. We investigated the relation between structure induced and pulse energy for a different composition sample of the p-(MMA/EA-BA) block copolymer and tried to confirm that the formation of the aggregation was not limited to a specific composition of the copolymers. The results are given in Fig. 7
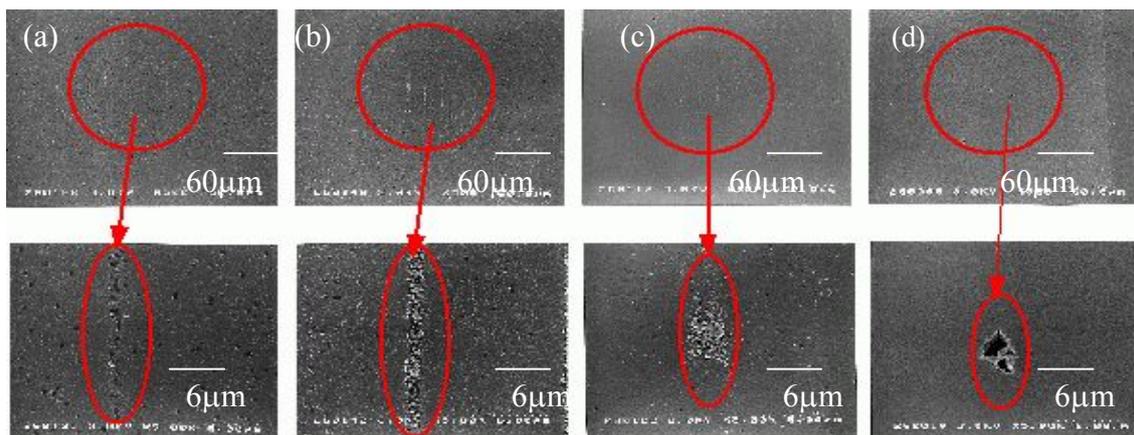
Fig. 7 SEM micrograph of aggregated stripe-like structure induced by laser irradiation for PMMA/EA-BA copolymer (PMMA; 50 wt%).
(a) 15 nJ/pulse, (b) 75 nJ/pulse, (c) 140 nJ/pulse, (d) 250 nJ/pulse.

28

The molecular weight (Mw) of the copolymer was 100,000 and PMMA content was 50 wt%. Line irradiation was carried out for the copolymer under the condition as follows: Irradiation depth (target depth); 50 μm, scanning rate; 500 μm/s, objective lens; 20X, pulse energies were changed from 15, 75, 140 to 250 nJ/pulse. As shown in Fig. 7, the irradiation with 15 nJ/pulse causes the ca. 60 μm length stripe aggregation of sub-micron scale deposit and more irradiation with 75 nJ/pulse leads that the stripe aggregation became more condense (stripe became thicker). Further high irradiation with 140 nJ/pulse results in that the aggregation became more condense and elliptical shape and the cracks with 2 - 3 μm diameter appeared for 250 nJ/pulse irradiation.

As shown in Figs 1, 2 and 3, T_g of polymer materials significantly relates to the structures formed by laser irradiation. During the line irradiation, in which the focused beam moves from one irradiated spot to adjacent spot, the irradiated spot is subjected to three-dimensional heating (spot is the center of three dimensional heated cube). Heating of the scanning direction (X axis direction) is kept by succeeding spot irradiation (superposition of heating) but heating of the direction perpendicular to the scanning direction of spot (Y axis direction) is limited and temperature decreases along the distance from the core of the irradiated spot to far in the direction of Y axis during irradiation. Therefore, inhomogeneous heating and cooling occur during irradiation. Polymer materials have viscoelastic properties involving molten and rubbery state above T_g and glassy state below T_g. Supposedly during the irradiation the continuous thermal gradient are formed along the distance from the core of the spot to far, along which the molten, rubbery (above T_g) and glassy states (below T_g) are successively produced. Instantaneous expanded volume derived from the heating effect of the irradiated spot makes compressive force to the solid region around the spot at which the crack or void is induced. Then thermal wave produced by laser irradiation causes the microscopic thermal gradient (molten and rubbery states) from the irradiated spot to the surface region, and volume expansion also follows this thermal gradient. Since, in the case of acrylic adhesive and olefin gel with T_g in the vicinity of or lower than room temperature, crack or void can be spread out to near the surface along the microscopic rubbery state with lower viscosity by heating effect and large thermal shrinkage takes place upon solidification process. These cooperative phenomena of movement of void or crack and large thermal shrinkage at the irradiated surface are significantly responsible for forming cave and channel structures with depth equal to the focused point from the surface and any void or crack cannot remain. On the contrary, for PES, PMMA and PC with high, T_g crack or void formed cannot be spread out to the surface because of higher viscosity of the matrix even though it is heated up by thermal

29

diffusion, but thermal gradient causes the volume expansion near the surface and expanded volume is subjected to the solidification with less thermal shrinkage at the surface. Therefore, the expanded volume plays an important role for creating volcano-like upheaval structure at the surface and crack or void remains at the position near irradiated point is formed.　Indeed, when irradiation energy is increased, the larger and higher volcano-like upheaval was induced on the surface for PC sample with high T_g. This result supports that the larger irradiation energy produces larger thermal energy to increase the local temperature near the surface. Then the increased local temperature induces volume expansion to form larger and higher volcano-like upheaval at the surface.

The block copolymer consists of separate block parts with high T_g and low T_g in which the influence of heating on thermal expansion is balanced adequately to form the deposit from the molten state. The structure of the sub-micron scale deposit is investigated by AFM analysis and FT-IR microspectrophotometric analysis. Figure 8 shows the AFM image of the cross-section of irradiated p-(MMA/EA-BA) copolymer in which MMA content is 70 wt% and Figure 9 shows the FT-IR microspectrophotometric spectra measured with ATR accessory of irradiated and un-irradiated samples of same block copolymer. AFM analysis revealed that the aggregation of deposit is swelling and has higher elasticity than un-irradiated region.
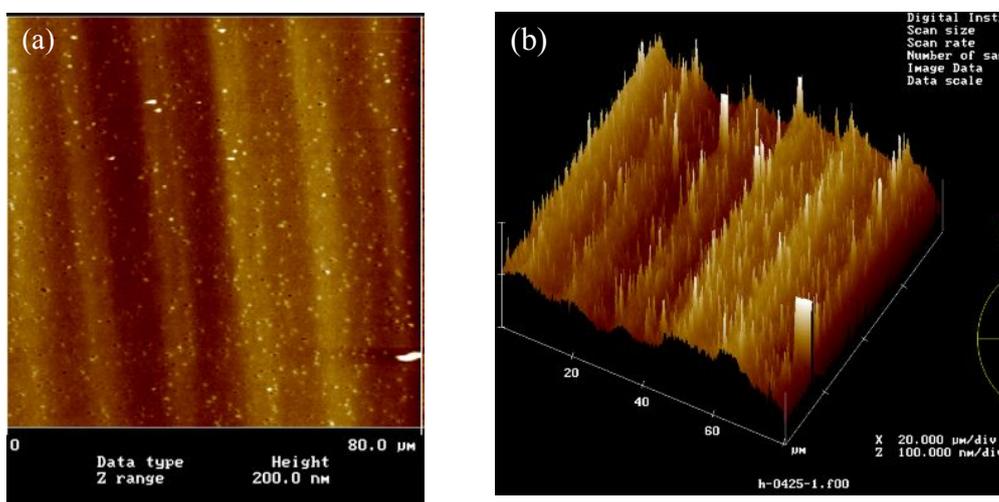
Fig. 8 AFM image of cross-section of irradiated p-(MMA/EA-BA) block copolymer (PMMA; 70 wt%).
(a) surface unevenness　(b) three dimensional imaging
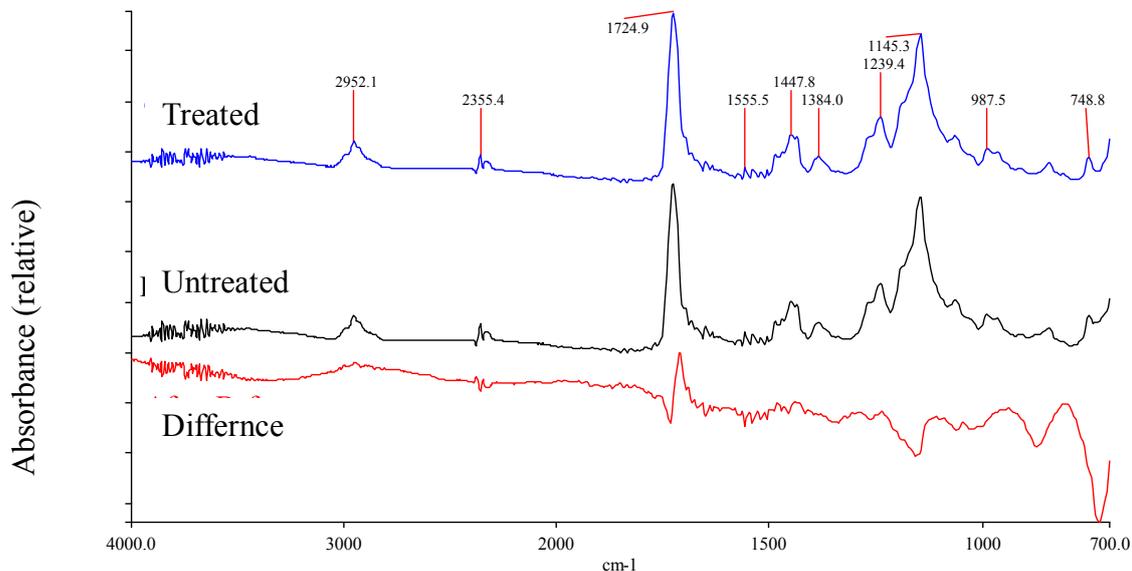
Fig. 9 FT-IR ATR microspectrophotometric spectra of irradiated
sample (treated) , un-irradiated sample (untreated) and difference
between them for p-(MMA/EA-BA) copolymer (PMMA; 70wt%).

The difference spectrum between treated and untreated ones reveals the decrease in IR absorbance due to ester group (1725 cm^{-1}) and the increase in that due to aldehyde group (1720 cm^{-1}). These results imply the photo-decomposition or photo-crosslinking of polymer chain components of PMMA and P-(EA-BA) induced by multi-photon excitation of femto-second NIR laser irradiation. Photo-induced decomposition of PMMA and copolymer with methyl acrylate under ultra-violet (UV) wavelength irradiation has been reported in the literature.[11] The aggregation has different optical properties from un-irradiated region. Preliminary experimental results show the efficient diffraction can be observed from the stripe structures induced laser radiation.

It has been reported that irradiation to inorganic glass materials brought the change in structure from thin stripe to thick one, to ellipse and finally cracks with increasing the irradiated pulse energy. The tendency of structure change with increasing pulse energy in irradiated p-(MMA / EA-BA) block copolymer samples was the same as the results obtained for inorganic glass materials. But there were two significant differences. First, required pulse energy to bring such change for polymer materials were 1/10 - 1/20 times lower than that for inorganic glass materials.[9] This is probably due to the significant difference of glass transition temperature and thermal conductivity. Second, no aggregations of deposit but uniform stripe-like structure, as shown in Fig.10, are

induced in inorganic glass materials. This is probably due to different mechanism for the formation of induced structures between two materials.
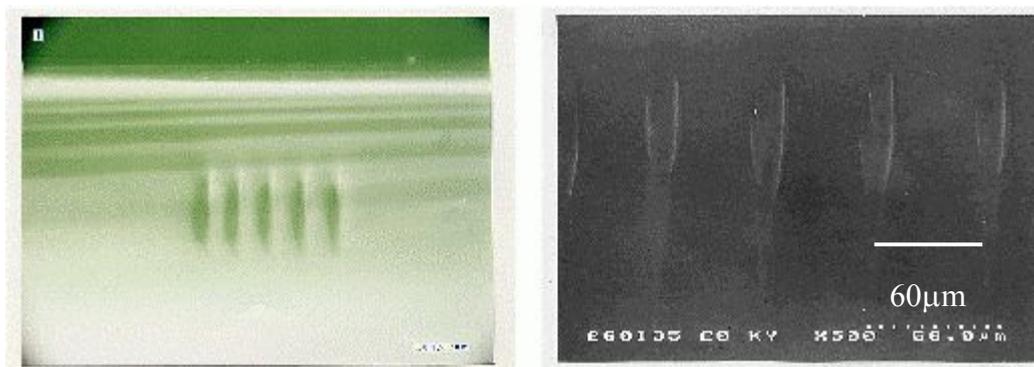
Fig. 10 Micrograph of structure induced by laser irradiation for inorganic glass materials (2500 nJ/pulse, 60 μm target depth).
(a) micrograph of optical microscope   (b) micrograph of SEM

3-4 Conclusion

We carried out line irradiation into polymer materials. In the case of shallow depth irradiation, for example 30 μm in depth, volcano-like upheavals was observed on the surface of irradiated sample for higher T_g polymers, such as PES, PMMA, PC but caves and channels for lower T_g polymers, such as acrylic adhesive and olefin gel. The induced structures had significant relation to T_g for the irradiated polymers. The irradiation in deep region, for example 90 μm in depth, induced voids and cracks in the irradiated spot for polymer materials with higher T_g. Stripe-like aggregation consisted of sub-micron deposit was observed for irradiated p-(MMA/EA-BA) block copolymers which have both higher T_g and lower T_g in the material. These stripe-like aggregations changed their shapes from thin stripe to thick one, and to ellipse and finally voids and cracks appeared with increasing the irradiated pulse energy. The change in structure in irradiated copolymers had the same tendency as in the case of the inorganic materials in qualitative manner. But in quantitative manner, inorganic glass materials required 10 - 20 times much energy than polymer materials to induce the equivalent change. The other significant difference in stripe-like structures induced between p-(MMA/EA-BA) copolymers and inorganic glass materials was that aggregation composed of sub-micron deposit was formed in polymer materials and not aggregation but uniform structure was formed in inorganic glass material. The analyses by AFM, and microspectrophotometric FT-IR revealed that sub-micron scale deposit might be re-produced structures after photo-decomposition or photo-crosslinking of polymer

chain components. This aggregation had different optical properties from un-irradiated region. These structures induced by irradiation of femtosecond laser pulse might be applicable for optical devices such as diffraction grating and optical guide and so on. Indeed, preliminary experimental results show the efficient diffraction can be observed from the structures induced laser radiation, which is in progress for studying and will be published elsewhere.

References and notes

(1) W. J. Tomlinson, I. P. kaminov, E. A. Chandross, R. L. Fork, W. T. Silfvast: Appl. Phys. Lett. **16** (1970) 486.

(2) K. Miura, J. Qiu, H. Inoue, T. Mitsuyu, K. Hirao: Appl. Phys. Lett. **71** (1997) 3329.

(3) Y. Kondo, J. Qiu, T. Miura, K. Hirao, T. Yoko: Jpn. J. Appl. Phys. **38** (1999) L1146.

(4) T. Toma, Y. Furuya, W. Watanabe, K. Ito, J. Nishii, K. Hayashi: Opt. Rev. **7** (2000) 14.

(5) Y. Kondo, T. Suzuki, H. Inoue, K. Miura, K. Hirao: Jpn. J. Appl. Phys. **37** (1998) 94.

(6) K. Hirao, K. Miura: Jpn. J. Appl. Phys. **37** (1998) 2263.

(7) K. Miura, H. Inoue, J. Qiu, K. Hirao: Nuclear Instruments and Methods in Physics Research **B141** (1998) 726.

(8) B. C. Stuart, M. D. Feit, A. M. Rubenchik, B. W. Sore, M. D. Perry: Phys. Rev. Lett. **74** (1995) 2248.

(9) K. M. Davis, K. Miura, N. Sugimoto, K. Hirao: Opt. Lett. **21** (1996) 1729.

(10) E. N. Glezer, M. Milosavljevic, L. Huang, R. J. Finlay, T. H. Her, J. P. Callan, E. Mazur: Opt. Lett. **21** (1996) 2023.

(11) J. P. Allison: J. Polym. Sci. Part A, **4** (1966) 1209.

Chapter 4: Grating structures induced by irradiation of NIR femtosecond laser pulse in polymeric materials and diffraction measurement of those structures

4-1 Introduction

In previous Chapter, we investigated the structures induced by irradiation of NIR femtosecond laser pulse in various polymer materials; olefin gel, acrylic adhesive as low glass transition temperature (T_g) polymers and poly-ether-sulphone (PES), poly-methyl-methacrylate (PMMA), poly-carbonate (PC) as high T_g polymers and p-(MMA/EA-BA) block copolymers as having both low and high T_g polymer. We confirmed that structures induced by line irradiation which was performed by scanning laser spot in polymer bulk depended on T_g of irradiated polymers; volcano-like upheaval structure on the surfaces for relatively high T_g polymers and cave or channel structures on the surfaces for relatively low T_g polymers and aggregation of sub-micron scale deposit for having both low and high T_g polymer (block copolymers). These aggregations of deposit had different refractive index from un-irradiated region and might induce interest optical properties.[11]

In this Chapter, we investigate the diffraction grating capability of those made from stripe-shape structures induced by irradiation of NIR femtosecond laser pulse in p-(MMA/EA-BA) block copolymer using transmission diffraction measurement and present new possibility of NIR femtosecond laser pulsing for manufacture of polymer optical devices.

4-2 Experimental

Irradiation system and methods of observation were same as described in Chapter 2. The used polymer samples were copolymers of methyl-methacrylate (MMA) and ethyl-acrylate-butyl-acrylate (EA-BA) (p-(MMA/EA-BA) copolymer) which were prepared by living-radical polymerization in laboratory of Nitto Denko Corporation. The diffraction measurement was carried out by the method described in Chapter 2. Diffraction efficiency (η) of each order was calculated by measuring each diffracted beam intensity. Diffraction efficiency is ordinarily defined by the ratio of diffraction beam intensity to incident beam intensity. Sample films were sandwiched between two glass-plates. Transmission beam intensity was ca. 70 - 75% of incident beam intensity because of optical intensity loss such as absorption and reflection of two glasses. Therefore we took sum of the each diffraction beam spot intensities instead of incident beam intensity for measurement of diffraction efficiency. Beam energy of each order

diffraction spots (0th, $\pm1^{st}$, $\pm2^{nd}$ so on) was measured by power meter and the distances between zeroth diffraction spot and each order diffraction spots were measured on the black screen placed at 300 mm far from the sample. Diffraction efficiency (η_m) of each order diffraction is calculated by the equation of

$$\eta_m = \frac{I_m}{\sum_{m=-\infty}^{\infty} I_m} \qquad (1)$$

In this equation: I_m is diffraction spot intensity of mth order. m^{th}-order diffraction efficiency (η_m) can be written as

$$\eta_m = J_m^2(\delta) = J_m^2(\frac{2\pi L \Delta n}{\lambda \cos\theta}) \qquad (2)$$

using Bessel Function.[12,13] In this equation : $J_m(\delta)$; Bessel Function, L; thickness of diffraction grating, Δn; refractive index change, λ; wavelength of incident beam, θ; angle of incident beam. Refractive index change (Δn) is calculated using equation (2).

Q value, a parameter used to judge on diffraction pattern, is given by the equation of

$$Q = \frac{2\pi\lambda L}{n\Lambda^2} \qquad (3)$$

In equation (3), n is refractive index of polymeric material, Λ is the interval between each diffraction grating.

4-3 Results and Discussion

We found that unique structures could be induced by femtosecond laser pulse for p-(MMA/EA-BA) block copolymer.[11] Femtosecond laser pulse line irradiation for these block copolymers brought no significant change on the surface of the irradiated samples but inside the samples the aggregation of deposit with sub-micron scale was developed from the focused point to the direction of laser propagation, which can be observed as a stripe structure. The length of the stripe structure developed was ca. 100 μm and the width was 3 - 5 μm. These structure are derived from the aggregation of deposit which are quite different from those for other polymer such as PMMA, PC, PES (higher Tg polymers) and olefin gel, acrylic adhesive (lower Tg polymers) as reported in previous paper.[11] The induced structure significantly depends on the irradiated pulse energy. SEM micrograph of induced structures is shown in Fig. 1. The sample is the copolymer with the molecular weight (Mw) 100,000 and PMMA content was 50 wt% (we call this polymer as polymer #1). Line irradiation conditions are as follows: irradiation depth (target depth); 50 μm, scanning rate; 500 μm/s, objective lens; 20X. Pulse energies were

changed from 15, 75, 140 to 250 nJ/pulse.
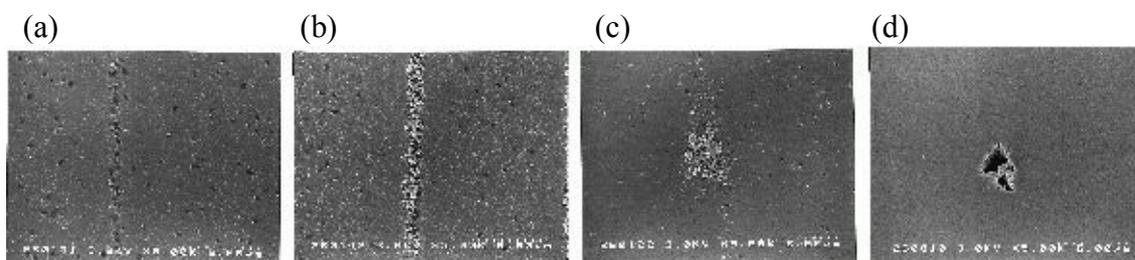
Fig. 1 SEM micrograph of aggregated stripe-like structure induced by laser irradiation for PMMA/EA·BA copolymer (PMMA; 50 wt%).
(a) 15 nJ/pulse, (b) 75 nJ/pulse, (c) 140 nJ/pulse, (d) 250 nJ/pulse

The irradiation with 15 nJ/pulse causes the ca. 60 μm length stripe aggregation of deposit with sub-micron scale and more irradiation with 75 nJ/pulse leads to the more condense stripe aggregation (stripe became thicker). Further high irradiation above 140 nJ/pulse causes the aggregation with more condense and elliptical shape or the cracks with 2 - 3 μm in diameter. The aggregation of deposit was also observed for another p-(MMA/EA-BA) block copolymer with different PMMA block content (PMMA block content; 70 wt%, Mw; 83,000. We call this as polymer #2).

Stripe-shape structures with ca. 3 - 5 μm in width and ca. 30 - 180 μm in thickness were obtained for both copolymers by adequate irradiated pulse energy. The ensemble of layers of these stripe-shape structures should work as transmission diffraction grating. We carried out femtosecond laser pulse irradiation for sample #1 and sample #2 to obtain transmission diffraction grating. Line irradiation conditions were as follows: irradiation depth (target depth); 80 μm, scanning rate; 500 μm/s, objective lens; 20X for sample #1, 10X for sample #2, changing irradiation condition were pulse energy (100, 150 nJ/pulse), number of diffraction grating N_G (10, 20, 40, 50 layers), interval between each diffraction grating Λ (7 μm, 10 μm, 15 μm, 30 μm); polymer #1 with photo-cross-linker of 0.5, 1.0, 2.0 weight part and #2 with photo-cross-linker of 1 weight part were used. Samples induced by irradiation of femtosecond laser pulse are listed with irradiation condition in Table 1.

Table 1. Grating properties for samples induced by irradiation of femto-second laser pulse

Sample No.	Polymer No. (photo-crosslinker) (weight part)	Irradiated pulse energy (nJ/pulse)	Inter-grating distance (μm)	Number of grating	Grating thickness (μm)
#1	#1(0.5)	100	15	10	49
#2	#1(0.5)	100	15	40	49
#3	#1(0.5)	100	7	20	49
#4	#1(1.0)	150	10	10	81
#5	#1(1.0)	100	7	20	63
#6	#1(1.0)	100	15	40	63
#7	#1(2.0)	100	15	10	29
#8	#1(2.0)	100	15	40	29
#9	#1(2.0)	100	7	20	29
#10	#1(2.0)	100	30	50	29
#11	#2(1.0)	150	15	10	219
#12	#2(1.0)	150	15	15	219

Diffraction patterns are shown with different Λ (7 μm, 15 μm, 30 μm) for sample #1 with photo-cross-linker of 1 weight part in Fig.2.

(a)   (b)   (c)
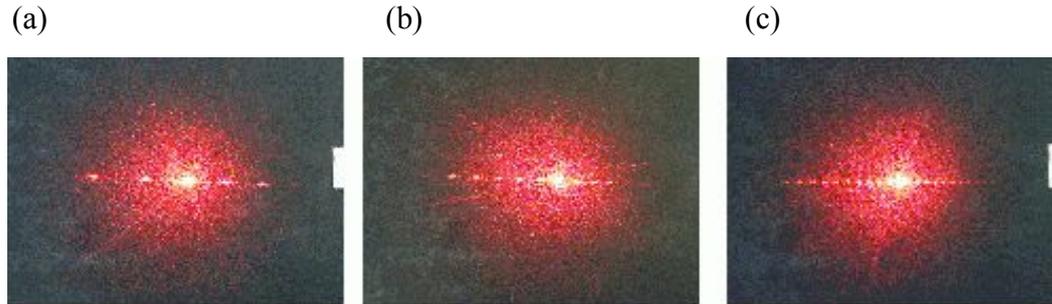
Fig. 2 Diffraction pattern photograph of different Λ for polymer #1. (photo-cross-linker; 1.0 weight part) (a) Λ=7 μm, (b) Λ=15 μm, (c) Λ=30 μm

As Λ increases, higher-order diffraction pattern are observed and the distance between zeroth diffraction and each order diffraction D (for example, D_1 is the 1st-order diffraction spot on black screen and the distance is noted as d_{01} in mm unit) becomes narrower. According to Bragg rule for diffraction, the following equation is satisfied,

$$2\Lambda \sin \theta = N \frac{\lambda}{n} \qquad\qquad\qquad (4)$$

In equation (4), N is integer, and $\sin\theta$ is nearly equal to $\tan\theta = d_{01}/300$ under the condition of $d_{01} \ll 300$. If same-order diffraction spots were selected for comparison (that is N is same integer), $2\Lambda\sin\theta$ would become constant in this case. Figure 3 shows linear relation of $\sin\theta$ vs. $1/\Lambda$ for N = 1 and we confirmed that the transmission diffraction occurred in the induced stripe-shape structures.
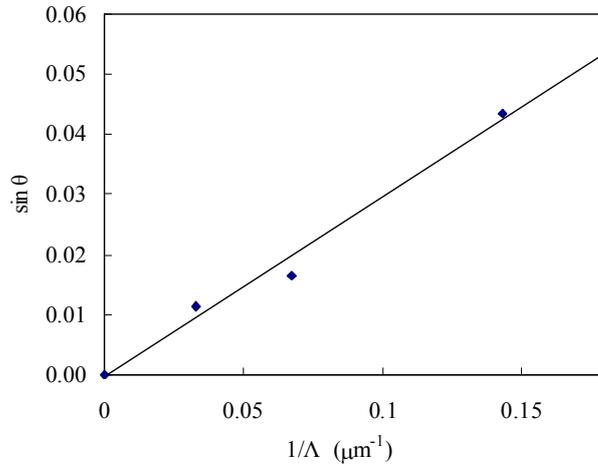
Fig. 3 Relation between distance of diffraction spot and 1/(interval between diffraction grating).
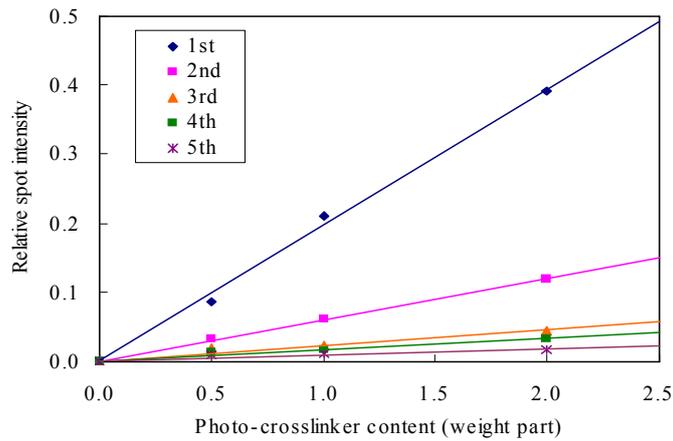
Fig. 4 Relation between diffraction spot intensity and photo-cross-linker content in polymer #1 for each order diffraction.

Figure 4 shows the linear relationship between intensities of each diffraction spot from 1st to 5th order and weight parts of photo-cross-linker in polymer #1 (the condition: $\Lambda = 15\,\mu m\ N_G = 40$). This result supports that the stripe-shape structure is formed through photochemical reaction in the area laser irradiated. The copolymer is transparent at the wavelength of 800 nm of fundamental laser beam, therefore one photon absorption at 800nm does not excite either copolymer or photo-cross-linker, triazine derivative, with maximum absorption wavelength of ca. 360 nm. However, in the case of femtosecond laser pulse irradiation, contribution of the multi-photons absorption to photo-excitation becomes larger and two-photon absorption excites photo-cross-linker to induce the photochemical cross-linking reaction.[14] Therefore we believe that two-photon photochemical reaction is significantly related to the stripe-shape structure.

Table 2. Results of transmission diffraction experiment

Sample No.	Q value	Maximum diffraction order	Sin θ	Diffraction efficiency (1 st order)	Refractive index change
			$(D_1/300)$	(%)	$(x10^3)$
#1	0.58	5 th	0.043	2.6	0.83
#2	0.58	2 nd	0.040	1.0	0.52
#3	2.7	7 th	0.095	6.5	1.4
#4	2.2	3 rd	0.069	3.5	0.61
#5	3.4	2 nd	0.097	2.6	0.71
#6	0.74	5 th	0.047	6.0	1.0
#7	0.34	7 th	0.047	3.7	1.8
#8	0.34	5 th	0.037	11	3.1
#9	1.6	2 th	0.095	4.7	2.0
#10	0.085	4 th	0.021	2.0	1.3
#11	2.6	2 nd	0.044	12	0.42
#12	9.2	1 st	0.073	3.0	0.20

Table 2 shows the experimental results of diffraction gratings (the notation of diffraction experiment number in Table 2 corresponds to diffraction grating structure number in Table 1). From Table 1 and Table 2, we confirm that larger Q value is, smaller the

maximum diffraction order became for sufficient diffraction spot intensity. It is said that Q is less than unity for Raman-Nath type diffraction and Q is larger than unity for Bragg type diffraction. However, it seems from the results in Table 2 that Q value should be larger than 5 to obtain perfect Bragg type diffraction. Obtained Q values, diffractive efficiencies, refractive index changes are ca. 0.1 - 9, ca. 1 – 13%, ca. $0.20 – 3.0 \times 10^{-3}$ respectively.

The optimization of the irradiation condition should be carried out to obtain complete Bragg type diffraction (thick grating). In this case, seven parameters, of PMMA content in co-polymer, photo cross-linker content in co-polymer (these parameters are concerned with co-polymer composition), magnification of objective lens, irradiation pulse energy, sample scanning rate (these parameters are concerned with dosed energy density), irradiated depth, distance between irradiated line (these parameters are concerned with uncertain effect) should be optimized. Robust design methodology developed in the field of quality engineering[15] was employed for the optimization.

Table 3. Controlling factors and levels in Robust design experiment

Controlling factor	(unit)	Level 1	Level 2	Level 3
PMMA content in co-polymer	(%)	50	70	-----
Photo cross-linker content in co-polymer	(weight part)	0.5	1.0	2.0
Magnification of objective lens	(X)	10	20	-----
Irradiated pulse energy	(nJ/pulse)	90	150	250
Sample scanning rate	(μm/s)	500	1000	750
Irradiated depth	(μm)	30	80	100
Distance between irradiated line	(μm)	7	10	15

We can seek and get effectively optimum material and fabrication conditions by carrying out limited number of experiments in the Robust design.[15] In Robust design,

controlling factors (seven parameters in this case) are selected in point of influence to get desired property (in this case thick grating) and levels of each controlling factor are conditions selected in the experimentally possible range by considering the results of preliminary experiments shown in Tables 1 and 2.

Table 4. Optimal condition by Robust design experiment

Controlling factor	(unit)	Optimal condition
PMMA content in co-polymer	(%)	50
Photo cross-linker content in co-polymer	(weight part)	2.0
Magnification of objective lens	(X)	10
Irradiated pulse energy	(nJ/pulse)	150
Sample scanning rate	(μm/s)	500
Irradiated depth	(μm)	100
Distance between irradiated line	(μm)	15

We selected seven parameters as controlling factors and selected levels for each controlling factor as listed in Table 3. The 18 experiments allotted by the levels of each controlling factor using L18 orthogonal array developed in Robust design[15] were carried out. The thickness of grating formed by laser irradiation is plotted as a function of dosed energy density calculated from irradiated power, sample scanning rate and irradiated spot radius (it depends on objective lens) for the 18 experiments selected by Robust design. As shown in Fig. 5, it was found that there is a threshold energy density to get diffraction grating and that thicker diffraction grating was obtained at relatively low energy region. The optimal condition to obtain thicker grating is shown in Table 4. Q value ($Q = 2\pi\lambda L/n\Lambda^2$) calculated with $\Lambda = 15$ μm, L = 170 μm and n = 1.485 is 2.6, which is a little bit lower for achieving Bragg type diffraction, narrower Λ of 7 μm experimentally controlled can be adapted.
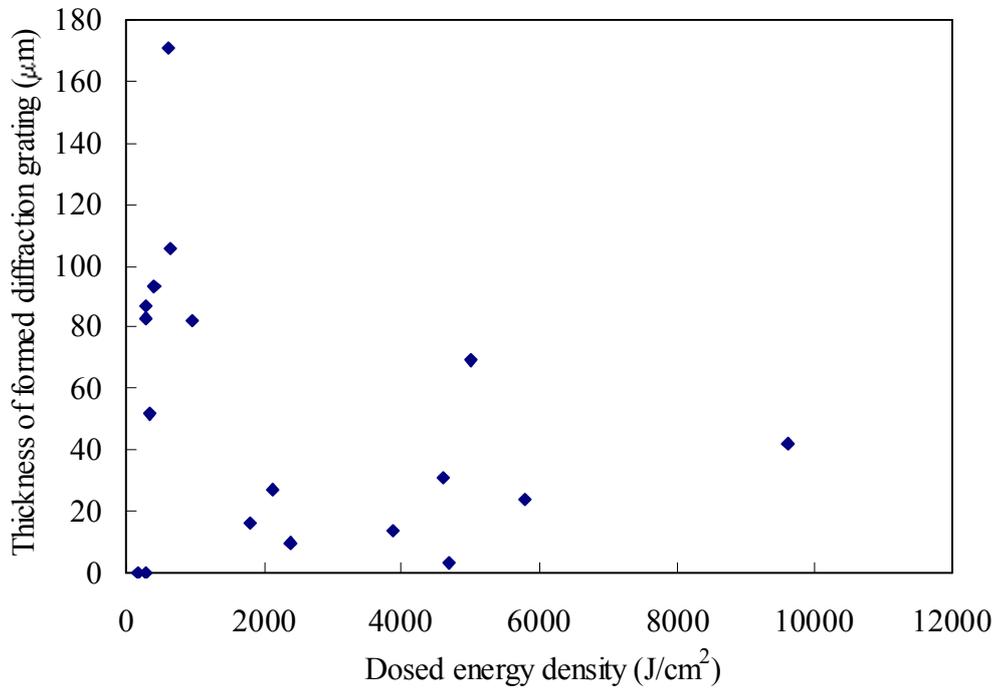
Fig. 5 Relation between thickness of diffraction grating formed and dosed energy density.

(a)   (b)
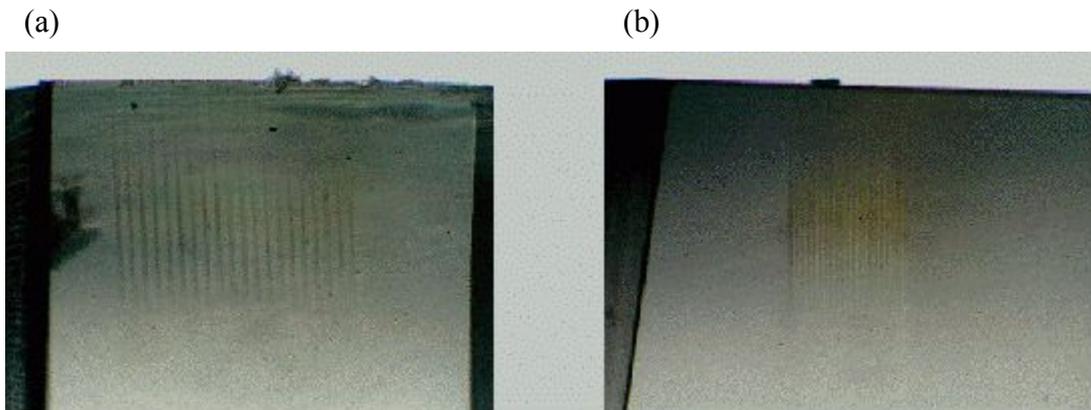
Fig. 6 Optical micrograph of diffraction grating (N_G=20).
(a) sample fabricated by the optimal condition : Λ=15 μ m
(b) sample fabricated with narrowest : Λ=7 μm

Figure 6 shows the comparison of the optical micrographs of diffraction grating (N_G = 20) induced by laser irradiation with Λ = 15 μm and with narrower Λ of 7 μm. As shown in Fig. 6, grating thickness is ca. 160 μm in both cases. The diffraction pattern of

each case is shown in Fig. 7. Second-order Raman-Nath type diffraction is observed for Λ = 15 μm and complete Bragg type diffraction for Λ = 7 μm. Table 5 summarizes the result of both diffraction experiments. The refractive index change was 0.30 – 0.31 x 10^{-3}.

  (a)   (b)
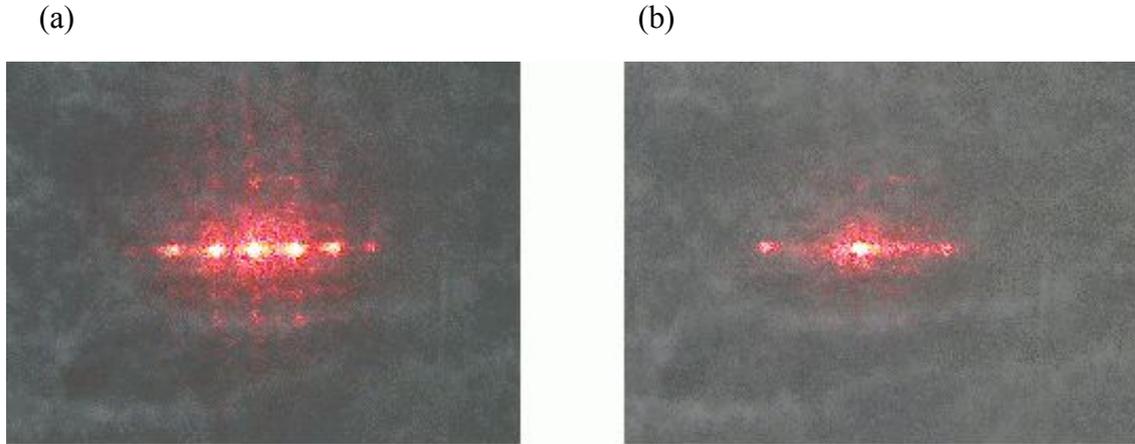
Fig. 7 Diffraction pattern photograph of sample fabricated by the optical condition and with narrowest Λ.
(a) sample fabricated by the optimal condition : Λ =15 μm
(b) sample fabricated with narrowest : Λ=7 μm

Table 5. Diffraction properties obtained by optimal condition using Robust design experiment

Sample No.	Grating thickness	Q value	Maximum diffraction order	Sin θ	Diffraction efficiency (1 st order)	Refractive index change
	(μm)			(D_1/300)	(%)	(x10^3)
No.1	161	1.9	2	0.042	5.9	0.31
No.2	160	8.7	1	0.097	5.5	0.30

Sample No.1: sample fabricated by optimal condition. (Λ=15 μm)
Sample No.2: sample fabricated with narrowest Λ.(Λ=7 μm)

Hirao *et al.* reported that multiple superimposed lines irradiation for Ge-doped silica glass produced the refractive index change larger (refractive index change increased 3.5 times after 10 superimposed lines irradiation).[9] We tried multiple lines (3 lines) irradiation for p-(MMA/EA-BA) block copolymer (polymer #1).

Figure 8 shows optical micrographs of diffraction grating ($N_G = 20$) induced by single line laser irradiation and that induced by the superimposed lines laser irradiation of 3 times. The thickness of grating was not changed by multiple superimposed lines irradiation, but the width of grating of the former seemed to be wider than that of the latter and color of lines of the latter changes black.
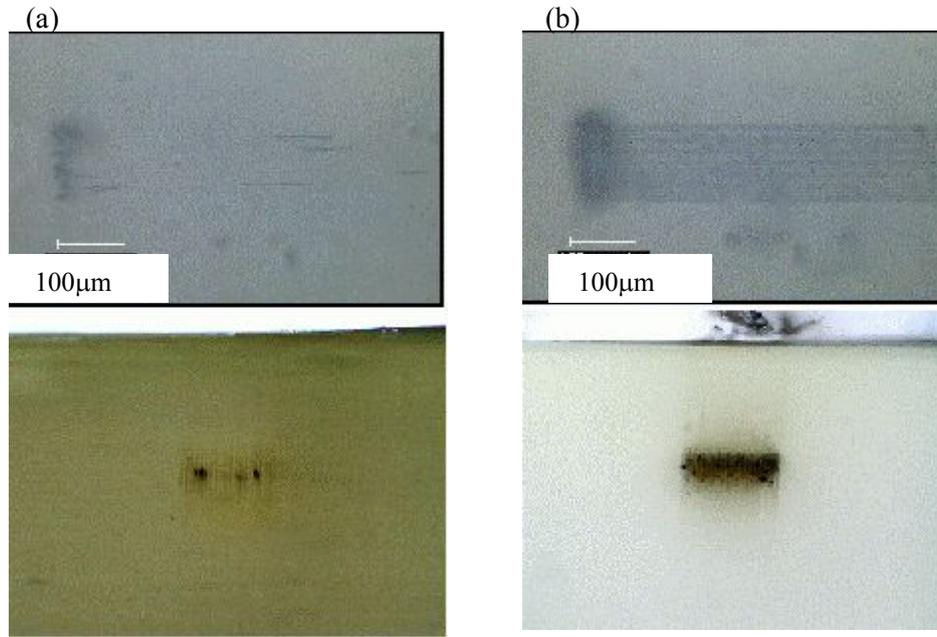
Fig. 8 Optical micrograph of diffraction grating fabricated by single and superimposed lines irradiation of 3 times.
(a) Single line irradiation   (b) Superimposed lines irradiation of 3 times

Table 6. Diffraction properties for single and multiple superimposed lines irradiation experiments

Sample No.	Grating thickness	Q value	Maximum diffraction order	Sin θ	Diffraction efficiency (1 st order)	Refractive index change
	(μm)			(D_1/300)	(%)	(x10^3)
No.1	84	4.6	1	0.093	1.7	0.30
No.2	72	3.9	2	0.092	13.5	1.1

Sample No.1: sample fabricated by single line irradiation.

Sample No.2: sample fabricated by multiple superimposed lines irradiation of 3 times.

As shown in Table 6, refractive index changes were 0.30 x 10^{-3} for single line irradiation and 1.1 x 10^{-3} for the superimposed lines irradiation of 3 times and the latter change is 3.7 times larger than the former one. We confirmed that multiple superimposed lines irradiation was effective to enlarge the refractive index change as inorganic glass materials. But color of the stripe structure created by the superimposed lines irradiation of 3 times changes black, suggesting some degradation or decomposition of the irradiated spots. Even though the possibility of some degradation, the superimposed lines irradiation with present energy condition might be favorable to enlarge the refractive index change. We convince that polymeric material also has a possibility for creating the ordered change of refractive index comparable to that in the order of 10^{-3} - 10^{-2} achieved in inorganic glass materials. [4,9)]

4-4 Conclusion

We carried out line irradiation of near-infrared (NIR) femtosecond laser pulse in block copolymers of methyl-methacrylate (MMA) and ethyl-acrylate-butyl-acrylate {p-(MMA/EA-BA)} and laser irradiation induced the aggregation of deposit with sub-micron scale which had different refractive index from un-irradiated region in the matrix. The shape of the deposit aggregation was changed by irradiated energy and adequate irradiated dosed energy density gave the ensemble of layers of stripe-shape structure which worked as diffraction grating. We evaluated obtained stripe-structure using diffraction measurement. We confirmed that transmission diffraction occurred on the basis of the linear relation of $\sin\theta$ vs. $1/\Lambda$. Linear relation between diffraction spot intensity vs. photo-cross-linker content for each order diffraction (for the condition of Λ = 15 μm N_G = 40) was observed. The Raman-Nath type and Bragg type transmission diffraction patterns which had ca. 1 – 13 % of diffraction efficiencies and ca. 0.1 - 9 of Q value were obtained and the refractive index change were calculated as ca. 0.20 – 3.0 x 10^{-3}. Optimized condition obtained using Robust design (Taguchi method) gave perfect Bragg type diffraction pattern with ca. 9 of Q value and 0.30 x 10^{-3} of refractive index change. It must be stressed here that Bragg type transmission diffraction grating can be formed *in situ* in desired place by irradiation of femtosecond laser pulse to these block copolymers. Furthermore, refractive index change can be cumulative by multiple superimposed lines irradiation as in the case of inorganic glass materials. Superimposed lines irradiation of 3 times produces the refractive index change in the order of 10^{-3}, which opens way for fabrication higher change of refractive index in the order of 10^{-3} - 10^{-2} in polymeric materials comparable to that in inorganic glass materials. Successive investigation to form strong Bragg type transmission diffraction grating with larger

change in refractive index is in progress.

References and notes

(1) W. J. Tomlinson, I. P. Kaminov, E. A. Chandross, R. L. Fork, W. T. Silfvast : Appl. Phys. Lett. **16** (1970) 486.

(2) K. Miura, J. Qiu, H. Inoue, T. Mitsuyu, K. Hirao: Appl. Phys. Lett. **71** (1997) 3329.

(3) Y. Kondo, J. Qiu, T. Miura, K. Hirao, T. Yoko: Jpn. J. Appl. Phys. **38** (1999) L1146.

(4) T. Toma, Y. Furuya, W. Watanabe, K. Ito, J. Nishii, K. Hayashi: Opt. Rev. **7** (2000) 14.

(5) Y. Kondo, T. Suzuki, H. Inoue, K. Miura, K. Hirao: Jpn. J. Appl. Phys. **37** (1998) 94.

(6) K. Hirao, K. Miura: Jpn. J. Appl. Phys. **37** (1998) 2263.

(7) K. Miura, H. Inoue, J. Qiu, K. Hirao: Nuclear Instruments and Methods in Physics Research **B141** (1998) 726.

(8) B. C. Stuart, M. D. Feit, A. M. Rubenchik, B. W. Sore, M. D. Perry: Phys. Rev. Lett. **74** (1995) 2248.

(9) K. M. Davis, K. Miura, N. Sugimoto, K. Hirao: Opt. Lett. **21** (1996) 1729.

(10) E. N. Glezer, M. Milosavljevic, L. Huang, R. J. Finlay, T. H. Her, J. P. Callan, E. Mazur: Opt. Lett. **21** (1996) 2023.

(11) S. Katayama, M. Horiike, K. Hirao, N. Tsutsumi: J. Polym. Sci. Part B: Polym. Phys.**40** (2002) 537.

(12) H. Kogelnik: Bell. Syst. Tech. J. **48** (1969) 2909.

(13) P. Yeh in "Introduction to Photorefractive Nonlinear Optics", (Wiley Intersciece, New York, 1993) p. 61 – 65.

(14) J. P. Allison: J. Polym. Sci. A-1. **4** (1966) 1209.

(15) T. Adachi: J. Imag. Soc. Jpn. (Japanese) **39** (2000) 116.

Chapter 5: Grating structures induced by irradiation of NIR femtosecond laser pulse in dyed polymeric materials and diffraction measurement of those structures

5-1 Introduction

In previous Chapter, the stripe-shape layered structures produced by the assembled deposit induced the modulation of refraction index in P-(MMA/EA-BA) block copolymer, which was evaluated using a transmission diffraction measurement.[14] We obtained a perfect Bragg type diffraction pattern with refractive index modulation of approximately 0.30 x 10^{-3}.[14] In our previous investigations,[13,14] it has been found that additives, such as cross-linking agent, sensitizer and dyes played an important roll for the structures induced by the irradiation of NIR femtosecond laser.

In this Chapter, we investigate the effect of dye doped in the polymer matrix on the structures induced by NIR femtosecond laser pulse irradiation and discuss the relation between the induced structures and the photo chemical and physical properties, including two-photon excitation by NIR femtosecond laser pulsing, of dyes doped polymer systems.

5-2 Experimental

Irradiation system and methods of observation were same as described in Chapter 2. The diffraction measurement was carried out by the method described in Chapter 2 and Chapter 4..

Structural formulae of polymer samples used for the laser irradiation are summarized in Fig. 1. The polymers, PMMA (Mitsubishi Rayon), thermoplastic epoxy resin (Epoxy) (Tohto Kasei) commercially available were used. P-(MMA/EA-BA block copolymer) was prepared in our laboratory using a living-radical polymerization. The detailed procedures for the preparation were reported in previous paper.[13] Structural formulae of dyes used are summarized in Fig. 2. Dye samples used are classified into two types of type 1 and type 2. Type 1 dyes are BTAPVB (Tokyo Kasei Kogyo), Azo dye, DR 1 (Mitsubishi Chemical), 9,10-diphenyl-anthracene (DPA) (Tokyo Kasei Kogyo) and 9,10-dibromo-anthracene (DBA) (Tokyo Kasei Kogyo) with absorption at 400 nm, and type 2 dye is anthracene (Tokyo Kasei Kogyo) with no absorption at 400 nm. 1 weight part of dye and 100 weight parts of polymer were dissolved in proper weight of ethyl acetate for PMMA and P-(MMA/EA-BA) block copolymer, THF for Epoxy to make 30 wt% solution. 1 weight part of triazine derivative as a photo-crosslinker (maximum absorption wavelength of triazine derivative is approximately 360 nm) was

added to 100 weight parts of P-(MMA/EA-BA) block copolymer. Approximately 500 μm thick films were prepared by casting the polymer solution onto a glass substrate and subsequent evaporating the solvent.

(a) PMMA

(b) Thermo-plastic epoxy resin

(c) p-(MMA/EA-BA) block copolymer
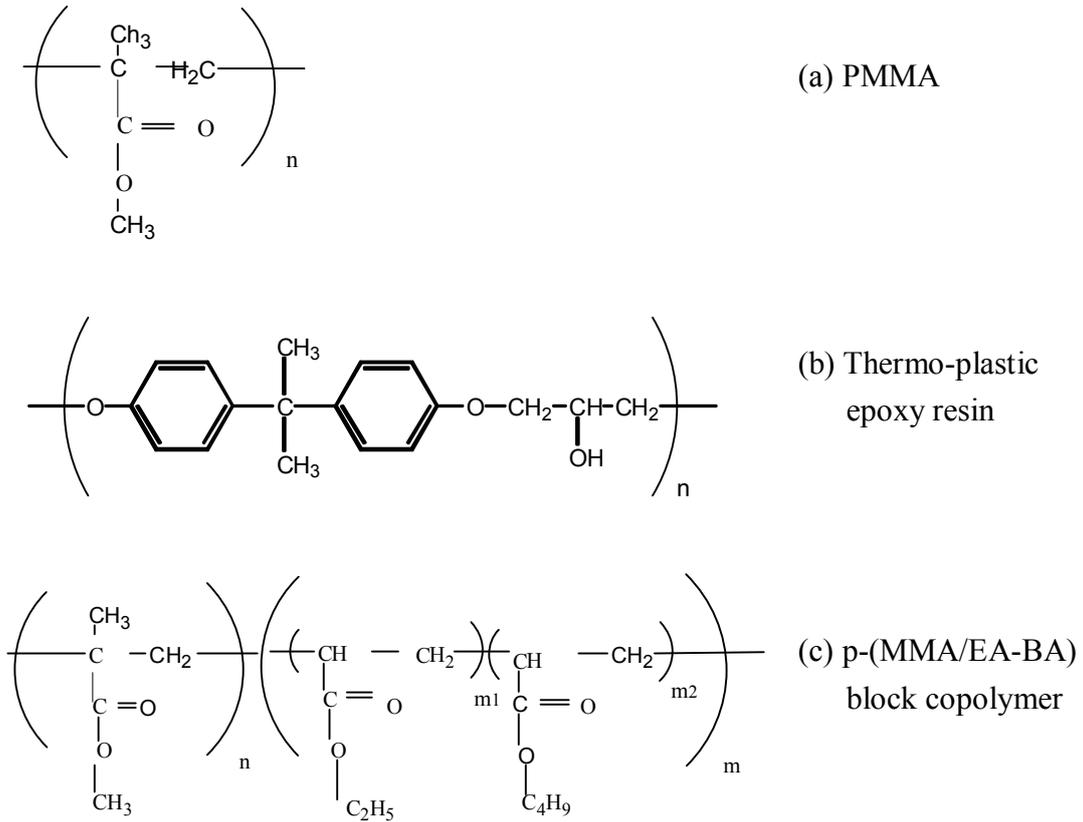
Fig. 1 Structural formulae of polymers used in this study.

(a) BTAPVB

(b) Azo dye

(c) Anthracene

(d) Di-phenyl anthracene (DPA)

(e) Di-bromo anthracene (DBA)

(f) DR 1
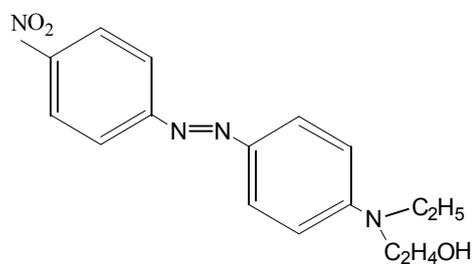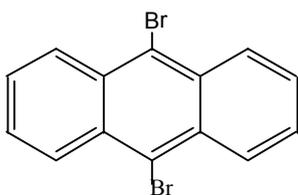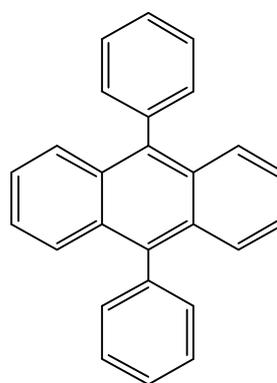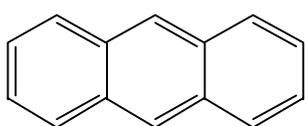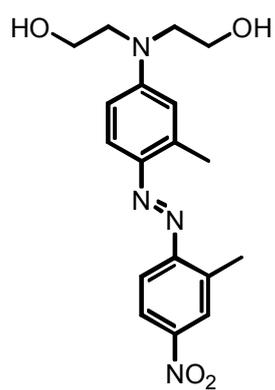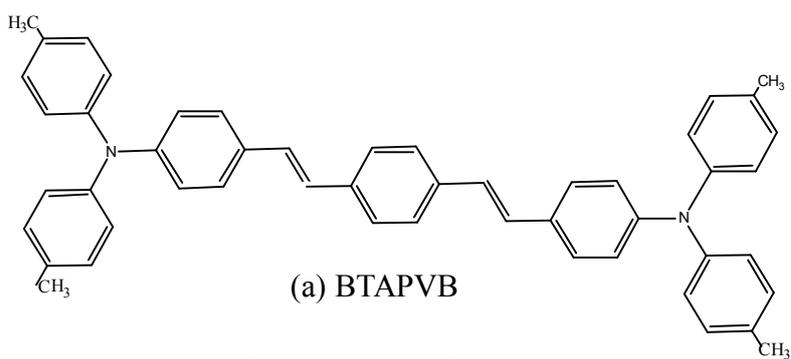
Fig. 2 Structural formulae of dyes used in this study.

5-3 Results and Discussion

In our previous papers,[13,14] we reported that only thinner grating structures with voids and cracks in PMMA were induced by the line irradiation of femtosecond laser pulse whereas laser irradiation to P-(MMA/EA-BA) block copolymer which contained 0.5-2.0 weight parts of triazine derivative as a photo-crosslinker (maximum absorption wavelength of the triazine derivatives is approximately 360 nm) to 100 weight parts of the block copolymer gave the aggregation of deposit with sub-micron scale developed from the focused point to the direction of laser propagation. Furthermore, the variation of irradiation energy to P-(MMA/EA-BA) block copolymer with triazine derivative changed the induced structures. Since P-(MMA/EA-BA) block copolymer and PMMA has the same chemical structures as shown in Figure 1, one could expect the same kind of structures as in P-(MMA/EA-BA) block copolymer would be induced in PMMA matrix. Preliminary experiments of the line irradiation were carried out for dyed P-(MMA/EA-BA) block copolymer and dyed PMMA. First, BTAPVB (laser dye) and Azo dye (nonlinear optical dye) were selected. Then femtosecond laser pulse was irradiated for dye doped PMMA and P-(MMA/EA-BA) block copolymer films with irradiation condition as follows: the irradiated depth, 30 μm (target depth); objective lens, X10; pulse energy, 165 nJ/pulse; sample scanning rate, 500 μm/s; line interval, 20 μm; number of lines, 20 lines.

Figure 3 and Figure 4 are optical micrographs (transmission patterns) of cross-section of grating structures induced by laser irradiation for P-(MMA/EA-BA) block copolymer and PMMA, respectively.
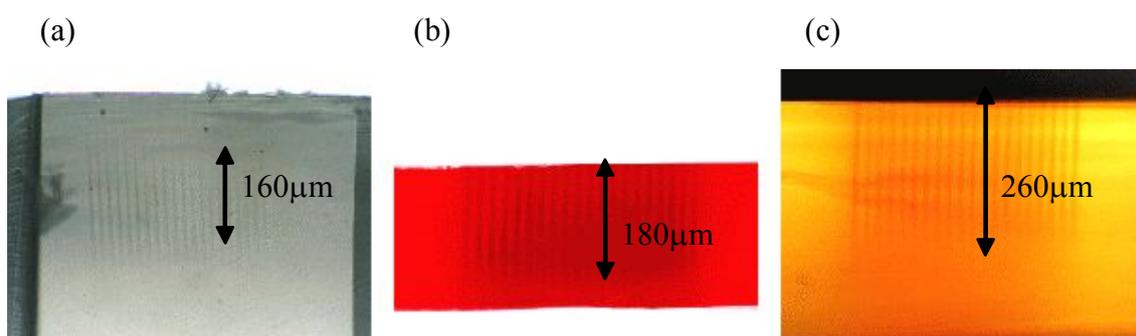
(a)   (b)   (c)

Fig. 3 Optical micrograph of grating structure induced by laser irradiation for p-(MMA/EA-BA) block copolymer. (a) copolymer without dye (b) Azo dye doped copolymer (c) BTAPVB doped copolymer.
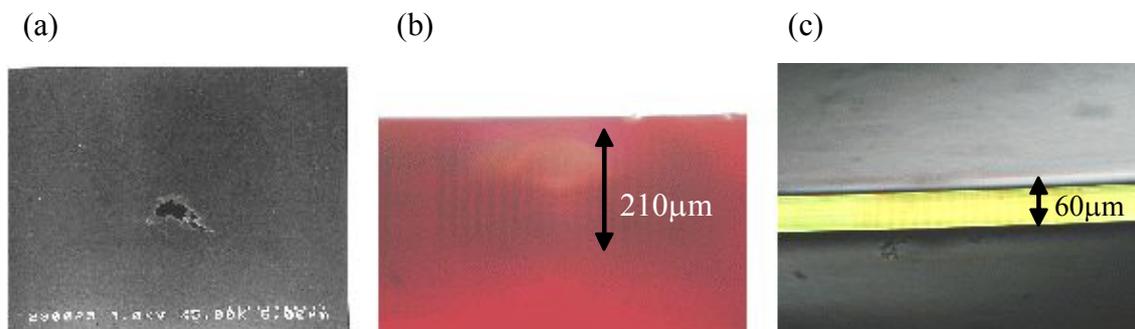
(a)   (b)   (c)

Fig. 4 Optical micrograph of grating structure induced by laser irradiation for PMMA. (a) PMMA without dye (b) Azo dye doped PMMA (c) BTAPVB doped PMMA.

The absorption properties of the induced structures differ from those in the un-irradiated region and it caused the slight dark stripe image. Longer line structures, thicker grating structures, were grown for dyed P-(MMA/EA-BA) block copolymer films as shown in Fig. 3 (b) and (c). Thicker grating structures were also observed for dyed PMMA as shown in Fig. 4. It is noted that higher pulse energy of 165 nJ/pulse is favored for the formation of grating structure in dyed PMMA. Whereas, the irradiation with 90 nJ/pulse, 115 nJ/pulse, 150 nJ/pulse to un-dyed PMMA caused only voids and cracks. It is confirmed that the energy dissipation through dyes plays an important role for producing these line structures. Next question is what kind of dissipation process should be considered for the formation of line structures. Dyes used above have absorption at 400 nm equivalent to the energy gap of two-photon excitation. We selected fluorescence dyes of anthracene with no absorption at 400 nm and DPA and DBA with absorption at 400 nm. DPA has high fluorescence quantum yield nearly unity and DBA has low fluorescence quantum yield less than 0.5. Additionally DR1 is selected as nonlinear optical dye with absorption at 400 nm (type 1 dye). Irradiation condition was as follows: the irradiated depth, 30 μm (target depth);objective lens, X10; pulse energy, 155 nJ/pulse; sample scanning rate, 500 μm/s; line interval, 20 μm; number of lines, 20 lines.

Figure 5 shows an optical micrograph (transmission patterns) of cross-section of induced structures for various dye doped PMMA. Anthracene doped PMMA gave voids and cracks as un-dyed PMMA. Rather longer line grating structures with a few voids and cracks were induced in DPA doped PMMA. Clear line structures with a fewer voids and cracks were induced in both DBA doped PMMA and DR 1 doped PMMA. As shown in Fig. 5, DR 1 doped PMMA had longer line structures, thicker grating

51

structures. On the contrary, the line irradiation for dye doped Epoxy gave voids in both case of type 1 and type 2 dyes. PMMA and P-(MMA/EA-BA) block copolymer have esteric moiety which is electron acceptor property and Epoxy has not. Obtained different results between PMMA, P-(MMA/EA-BA) block copolymer and Epoxy matrix polymers are supposed to be related to the difference of electron acceptor properties.
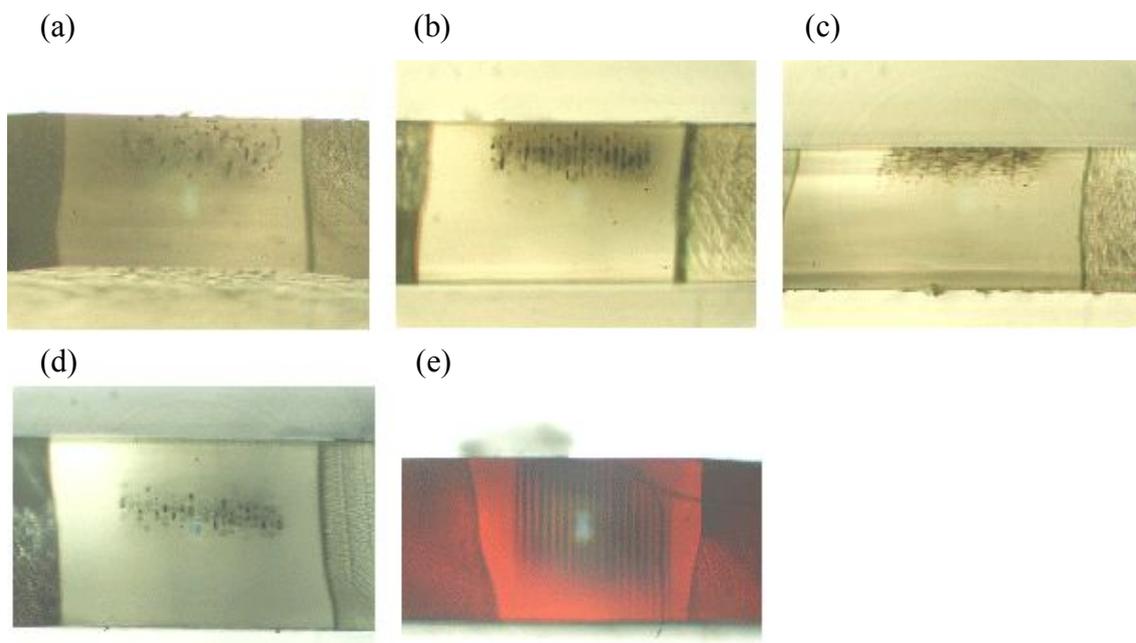
(a)

(b)

(c)

(d)

(e)

Fig. 5 Optical micrograph of structures induced by laser irradiation for PMMA. (a) PMMA without dye (b) DPA doped PMMA (c) Anthracene doped PMMA (d) DBA doped PMMA (e) DR 1 doped PMMA.

The presented structures induced by the femtosecond irradiation were supposed to be related to the excitation including multi-photon excitation and fluorescence properties of added dyes. Typical absorption and fluorescence spectra are shown in Fig. 6 and 7, respectively. Type 1 dyes of DPA, DBA and DR 1 have absorption at 400 nm with coefficient in the order of DR1 > DBA > DPA, which corresponds to the two-photon excitation by the pulse laser. Absorbed energy was dissipated via radiative transition process (fluorescence) and non-radiative transition process. As for the type 1 dyes, fluorescence intensities excited at 400 nm are as follow; DPA > DBP >> DR 1 ~ 0 as shown in Fig. 7. It is found that larger absorption coefficient at 400 nm and lower fluorescence efficiency of dyes is favored for the formation of induced line structures in dyed PMMA. Laser irradiation gave rise to the distinct decrease of infrared absorption

of carbonyl group at 1713 cm^{-1} even for PMMA containing DR1 dye which might have possibility of cis-trans isomerization by absorption of wavelength at 400 nm. Photoisomerization and chemical reaction might competitively be occurred in DR1 doped polymers. Supposedly the photo-crosslinking would be occurred in dyed PMMA as in the case of P-(MMA/EA-BA) block copolymer reported in our previous paper.[14]
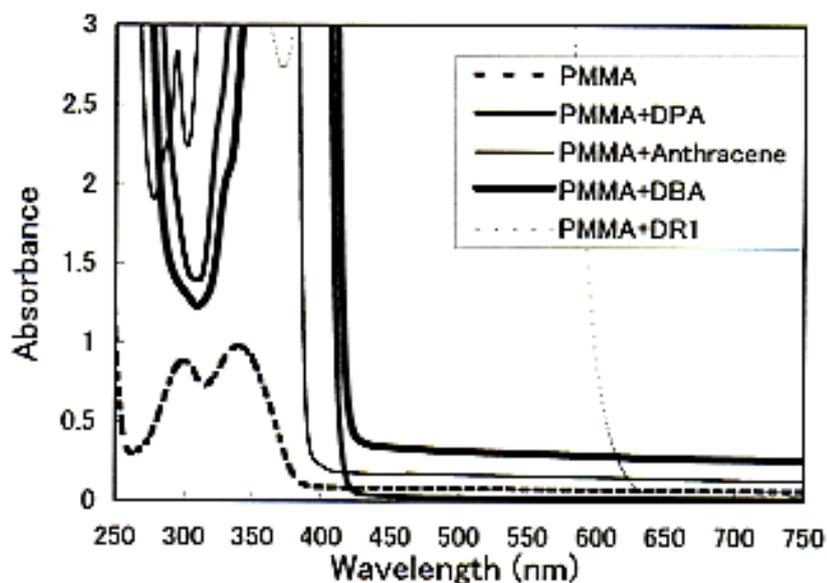
Fig. 6 Absorption spectra of PMMA and dye-doped PMMA samples.
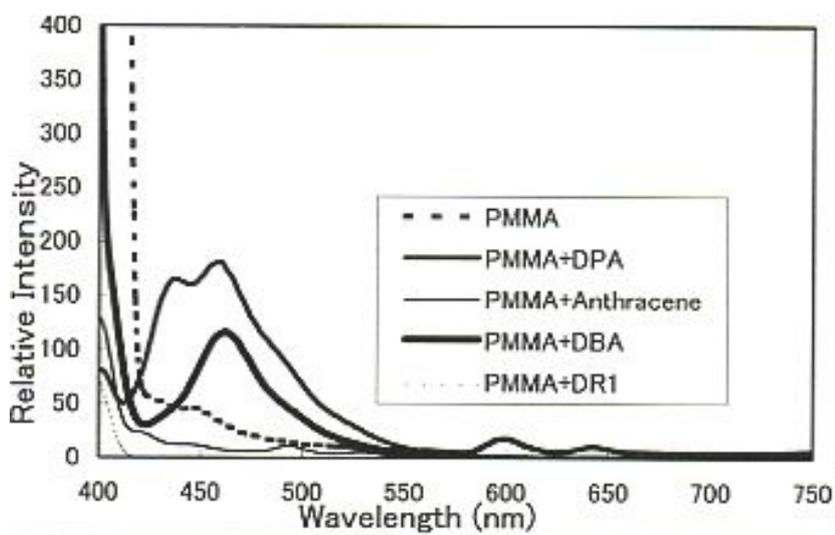
Fig. 7 Fluorescence spectra of PMMA and dye-doped PMMA samples (excitation wavelength: 400 nm).

These results would propose a new methodology of formations of the controlled structures of polymeric materials by short-pulse laser pulse irradiation and might give an information for the control and the protection of photo-chemical damage in polymer materials by laser irradiations.

The obtained line structures are worked as a transmission diffraction grating. The transmission diffraction properties of those grating structures were measured for dyed block copolymer (refractive index n: 1.485) and dyed PMMA (refractive index n: 1.493). The thickness of grating (L) and the interval between two gratings (Λ) were measured by an optical micrograph of cross-section of grating structures. The Q value was calculated using L, Λ, n and wavelength (λ) of incident beam (He-Ne laser) in equation (3) and the transmission diffraction efficiency was calculated using equation (1) with the diffraction intensity obtained by the diffraction measurement and the modulation of refractive index, Δn, was calculated using equation (2) with an obtained diffraction efficiency as described in previous chapter.. Typical data were shown in Table 1.

Table 1. Transmission diffraction measurement data of dye doped P-(MMA/EA-BA) block copolymer and PMMA.

Sample	Thickness of induced grating ($\square$m)	Refractive index change ($\times 10^3$)	Q value	Diffraction efficiency (1storder) (%)
1. P-(MMA/EA-BA) block copolymer +				
1) Azo dye	180	1.1	1.2	43
2) BTAPVB	255	0.45	1.7	24
2. PMMA +				
1) Anthracene	------	------	------	----
2) DPA	121	1.1	0.8	24
3) DBA	113	1.1	0.7	27
4) DR 1	344	0.45	2.3	48

The Q value were approximately 1-2 and larger Q value for Bragg diffraction (Q>5) can be obtained by narrowing the interval between each diffraction grating (Λ) as previously reported.[14] The diffraction in this case is caused by the index modulation and the absorption modulation due to the induced structures. It is noted that Δn estimated here includes both effects, because of the difficulty of separate estimation of both effects. The Δn due to the index modulation should be smaller. Line structures induced in dye doped PMMA gave approximately 25-50 % diffraction efficiencies, and the diffraction efficiencies did not change at all after the storage for 3 months at room temperature. We expect that these structures may work as optical devices such as a beam splitter in wave-guide.

5-4 Conclusion

The structures induced by the irradiation of NIR femtosecond laser pulse were investigated in dye doped polymeric materials; PMMA, Epoxy and P-(MMA/EA-BA) block copolymer. PMMA and P-(MMA/EA-BA) block copolymer showed a dye additive effect in which dyes having absorption at 400 nm (two-photon absorption of irradiated femtosecond laser pulse) and lower fluorescence quantum yield favored for the formation of thicker grating structures. To the contrary, Epoxy did not show the dye additive effect. The mechanism of the dye additive effect phenomenon for PMMA and P-(MMA/EA-BA) block copolymer was discussed on the basis of two-photon excitation (absorption) by dye at 400 nm and the following non-radiative transition process of the absorbed energy to polymer matrix which lead to the photo-degradation and photo-cross-linking of PMMA. We measured the transmission diffraction property of the grating structures induced by the irradiation of femtosecond laser pulse and confirmed that they are useful to be a transmission diffraction grating. Results obtained would pave the way for new methodology of short-pulse laser irradiation for the production of polymeric optical device and might be useful for the control and the protection of photo-chemical damage in polymer materials by laser irradiation.

References and notes
(1)   W. J. Tomlinson, I. P. kaminov, E. A. Chandross, R. L. Fork, W. T. Silfvast: Appl. Phys. Lett. **16** (1970) 486.
(2)   K. Miura, J. Qiu, H. Inoue, T. Mitsuyu, K. Hirao: Appl. Phys. Lett. **71** (1997) 3329.
(3)   Y. Kondo, J. Qiu, T. Miura, K. Hirao, T. Yoko: Jpn. J. Appl. Phys. **38** (1999) L1146.

(4) T. Toma, Y. Furuya, W. Watanabe, K. Ito, J. Nishii, K. Hayashi: Opt. Rev. **7** (2000) 14.

(5) Y. Kondo, T. Suzuki, H. Inoue, K. Miura, K. Hirao: Jpn. J. Appl. Phys. **37** (1998) 94.

(6) K. Hirao, K. Miura: Jpn. J. Appl. Phys. **37** (1998) 2263.

(7) K. Miura, H. Inoue, J. Qiu, K. Hirao: Nuclear Instruments and Methods in Physics Research **B141** (1998) 726.

(8) B. C. Stuart, M. D. Feit, A. M. Rubenchik, B. W. Sore, M. D. Perry: Phys. Rev. Lett. **74** (1995) 2248.

(9) K. M. Davis, K. Miura, N. Sugimoto, K. Hirao: Opt. Lett. **21** (1996) 1729.

(10) E. N. Glezer, M. Milosavljevic, L. Huang, R. J. Finlay, T. H. Her, J. P. Callan, E. Mazur: Opt. Lett. **21** (1996) 2023.

(11) H. B. Sun, S. Matsuo, H. Misawa: App. Phys. Lett. **74** (1999) 786.

(12) S. Kawata, H. B. Sun, T. Tnaka, K. Takada: Nature. **412** (2001) 697.

(13) S. Katayama, M. Horiike, K. Hirao, N. Tsutsumi:J. Polym. Sci. Part B. **40** (2002) 537.

(14) S. Katayama, M. Horiike, K. Hirao, N. Tsutsumi: Jpn. J. Appl. Phys. **41** (2002) 2155.

(15) H. Kogelnik: Bell Syst. Tech. J. **48** (1969) 2909.

(16) P. Yeh: Introduction to Photorefractive Nonlinear Optics; Wiley-Interscience: New York, (1993) 61-65.

Chapter 6: Upheaval structures on the surface induced by irradiation

of NIR femtosecond laser pulse in polymeric materials and application for micro-lens of those structures

6-A Laser molding in polymeric materials using NIR femtosecond laser pulse and replication via electroforming

6-A-1 Introduction

In Chapter 3, we confirmed that the structures induced by line irradiation which was performed by scanning a laser spot in polymer bulk significantly depend on T_g of polymers and two unique induced structures were found; the first one is stripe-shaped induced structure composed of assemble of aggregated deposits with sub-micron size and the other one is upheaval induced structure. The former was investigated in detail in Chapter 4. We were also interested in the formation of the periodic upheaval structures in the polymeric materials which had not been reported in literature for inorganic materials. We were also interested in a possibility of mass-production of the periodic upheaval structures on the polymer surface by replication method.

Micro-machining technology has greatly developed recently and broad application of that technology to electrical, optical and mechanical fields has been investigated. The Lithographie, Galvanoforming and Abformtechnik (LIGA) process developed at the Karlsrule Nuclear Research Center is one of the most promising micro-machining technologies and is composed of deep x-ray lithography (DXL), electroforming (electroplating) and molding.[12,13] The LIGA process has the advantage of being able to mass-produce micro structures up to several hundred μm in size. We recognized this ability and the possibility of this process to replicate the upheaval structure of polymers.

In this Chapter, we investigated the formation of the upheaval structures in polymer materials induced by NIR laser irradiation and the possibility of mass-production of the structures on the polymer surface by replication method using electroforming and molding (pseudo-LIGA process).

6-A-2 Experimental

Irradiation system was same as described in Chapter 2. The upheaval structures on the surface of the polymer materials induced by the pulse laser irradiation were observed through an optical interference microscope. The cross section was observed through both an optical microscope and a scanning electron microscope (SEM). The micro-lens effect of the upheaval structure was checked by He-Ne laser beam irradiation from the backside of the structure and by observing the focused beam. The polymer samples used for laser irradiation are commercially available polycarbonate (PC) (Teijin

Chemicals, Ltd.), polyether imide (PEI) (GE Plastics Japan Ltd.), poly(acrylonitrile-styrene) (AS) copolymer (Nippon A&L Inc.), and poly (acrylonitrile-butadiene-styrene-methyl metacrylate) (ABSM) copolymer (Nippon A&L Inc.). A PC sheet sample approximately 0.5 mm thick and a PEI sheet approximately 2 mm thick were used without any additional processing. AS and ABSM copolymer films approximately 500 mm in thickness were cast onto glass substrates from 30 wt% THF solution and 15 wt% acetone solution, respectively.

The periodic upheaval structure on the surface of PC induced by NIR pulse laser irradiation was electroformed. First, a non-electrolytic plating of Ni was carried out to obtain pre-coated samples approximately 1 μm in thickness followed by an electrolytic plating of Ni using pre-coated samples as negative electrode and Ni plate as positive electrode in a nickel sulfamic acid plating bath. Finally, coated samples with Ni of approximately 36 μm in thickness were formed as an electroformed mother mold. These electroforming processes occur as follows.

1) Degrease.
2) Etching.
3) Neutralization.
4) Surface adjustment (cationic adsorption).
5) Deposition of catalyst.
6) Activation of catalyst.
7) Non-electrolytic plating of Ni.
8) Electrolytic plating of Ni.

The process of the fabrication of a mother mold is shown in Fig. (1a - 1d). The chemicals used for non-electroplating and electroplating processes were commercially available products from Okuno Chemical Industries Co., Ltd. Molding was carried out by potting AS copolymer dissolved in THF solution (approximately 30 wt%) into the electroformed mother mold and then evaporating the solvent. The replicated sample, of molded AS copolymer was removed from the electroformed mother mold. The process of replication is shown in Fig. (1e - 1f).
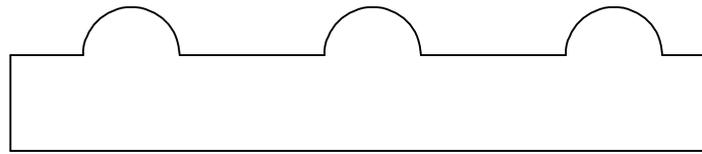
(a) Original bell-shaped structure by laser irradiation.
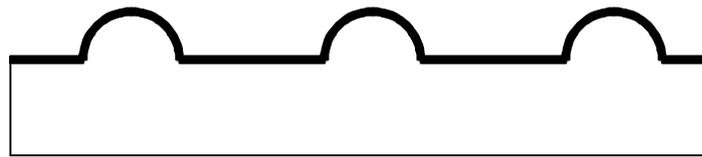
(b) Non-electrolytic plating of Ni.
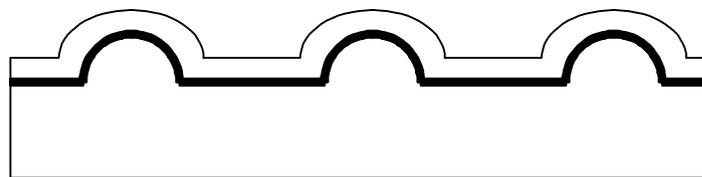
(c) Electrolytic plating of Ni over pre-coated Ni.
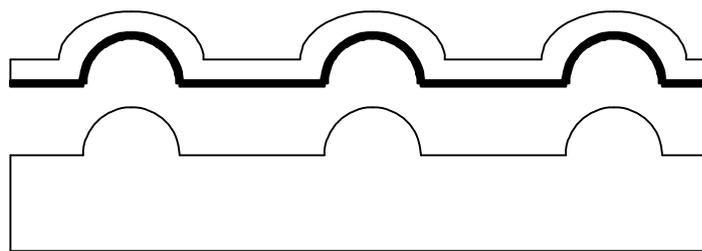
(d) Removal of the mother mold from original bell-shaped
    structure.
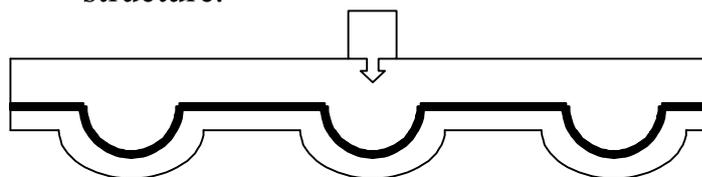
(e) Potting molding material into the mother mold.
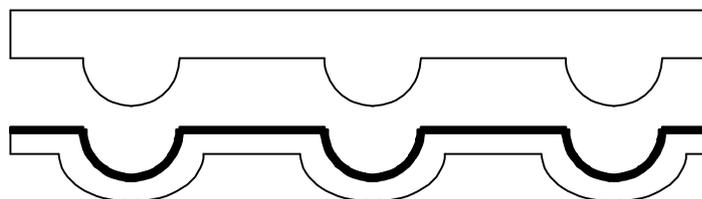
(f) Removal of replicated upheaval structure from the mother
    mold.

Fig. 1 The processes of fabrication of the mother mold and replication
of bell-shaped structure.

6-A-3 Results and Discussion

Line irradiation in PC, PEI, AS copolymer and ABSM copolymer were carried out under the following conditions: target depth, 60 μm; objective lens, 20X; scanning rate, 100 μm/s. Irradiation energies optimally selected for each polymer to obtain the upheaval structures under in situ observation were 150 nJ/pulse for PC, 90 nJ/pulse for PEI, 175 nJ/pulse for AS, and 180 nJ/pulse for ABSM. The shape, average diameter of the basal plane and height of the induced upheaval structures are shown in Table 1.

Table 1. Induced upheaval structures by irradiation with femto-second pulse laser for PC, PEI, AS, ABSM.

Sample	Shape	Diameter (μm)	Height (μm)
PC	Bell-shape	45	8
PEI	Bell-shape	18	10
AS Copolymer	Flat-top upheaval	47	18
ABSM Copolymer	Flat-top upheaval	41	20

Figure 2 is an optical micrograph of an upheaval structure of PC induced by another irradiation condition: target depth, 50 μm; objective lens, 10X; scanning rate, 500 μm/s. Irradiation energy, 150 nJ/pulse. The average diameter of the basal plane of this upheaval structure was 21.6 μm with standard deviation (σ) of 1.4 μm（number of measured samples, 100）.
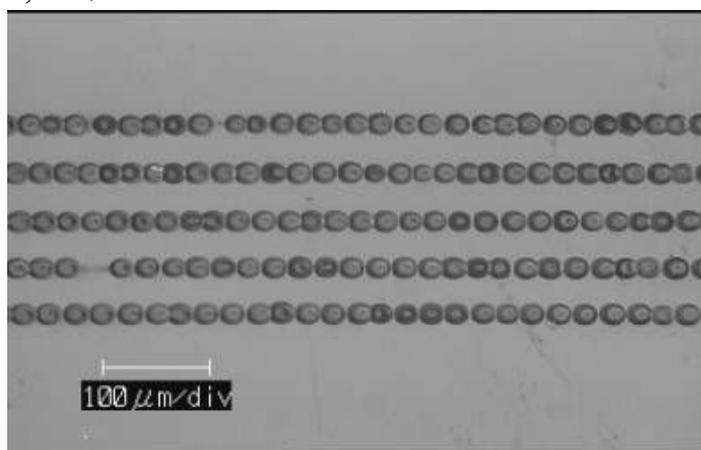
Fig. 2 An optical micrograph of a bell-shaped upheaval of PC.

Figures. 3a and 3b are optical micrographs of the upheaval structures of ABSM copolymer and AS copolymer, respectively; Figure 4a and 4b are SEM micrographs of front view and cross sectional view of the upheaval structure of ABSM copolymer, respectively.
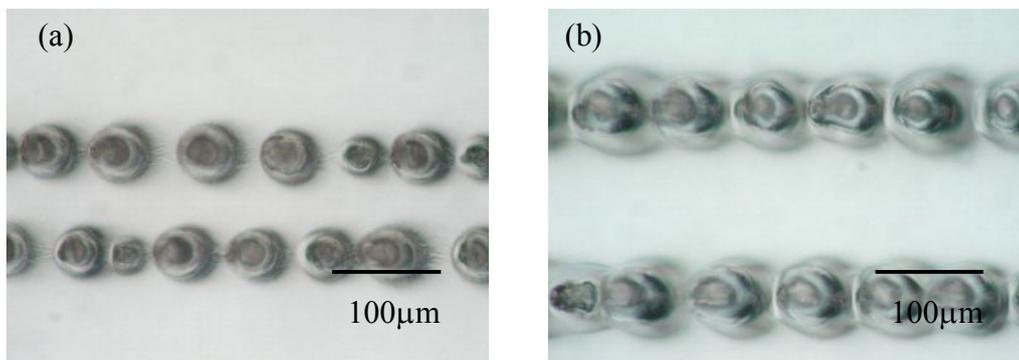
Fig.3 Optical micrographs of upheaval structures of (a) ABSM copolymer and (b) AS copolymer.
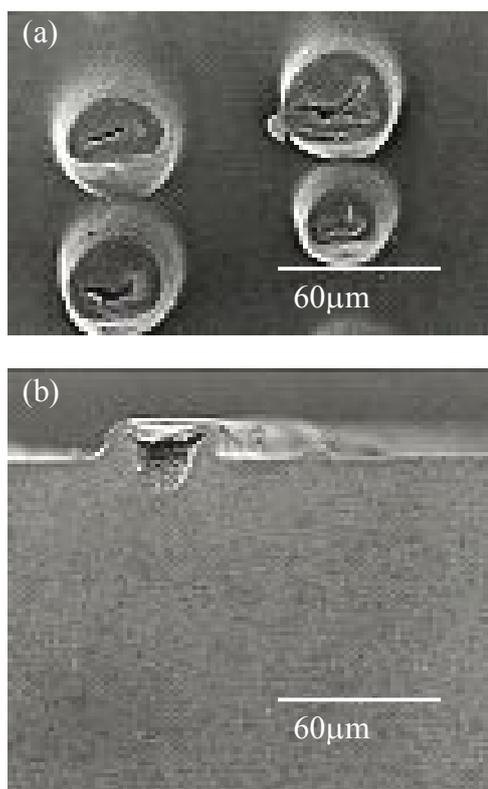
Fig. 4 SEM micrographs of upheaval structure of ABSM copolymer.
(a) Front view. (b) Cross sectional view.

As shown in Figs. 3 and 4, AS copolymer and ABSM copolymer samples showed periodic upheaval structures with a flattop. The upheaval structure induced on the surface of PC in Fig. 2 was bell-shaped as described in our previous report.[10] The mechanism of the formation of these upheaval structures in polymers with relatively high T_g's was described earlier as follows: cracks or voids due to abrupt thermal expansion to surrounding region are generated at the irradiated spot and move toward the surface along the microscopic thermal gradient from the irradiated spot to the surface region, but they are unable to spread out on the surface because of higher viscosity of the matrix and uphold the surface.[10] In the case of ABSM copolymer and As copolymer with a relatively lower T_g component than PC, expanded volumes around the surface were larger and the micro-cracks nearly reached the surface during the mobilized condition; mobile micro-cracks broke the thin surface layer and the flat-top structure might have been formed.

As shown in Fig. 4b, voids were observed in the upheaval structure just beneath the surface and seemed to uphold the structure on the surface and to interconnect to form a flattop, just like the crater of a volcano. The mobility of the polymer chain was assumed to play an important role in the formation of the upheaval structures.

The bell-shaped upheaval structure without a flattop in the PC sample showed a micro-lens effect but ABSM copolymer and AS copolymer samples with a flattop did not. The periodic bell-shaped upheaval structure in the PC sheet was replicated using electrolytic plating. Non-electrolytic plating of Ni approximately 1 mm in thickness was deposited on the surface of the bell-shaped upheaval structure in PC, and then Ni of electrolytic plating approximately 36 mm thick was overlaid onto the surface of the pre-coated Ni non-electrolytic plating layer. The PC sheet with the bell-shaped upheaval structure was removed from the electroformed Ni mold and the electroformed mother mold was reproduced as shown in Fig. 1(d).
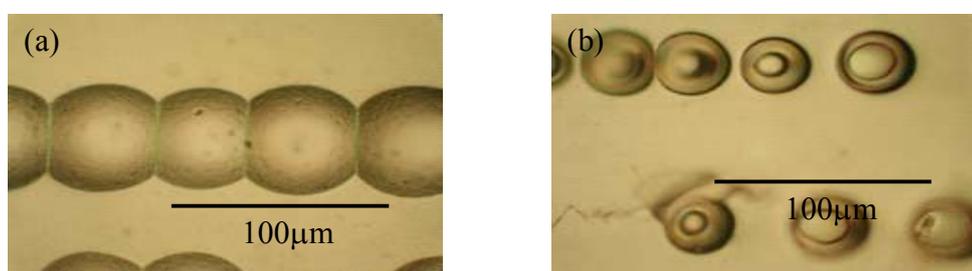
Fig. 5 Optical micrographs of the mother mold obtained by the electroforming process. (a) Front view. (b) Back view.

62

Figure 5 shows optical micrographs of the mother mold obtained by the electroforming process. Finally, the bell-shaped upheaval structures were replicated by potting approximately 30wt% THF solution of AS copolymer into the electroformed Ni mother mold, evaporating the solvent and then removing it from the mother mold as shown in Fig. 1(f). Our replication method using the pseudo-LIGA process has the following advantages: non-selectivity of original polymer materials and structures for fabrication of the mother mold, sufficient toughness of the mother mold to repeat the replication, non-selectivity of replicated material and adequate precision in replication. The size of the upheaval structure in an original PC and the corresponding replicated AS copolymer were, for example, 23.8 μm and 23.5 μm in diameter of the basal plane and 4.5 μm and 4.9 μm in height, respectively. We confirmed that the replica was reproduced with sufficient precision. Figure 6 shows a micrograph of the transmission image of the replicated upheaval structure by potting the AS copolymer. As shown, we could obtain the replica of the bell-shaped upheaval structure in PC by potting a different polymer material. In the case of laser molding, AS copolymer showed the upheaval structure with the flattop but we were able to obtain the bell-shaped upheaval structure without the flattop of As copolymer by replication via electroforming.
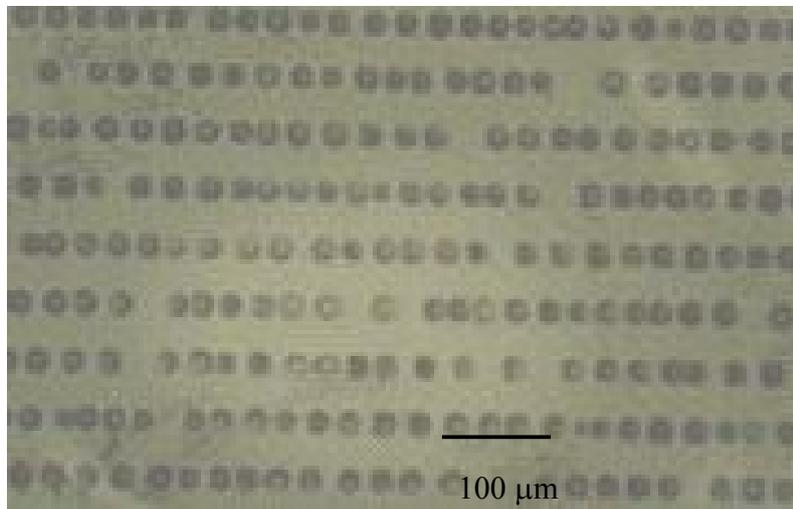
Fig. 6 Optical micrograph of replicated bell-shaped upheaval structure of AS copolymer.

Figure 7 shows the micrographs of the transmission images of (a) focused and (b) unfocused positions of a bell-shaped PC micro-lens. Schematic of micro-lens effect is shown in Fig. 5 of Chapter 2. Figure 7(a) clearly shows a micro-lens effect of the

bell-shaped structure induced in PC by laser molding. Figure 8 shows micrographs of the transmission images of (a) focused and (b) unfocused positions of the replicated AS copolymer micro-lens.
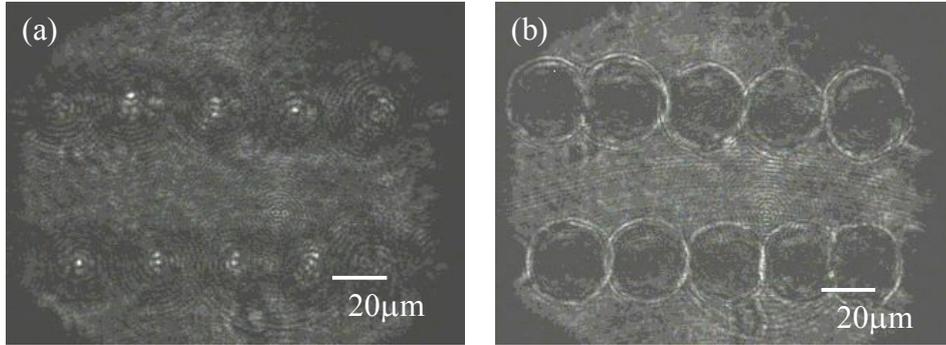
Fig. 7 Micrographs of the transmission images of (a) focused position and (b) un-focused position.
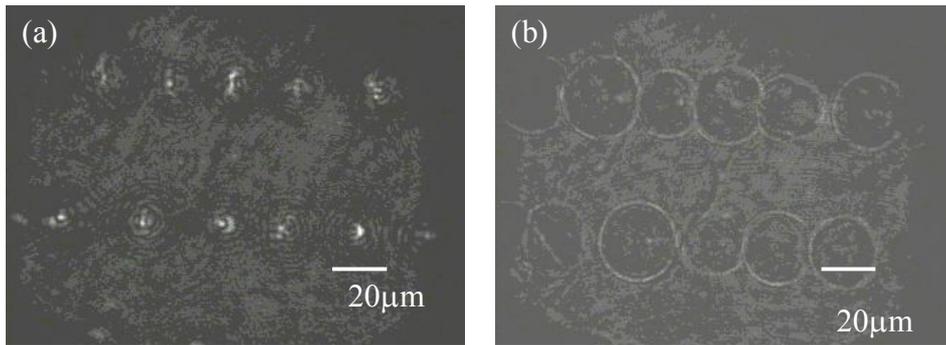
Fig. 8 Micrographs of the transmission images of (a) focused position and (b) un-focused position of replicated AS copolymer micro-lens.

As shown in Figs. 7 and 8, we confirmed the same micro-lens effect for the replicated structure as for the original structure. The focal length (f) of a semi-spherically shaped micro-lens is presented as $f = R / (n-1)$. In this equation, R is radius of the semi-sphere, and n is refractive index of the polymeric material for the micro-lens. The focal length becomes shorter with decreasing R or by using polymeric material with a higher refractive index. The fundamental micro-lens effect was confirmed for bell-shaped upheaval structures by laser molding and replication via electroforming, but the radius of the bell-shaped upheaval obtained was not uniform and had broad distribution. We continue to try to obtain a smaller and more uniform bell-shaped upheaval structure induced by laser molding and replication via electroforming.

The combination of the laser molding and the subsequent replication process using the electroformed mother mold will pave the way for the mass-production of micro-scale polymeric optical-devices, such as a micro-lens array.

6-A-4 Conclusion

Upheaval structures on the surface of polymer induced by the line irradiation of NIR femtosecond laser pulse in the polymer bulk was investigated. Bell-shaped upheaval structures were obtained in PC and PEI, but ABSM copolymers and AS copolymers gave the structures with a flattop. It was demonstrated that the periodic bell-shaped upheaval structure obtained in PC acts as a micro-lens but ABSM copolymers and AS copolymers do not show a micro-lens effect. The periodic bell-shaped upheaval structure in PC was replicated by electroforming (non-electrolytic plating of Ni and the following electrolytic plating of Ni) and potting AS copolymer of approximately 30wt% THF solution into the electroformed mother mold as done in the LIGA process. The replicated upheaval structure made of AS copolymer also showed the micro-lens effect. We propose here a novel methodology for a micro-scale polymeric optical device like a micro-lens array by means of laser molding in polymeric materials using a femtosecond laser pulse and additional mass production using the pseudo-LIGA process.

References and notes

(1) K. Miura, J. Qiu, H. Inoue, T. Mitsuyu, K. Hirao: Appl. Phys. Lett. **71** (1997) 3329.

(2) Y. Kondo, J. Qiu, T. Miura, K. Hirao, T.Yoko: Jpn. J. Appl. Phys. 38 (1999) L1146.

(3) T. Toma, Y. Furuya, W. Watanabe, K. Ito, J. Nishii, K. Hayashi: Opt. Rev. **7 (**2000) 14.

(4) Y. Kondo, T. Suzuki, H. Inoue, K. Miura, K. Hirao: Jpn. J. Appl. Phys. **37** (1998) 94.

(5) K. Hirao, K. Miura: Jpn. J. Appl. Phys. **37** (1998) 2263.

(6) K. Miura, H. Inoue, J. Qiu, K.Hirao: Nuclear Instruments and Methods in Physics Research **B141** (1998) 726.

(7) B. C. Stuart, M. D. Feit, A. M. Rubenchik, B. W. Sore, M. D. Perry: Phys. Rev. Lett. **74** (1995) 2248.

(8) K. M. Davis, K. Miura, M. Sugimoto, K. Hirao: Opt. Lett. **21** (1996) 1729.

(9) E. N. Glezer, M. Milosavljevic, L. Huang, R. J. Finlay, T. H. Her, J. P. Callan,E. Mazur: Opt. Lett. **21** (1996) 2023.

(10) S. Katayama, M. Horiike, K. Hirao, N. Tsutsumi: J. Polym. Sci. Part B. **40** (2002)

537.

(11) S. Katayama, M. Horiike, K. Hirao, N. Tsutsumi:. Jpn. J. Appl. Phys. Part1. **41** (2002) 2155.

(12) A. Rogner, J. Eicher, D. Münchmeyer, R. P. Peters, J. Mohr: J. Micromech. Microeng. **2** (1992) 123.

(13) Y. Hirata, H. Okuyama, S. Ogino, T. Numazawa, H. Tanaka: Proc. IEEE. MEMS'95. (1995) 191.

6-B Periodic bell-shaped upheaval structure on surface of polycarbonate by irradiation of NIR femtosecond laser pulse

6-B-1 Introduction

In Chapter 6-A, upheaval structures on the surface of polymers including PC and PEI, ABSM copolymers and AS copolymers induced by the line irradiation of NIR femtosecond laser pulse in the polymer bulk was investigated. Bell-shaped upheaval structures were obtained in PC and PEI, but ABSM copolymers and AS copolymers gave the upheaval structures with flattop. It was demonstrated that the periodic bell-shaped upheaval structure obtained in PC acts as micro-lens but ABSM copolymers and AS copolymers did not show micro-lens effect. The replicated upheaval structure made of AS copolymer also showed micro-lens effect. The formation of upheaval structures had not been reported in literature for inorganic materials and it might be related to intrinsic viscoelastic property and thermal property of polymer materials which are composed of long chin backbones and have entanglement.

We are especially interested in the formation of the periodic upheaval structures in the polymeric materials. The observation of internal induced structure by means of various microscopes might offer the key to analyze the mechanism. In this Chapter, we investigate in more detail the formation of upheaval structures in PC induced by NIR laser irradiation under a wide range of irradiation conditions and by means of additional observation using a differential interference laser scanning microscope and discuss the mechanism of the formation of upheaval structures.

6-B-2 Experimental

Irradiation system was same as described in Chapter 2. The upheaval structures on the surface of the polymer materials induced by the pulse laser irradiation were observed by an optical microscope and an optical interference microscope. To measure the cross section of the irradiated regions of the irradiated sheet samples, the samples were cut using a microtome. The cross-sectional and transmission image obtained using an optical microscope was observed and we obtained information on the transmission property of the irradiated and non-irradiated regions. We obtained information on the refractive index property of the irradiated and non-irradiated region based on the differential interference contrast images obtained using a laser scanning microscope (wavelength of laser, 488 nm; observation mode, transmitted mode; optically sliced thickness, 5 μm; number of stacked layers, approximate 30 layers). We also observed the morphology of the cross section using a SEM.

Polycarbonate (PC) (Teijin Chemicals Ltd.) sheet samples used for laser irradiation

are commercially available approximately 0.5 mm thick and were used without any additional processing.

6-B-3 Results and Discussion

3.1 Experimental results

First, the line irradiation of PC was carried under the following conditions: target irradiation depth, 30 μm; objective lens, 10X; scanning rate, 500 μm/s; irradiation energy, 75 nJ/pulse. line interval, 50 μm. Figure 1 is an optical interference micrograph of an upheaval structure. A periodic bell-shaped upheaval structure on the surface of PC was observed.
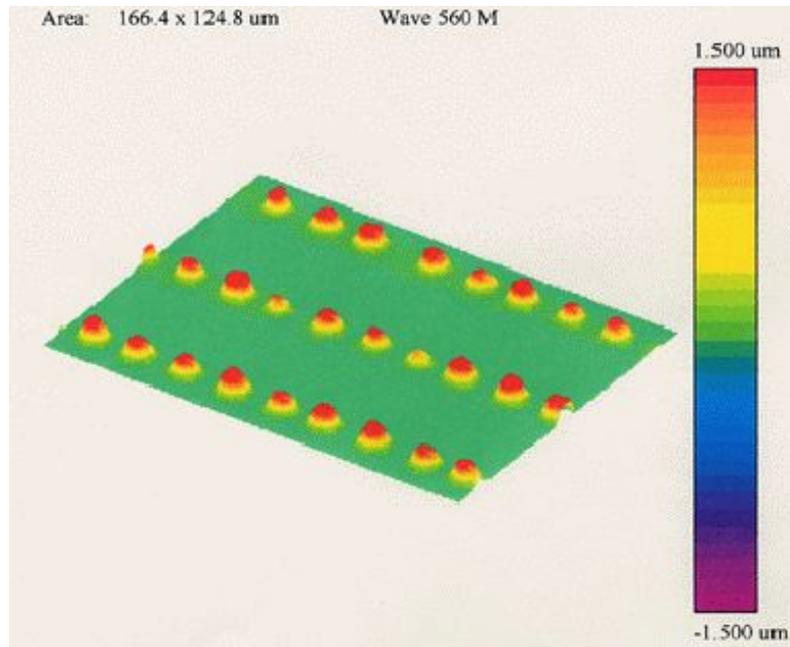
Fig. 1 An optical interference micrograph of an upheaval structure
of PC on the surface.

Two sets of experiments for PC were carried out with different irradiation conditions to confirm the relationship between the induced structures and the irradiation conditions. The irradiation conditions were as follows:

Experiment 1: irradiation energy, 100 nJ/pulse; objective lens, 10X; scanning rate, 500 μm/s; line interval, 50 μm. Variable parameter: target irradiation depth was changed from 10, 30, 50, 80 to 100 μm.

Experiment 2: target irradiation depth, 50 μm; objective lens, 10X; scanning rate, 500μm/s; line interval, 50 μm. Variable parameter;

irradiation energy was changed from 50, 100, 150, 250, 350, 400, 450 to 500 nJ/pulse.

The obtained experimental results are shown in Table 1. Figure 2 shows the optical micrograph and transmitted differential interference laser scanning micrograph for various structures induced by changing the target irradiation depth (Experiment 1). The SEM image of the cross section of the PC bulk with changing target irradiation depth was already shown in our previous report.[11] Figure 3 shows the optical micrograph, transmitted differential interference laser scanning micrograph and SEM images of various structures induced by changing irradiation energy (Experiment 2).

Table 1. Results obtained by irradiation with femtosecond pulse laser for PC under various irradiation conditions.

Irradiated Energy (nJ/pulse)		50	100	150	250	350	400	450	500
Irradiated Depth (μm)	10		+						
	30		+						
	50	-	+	+	=	=	=	++	++
	80		-						
	100		-						

+ : small bell-shaped upheaval structure.

++ : large bell-shaped upheaval structure.

- : no specific upheaval structure.

= : continuous band-shape not having clear upheaval structure.
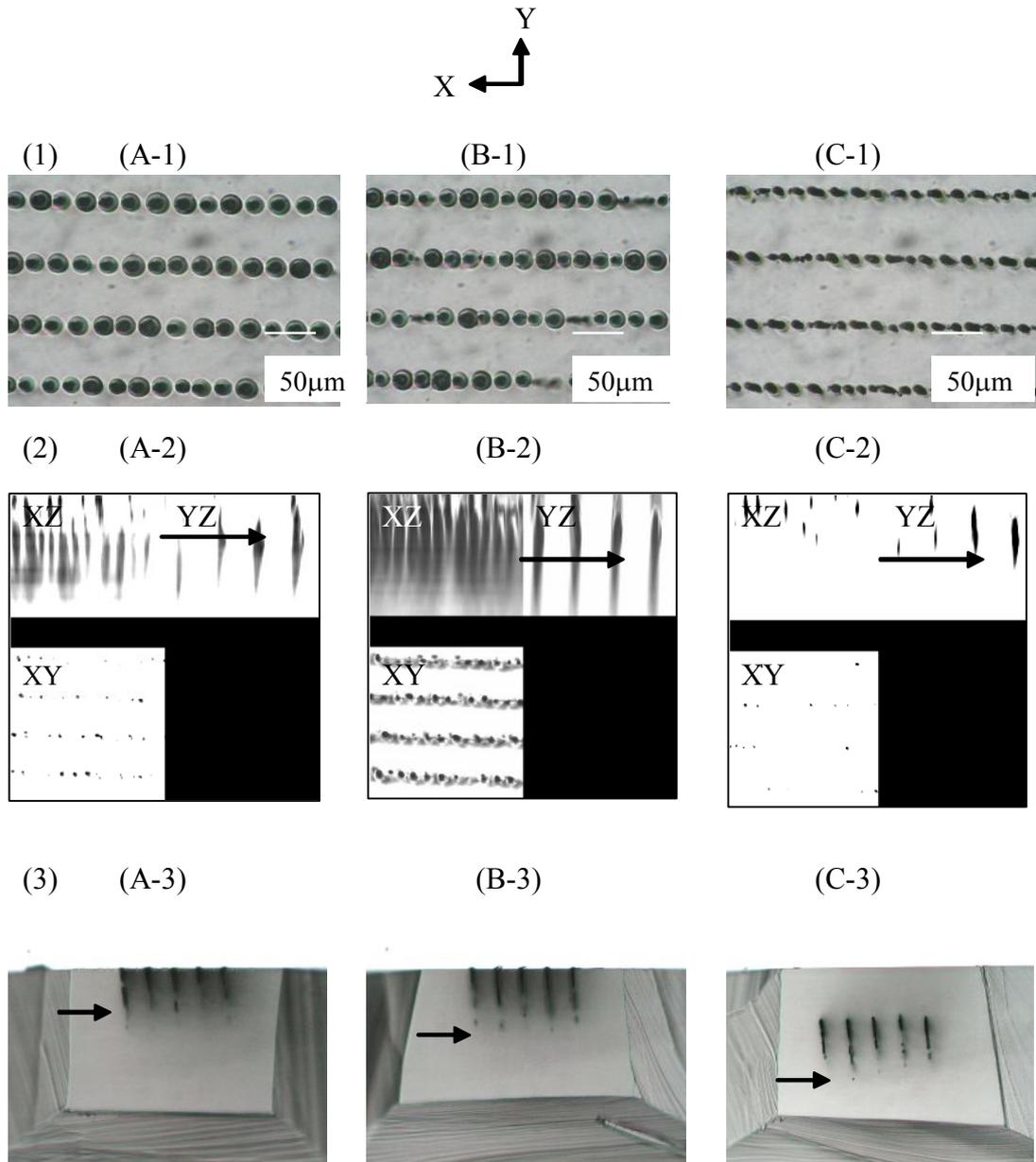
Fig. 2 Micrographs of induced structures by laser irradiation of PC under a condition of constant irradiation energy (100 nJ/pulse) (arrow shows the target depth).

A: target irradiation depth, 10 μm; B: target depth, 30 μm; C: target depth, 80 μm.

(1): optical micrographs (front-view; transmission images).

(2):differential interference laser scanning micrographs (transmitted differential interference contrast images).

(3): optical micrographs (cross-sectional view; transmission images).
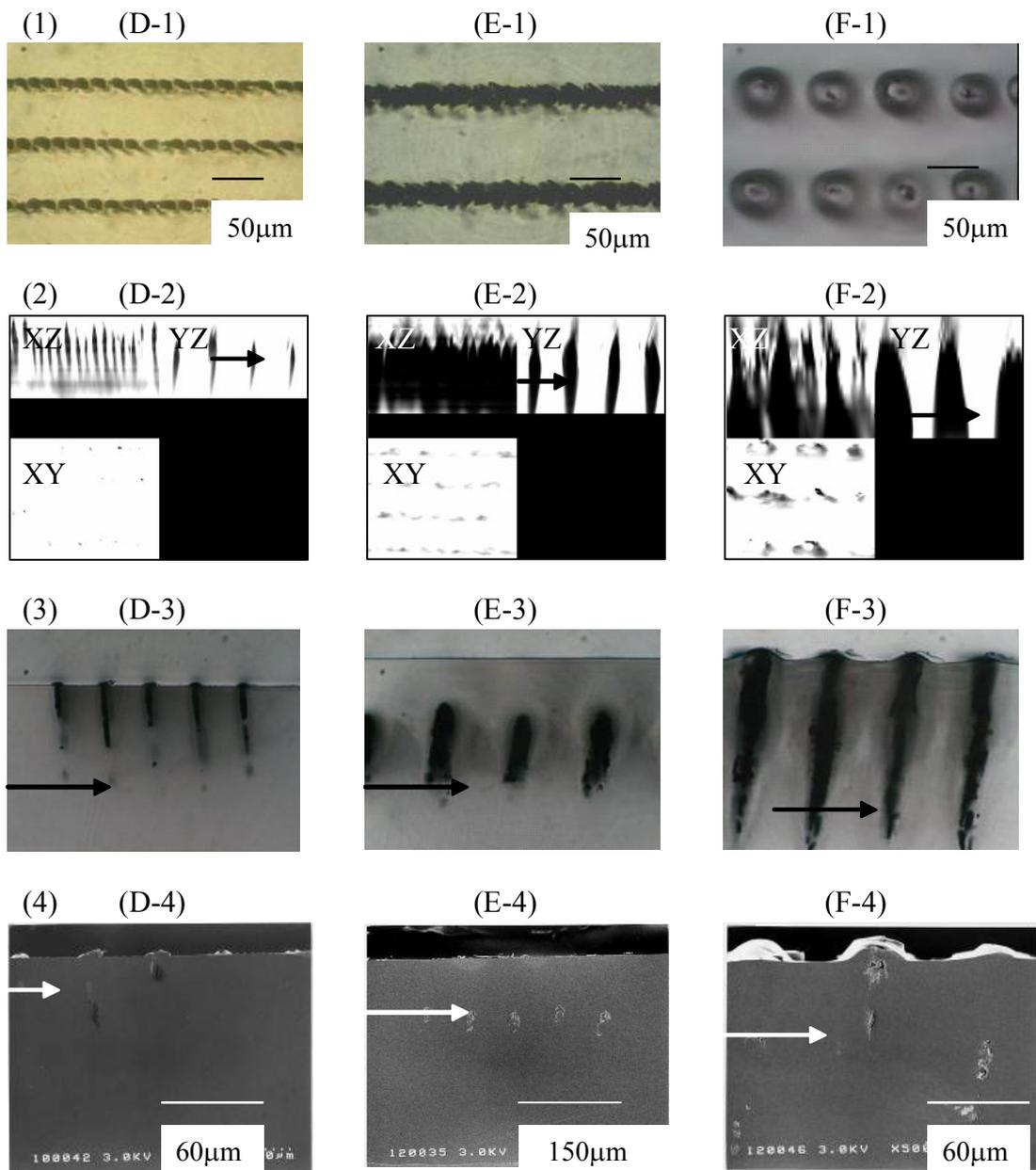
Fig. 3 Micrographs of induced structures by laser irradiation of PC under a condition of constant target irradiation depth (50 μm) (arrow shows the target depth).

D: irradiation energy, 150 nJ/pulse; E: irradiation energy, 400 nJ/pulse;

F: irradiation energy, 500 nJ/pulse.

(1): optical micrographs (front view; transmission images).

(2):differential interference laser scanning micrographs (transmitted differential interference contrast images).

(3): optical micrographs (cross-sectional view; transmission images).

(4): SEM images

A bell-shaped upheaval structure was not formed at a deeper target depth with a lower irradiation energy. Under a constant-depth (50 μm) irradiation condition, with increasing irradiation energy, changes in structures from small bell-shaped to continuous band-shaped and then to large bell-shaped were observed as shown in Table 1. These changes are visually shown in the optical micrographs of the front view in Figs. 2 (A-1, B-1, C-1) and 3 (D-1, E-1, F-1). There are two optimal irradiation energy regions for forming the periodic bell-shaped upheaval structure for a given irradiated depth. The size of the bell-shaped upheaval structure changed from approximately 15 μm to 45 μm in diameter of a basal plane upon varying the irradiation conditions.

1) differential interference laser scanning microscopy

The transmitted differential interference contrast images obtained by laser scanning microscopy (Figs. 2 and 3) show the periodic formation of a rodlike and/or elliptic induced structure with refractive index modulation along the incident laser path, as shown in A-2, B-2, C-2 and D-2, E-2, F-2. In Fig. 2 at a constant irradiation energy (Experiment 1), transmitted differential interference contrast image of the structure with a target irradiation depth of 30 μm was clearer than those with target irradiation depths of 10 and 80 μm. In Fig. 3, at a constant target irradiation depth (Experiment 2), the induced structures widens with the increase in irradiation energy as shown in the YZ sectional views. Narrow and wide differential interference contrast images are observed in D-2 for 150 nJ/pulse and in F-2 for 500 nJ/pulse, respectively. The transmitted differential interference contrast of a laser scanning microscope is obtained based on phase difference, which is a product of the refractive index change (Δn) and thickness (X) of the induced structures, and a contrast image can be observed in our experiment under the condition of $(\Delta n)(X) > 50$ nm. The thickness (X) of the rodlike and/or elliptic induced structure was approximately $5 - 25$ μm, therefore the refractive index change (Δn) was assumed to be approximately $> 2 \times 10^{-3}$. This value of refractive index change is comparable with those of other polymers reported previously.[12-14] The width of the periodic differential interference contrast images corresponded to the size of bell-shaped upheaval structures on the surface. The XZ cross-sectional view of irradiation energy with 400 nJ/pulse does not show a discrete but rather a continuous differential interference contrast image, as shown in E-2.

2) Optical microscopy

Under a constant-irradiation-energy condition, optical micrographs show transmitted contrast images with approximately the same lengths and widths but different positions

corresponding to the focused point, as shown in Fig. 2; A-3, B-3, C-3 (arrow shows the target irradiation depth). On the contrary, under a constant-depth condition, optical micrographs show that transmitted contrast images become wider with an increase in irradiation energy, as shown in Fig. 3 (D-3, E-3 and F-3). In the case of the formation of bell-shaped upheaval structures, these transmitted contrasts reached the surface (A-3, B-3 in Fig. 2 and D-3, F-3 in Fig. 3) but did not reach the surface for no specific upheaval structure (C-3 in Fig. 2, E-3 in Fig. 3). Transmitted contrast images would yield information on the transmission property of the irradiated and non-irradiated regions, therefore they seemed to show a locus of movement of products, such as carbonized species at the focused spot of the laser beam.

3) SEM

There are voids and cracks at the irradiated point beneath the bell-shaped upheaval structure in PC bulk. Voids and cracks maintain the upheaval structure on the surface as shown in D-4 and F-4, but they stay at the focused point and do not to maintain the continuous band-shaped structure as shown in E-4.

3.2 Discussion

We used irradiated target depth of 50 μm with changing irradiation energy as a model irradiation condition in considering mechanism of the formation of induced upheaval structure on the surface of PC. In this model irradiation condition, incident laser beam was focused at upper part of PC sheet with thickness of approximately 500 μm. The observed differential interference contrast images which seem to be induced structure by multi-photon absorption are rodlike and/or elliptic as shown in Fig. 2 and Fig. 3. PC has significant absorption at 267 nm and no significant absorption at 400 nm. 267 nm and 400 nm are wavelengths of three-photon and two-photon excitation of used laser pulse, respectively. As the probabilities of the two-photon and three-photon absorption are in proportion to square and cubic of the power density (photon density), therefore multi-photon absorption including two-photon, three-photon absorption and so on occurs in PC by irradiation of femtosecomd laser pulse.

Power density (PD) of incident laser beam is generally given by

$$PD=(\sin(cz)/cz)^2 \qquad (1)$$

In eq. (1), c is a constant which is determined by wavelength of incident beam and the numerical aperture (NA) of the objective lens and z is the distance from the focused point along the Z direction (z=0 at the focused point). The probabilities of the

two-photon and three-photon absorption are in proportion to square and cubic of the power density (photon density), therefore $(\sin(cz)/cz)^4$ and $(\sin(cz)/cz)^6$, respectively. Figure 4 shows functional shapes of $(\sin(cz)/cz)^2$, $(\sin(cz)/cz)^4$ and $(\sin(cz)/cz)^6$ which are normalized at each peak value. The multi-photon absorption occurs symmetrically according to the functional profiles along the incident path and the absorbed energy was maximum at the focused point in PC as shown in Fig.4 and as reported in paper.[16] The lower the NA of objective lens used is selected, the wider the distribution of the profiles of $(\sin(cz)/cz)^2$, $(\sin(cz)/cz)^4$ and $(\sin(cz)/cz)^6$ appears. As mentioned above, the obtained differential interference contrast images by laser scanning microscope were not maximum at the focused point but rod-like and/or elliptic. It is mostly due to low NA of objective lens (NA is 0.3 for 10X objective lens) in our experiment. We had already observed analogous phenomena using objective lens with low NA (NA; 0.30) that crystallized relief structures were formed far from a focused point in amorphous inorganic (In_2O_3 + 1 wt% TiO_2) film. Shapes of crystallized relief structures were sensitive to the irradiation conditions (focused height and scanning rate of irradiation) and cone-shaped structures in cross section image were obtained by the optimized irradiation condition.[17]
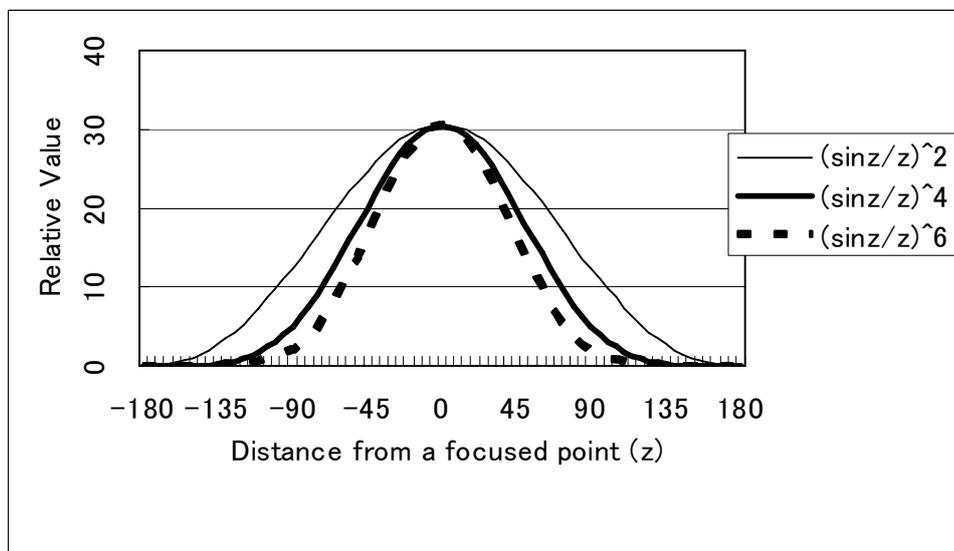
Fig.4. Schematic functional patterns of power density $(\sin z/z)^2$, probability of two-photon absorption $(\sin z/z)^4$ and three-photon absorption $(\sin z/z)^6$. In these patterns, relative values are normalized by adjusting same peak value.

In the line irradiation with NIR laser pulse for 150 femtoseconds, irradiated pulse

was not single but continuously moving along the X-axis at a constant depth in the Z-axis. The periodic bell-shaped upheaval structure on the surface formed by laser irradiation onto PC bulk is caused by the movement of products such as carbonized species at the focused point to the surface as shown in the cross-sectional optical micrographs (Fig. 2; A-3, B-3 and Fig. 3; D-3, F-3) and by upholding voids as shown in the SEM micrographs (Fig. 3; D-4, F-4). Periodic emergence of bell-shaped upheaval reminds us of the formation of the dissipative structures by spatio-temporal self-oscillation as reported in papers.[18,19]. The repetition rate of irradiation source used for our experiments was 200 kHz and scanning rate of our experiments was 500 μm/s and scanning pitch of the computer-controlled XYZ stage was 0.1 μm, therefore there were continuously 40 pulses per 0.1 μm (in 200 μs) in the scanning direction. The irradiated spot focused by a 10X objective lens has a diameter of approximately 5 μm in our experiment, therefore there were continuously 2000 pulse (in 10 ms) until next 5 μm scanning of focused spot center. The value of 10 ms was enough longer than thermal diffusion time constant (>20 pico-second). The focused spot center is scanning on the place which is subjected to preceding irradiation in the X direction (scanning direction). The observed size of voids was approximately 7 − 15 μm in a diameter which were approximately 1/3 times as small as those of size of bell-shaped upheaval structure on the surface in a diameter of the basal plane as shown in Fig. 3 (SEM micrographs). Voids which seem to be assembly of micro-cracks supposedly have an initial size (supposedly be approximately 5 μm) and become larger by thermal expansion. Figure 5 shows schematic presentation of the formation of micro-cracks and scanning of focused spot. As shown in Fig. 5, when micro-cracks has already been formed in the domain of focused spot center A and focused spot center moves from A point to B point, part of irradiation energy for forming micro-cracks is not required in the region of having preformed micro-cracks within the domain of focused spot center A during movement of the focused center from A toward B. This extra energy is allotted to induce another structure such as refractive index change and carbonized species. As the movement of focused center goes on, micro-cracks on the domain of focused center A begin to move from the target depth toward the surface according to anisotropic thermal gradient in the Z-axis which is mentioned later and then non-micro-cracks region appears at the target irradiation depth in the Z-axis. Allotment of the irradiation energy to the formation of induced structures is switching on micro-cracks from such as refractive index change and carbon species. In the case of spatio-temporal self-oscillating gel, periodic swelling-deswelling change is achieved by autonomous pH-oscillating.[19] In our case, periodic upheaval structure is supposedly by autonomous switching of irradiation

energy between the formation of micro-cracks and that of induced products such as refractive-index change and carbonized species.
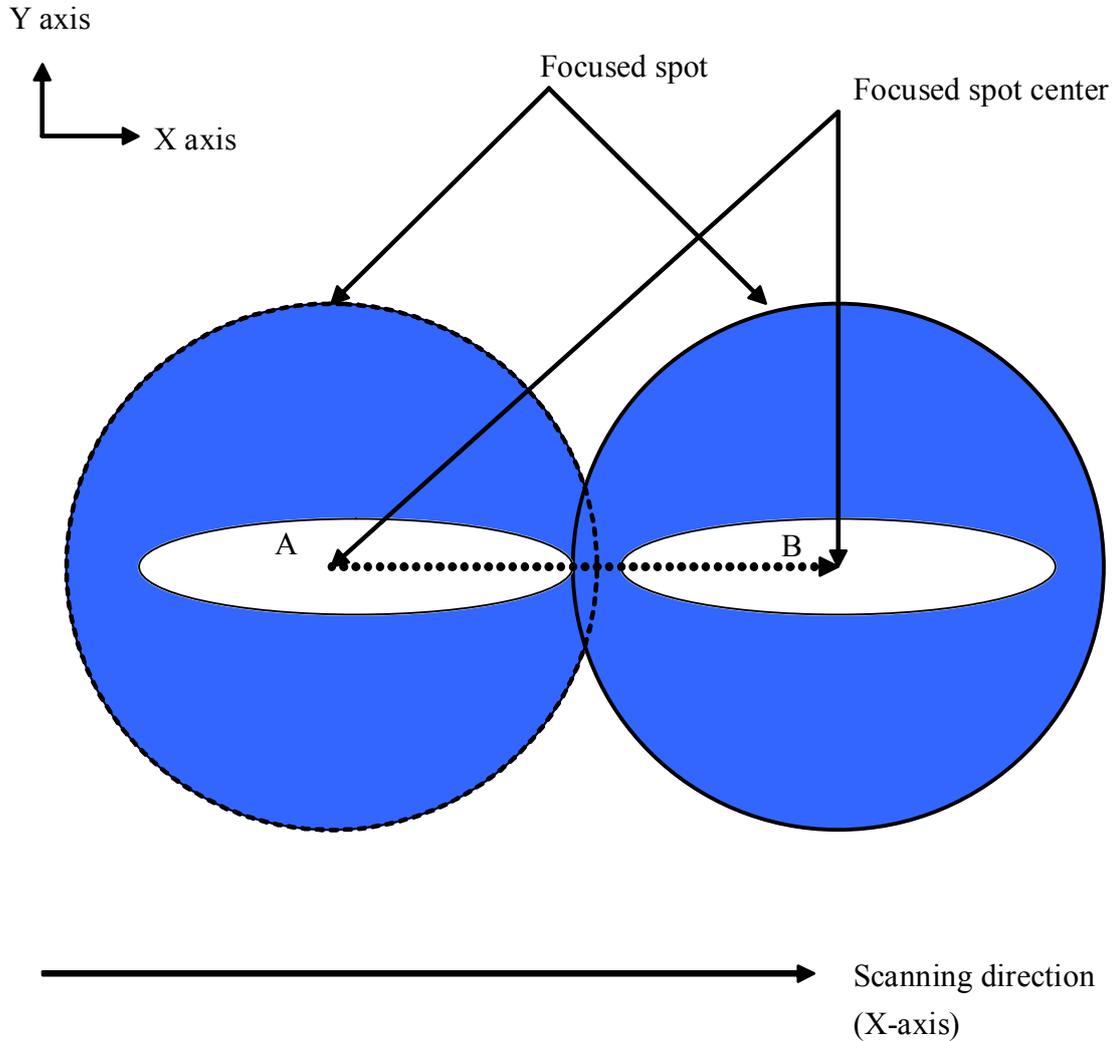
Fig.5 Schematic of the formation of micro-cracks and scanning of focused spot (Open ellipse are micro-cracks).

The mass transfer of voids and induced products is significantly associated with the property of the polymeric matrix. In comparison with metal and inorganic materials, polymeric materials have lower thermal conductivity and lower T_g (although T_g of PC is relatively higher among polymeric materials). These properties seem to bring about significant thermal effects on the irradiation with the ultra-short laser pulse. Lower thermal conductivity brings about long-time thermal influence during the irradiation and lower T_g brings about mobilization of the matrix polymer under these thermal

influences. Polymeric materials have viscoelastic properties involving molten and rubbery states above T_g and a glassy state below the T_g, and these viscoelastic properties appear according to the temperature induced and thermally diffused by irradiation with a laser pulse. The mobilization of polymer materials on the basis of the lower thermal conductivity and lower T_g seemd to play a significant role in the formation of inner induced structures in PC bulk which is responsible for the formation of the resultant upheaval structure on the surface of PC.

Figure 6 is a schematic representation of the mechanism of the formation of the upheaval structure induced by line irradiation of NIR laser pulse in the case of the target irradiation depth of 50 μm; 6-A is a schematic process of the formation of the rodlike and/or elliptic induced structure in PC by the multi-photon absorption along the incident laser path, 6-B is a schematic process of the thermal influence at the focused point by irradiation and thermal diffusion behavior from the focused point and the resultant formation of anisotropic thermal gradient, 6-C is schematic process of the formation of voids and cracks at the focused point and their growth and movement toward the surface according to rodlike and/or elliptic induced structure (6-A) and anisotropic thermal gradient (6-B) and the resultant formation of the upheaval structure. In Fig. 6, lateral axis shows time passage after irradiation of laser pulse (from left side to right side) and continuous irradiation of laser pulse in line irradiation was shown as superimposed flame on the left side. At the moment of irradiation, multi-photon absorption (a1) and micro-crack by micro-explosion as thermal influence (b1) occurs around the irradiated spot. After more than 20 pico-second from the irradiation, thermal diffusion occurs which assists gathering of micro-cracks (c1). Concentric thermal diffusion occurs from the focused point to surrounding area in which matrix polymer plays as thermal absorber and this concentric thermal diffusion occurs except for the direction to the surface because of adiabatic effect of air adjacent to the surface. (b2) shows isothermal curve formed by thermal diffusion and thermal absorbance in polymer matrix. Polymer is able to be mobile within broken line. As time passes, mobile region becomes narrower (b3) and resultantly anisotropic thermal gradient is formed in the case of the target depth of 50 μm (b4). The multi-photon-absorption profile (a1) also shows anisotropic thermal gradient due to non-radiative process after excited state. These two anisotropic thermal gradients control the mobility of PC polymer matrix and the movement of assemble of voids and cracks. The mobilization of PC polymer matrix is allowed in the thermal gradient region and the diffusion of voids and cracks with expanded volume and induced product by irradiation occur toward the surface in the thermal gradient region.
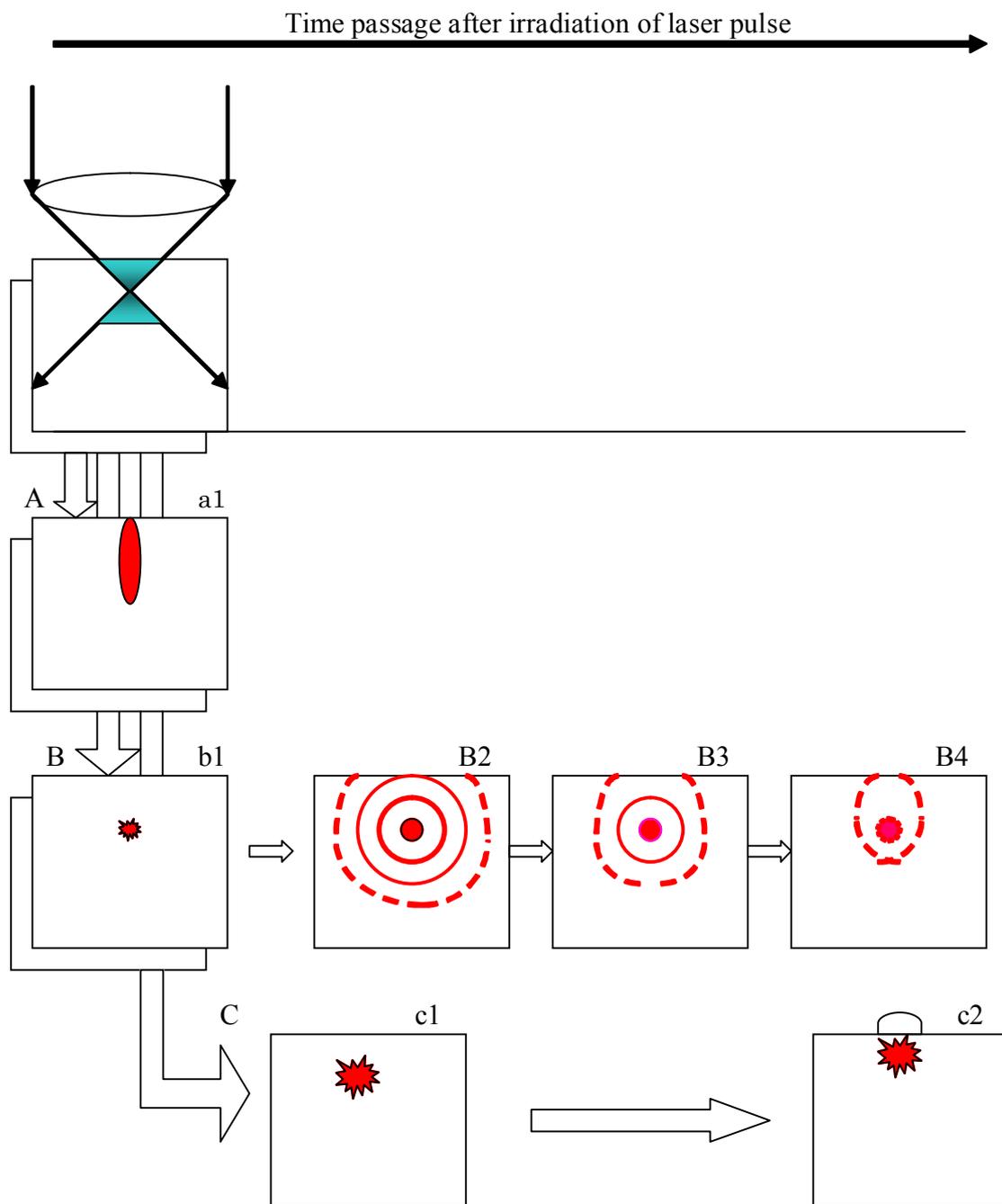
Fig. 6 Schematic representation of induced phenomena by line irradiation of NIR laser pulse in PC at the target irradiation depth 50 μm.

A: multi-photon absorption along the incident laser path.

B: thermal diffusion at the focused point and resultant thermal gradient toward the surface.

C: voids and cracks at the focused point and their growth and movement toward the surface and resultant formation of the upheaval structure on the surface.

Finally, the diffusions of the assembly of voids and cracks and product are terminated at a place where enough mobility can not be obtained and immobilization occurs upholding polymer surface to be a bell-shaped upheaval structure on the surface (c2). Movement of products, such as carbide, shows a locus as shown in optical micrographs (Fig. 2; A-3, B-3, Fig. 3; D-3, F-3).

Figure 6 showed schematic representation of in the case of the bell-shaped upheaval structure on the surface. But we observed continuous band-shaped structure without clear upheaval structure on the surface at an intermediate irradiation energy in a constant depth (50 μm) irradiation condition. We supposed that the induced rodlike and/or elliptic structure in PC by multi-photon absorption is overlapped with the increase of irradiation energy. As shown in Fig.3; E-2, continuous band-like consolidation of rodlike and/or elliptic structure in PC means lack of independence of each rodlike and/or elliptic structure and assemble of voids and cracks. It brings interconnection of assemble of voids and cracks in the X direction. Interconnected voids and cracks are hard to move toward the surface because of necessity of consolidated movement with long distance region

The formation of periodic bell-shaped upheaval structures is very interesting and seems to have a chaotic nature as a dissipative structure but its origin unfortunately is not sufficiently clear at the present stage. Further study is in progress now.

The application of these periodic upheaval structures for optical devices such as a micro-lens array has been published elsewhere.[20]

6-B-4 Conclusion

The formation of periodic upheaval structures on the surface of PC induced by line irradiation of NIR femtosecond laser pulses onto polymer bulks were investigated. In order to clarify the mechanism of the formation of these upheaval structures, irradiation experiments involving changing the irradiation conditions were performed. The induced structures were observed in detail using an optical microscope, SEM and differential interference laser scanning microscope. The upheaval structure was not formed under the condition of deeper target irradiation depth and lower irradiation energy. At a constant target irradiation depth of 50 μm, periodic bell-shaped upheaval structures on the surface changed from small to large with the increase in irradiation energy from small. We found a continuous band-shaped structure on the surface at the intermediate irradiation energy region. The periodic upheaval structures on the surface were observed to be maintained by voids and cracks in the SEM images. Differential interference

contrast images by laser scanning micrographs were rodlike and/or elliptic and showed a low NA effect. On the basis of obtained results of experiments and consideration of multi-photon absorption probability, viscoelastic property of polymeric material and so forth, we supposed the mechanism of the formation of upheaval structures on PC. For the formation of a periodic bell-shaped upheaval structure in PC, it is necessary that induced structure with refractive index modulation formed in PC bulk by multi-photon absorption are to be discrete in the X axis and periodic upheaval structure is supposedly formed by autonomous irradiation energy distribution to form induced structures including voids, induced products, refractive-index change. The anisotropic thermal gradient induced by the diffusion of focused energy allows the mass transfer of voids, cracks and products from the focused point to the surface.

References and notes

1) K. Miura, J. Qiu, H. Inoue, T. Mitsuyu, K. Hirao: Appl. Phys. Lett. **71** (1997) 3329.

2) Y. Kondo, J. Qiu, T. Miura, K. Hirao, T. Yoko: Jpn. J. Appl. Phys. **38** (1999) L1146.

3) T. Toma, Y. Furuya, W. Watanabe, K. Ito, J. Nishii, K. Hayashi: Opt. Rev. **7** (2000) 14.

4) Y. Kondo, T. Suzuki, H. Inoue, K. Miura, K. Hirao: Jpn. J. Appl. Phys. **37** (1998) 94.

5) K. Hirao, K. Miura: Jpn. J. Appl. Phys. **37** (1998) 2263.

6) K. Miura, H. Inoue, J. Qiu, K. Hirao: Nuclear Instruments and Methods in Physics Research **B141** (1998) 726.

7) B. C. Stuart, M. D. Feit, A. M. Rubenchik, B. W. Sore, M. D. Perry: Phys. Rev. Lett. **74** (1995) 2248.

8) K. M. Davis, K. Miura, N. Sugimoto, K. Hirao: Opt. Lett. **21** (1996) 1729.

9) E. N. Glezer, M. Milosavljevic, L. Huang, R. J. Finlay, T. H. Her, J. P. Callan, E. Mazur: Opt. Lett. **21** (1996) 2023.

10) D. Du, X. Liu, G. Korn, J. Squier, G. Mourou: Appl. Phys. Lett. **64** (1994) 3071.

11) S. Katayama, M. Horiike, K. Hirao, N. Tsutsumi: J. Polym. Sci. Part B **40** (2002) 537.

12) S. Katayama, M. Horiike, K. Hirao, N. Tsutsumi: Jpn. J. Appl. Phys. **41** (2002) 2155.

13) S. Katayama, M, Horiike, K. Hirao, N, Tsutsumi: J. Polym. Sci. Part B **40** (2002) 2800.

14) S. Katayama, M. Horiike, M. Urairi, K. Hirao, N. Tsutsumi: Chem. Phys. Lett. **373** (2003) 140.

15) Y. Sato, A. Sekihata, Y. Tanagisawa, M. Yamamoto, Y. Shimada, K. Ozaki, A.

Kusumi: J. Microsc. **185** (1997) 9.

16) H. Ueki, Y. Kawata, S. Kawata: Appl. Opt. **35** (1996) 2457.

17) S. Katayama, M. Horiike, T. Nakamura, K. Hirao, N. Tsutsumi: Appl. Phys. Lett. **81** (2002) 832.

18) G. Rabai, K. Kustin, I. R. Epstein: J. Am. Chem. Soc. **111** (1989) 3870.

19) R. Yoshida, T. Takahashi, T. Yamaguchi, H. Ichijo: J. Am. Chem. Soc. **118** (1996) 5134.

20) S. Katayama, M. Horiike, K. Hirao, N. Tsutsumi: Opt. Rev. (in press)

Chapter 7: Structures induced by irradiation of NIR femtosecond laser pulse in amorphous materials

7-A Crystallization and permanent relief grating structures induced by irradiation of NIR femtosecond laser pulse in amorphous inorganic (In₂O₃+1 wt% TiO₂) films

7-A-1 Introduction

In the literature, it has been reported that ultra-short pulse lasers with high peak power, such as, high peak power femtosecond laser in the NIR region, induced phase changes (phase transition) from amorphous to crystalline by irradiation in inorganic glass materials.[4] Induced structures including phase changes and refractive index modulation are reported to be locally confined to the region subjected to irradiation.[1-9] Crystalline polymer materials have not ordinarily perfect crystallinity and have intrinsic pseudo-crystal structure. Therefore, phase change from amorphous to crystalline in polymer materials could not be apparent and subtler than in inorganic materials. On the other hand, inorganic thin layers are widely used as components of organic and inorganic composite and phase changes from amorphous to crystalline might be useful tool to produce organic-inorganic composite with high performance.

Thin layers of indium oxide (In_2O_3) and tin oxide (SnO_2) doped In_2O_3 (ITO) with sub-micron thickness have been widely used for planar transparent electrodes and touch panel sensors for display devices. Thin layers of amorphous In_2O_3 and other components doped In_2O_3 can be obtained by sputtering onto a lower temperature substrate and under a condition with small amount of water.[10] These amorphous thin layers can be dissolved in a hydrochloric acid (HCl) solution. On the other hand, crystallized thin layers which can be obtained by sputtering onto a higher temperature substrate without water or thermally annealing amorphous thin layers at higher temperature (for example; above 200 ℃）, cannot be dissolved in HCl solution. Therefore, selective solubility of the amorphous region in thin layers of In_2O_3 and doped In_2O_3 would produce patterned structures if the periodic crystalline structures were induced in the thin layer. Recently, we found that specific and unique structures can be created by NIR femtosecond laser irradiation on the surface and inside the bulk of polymeric materials[11] and reported a diffraction measurement of grating structures induced by irradiation of acrylate block copolymers with femtosecond laser pulses.[12] Structures induced by irradiation with femtosecond laser pulses could be used to fabricate new optical devices such as a DFB laser with a combination of polymer materials and inorganic materials

In this Chapter, we investigated the relief grating structures induced by irradiation of NIR femtosecond laser pulses with approximately 5 μm focused beam diameter on amorphous ($In_2O_3+1wt\%TiO_2$) films with 100 nm thickness under various irradiation conditions and studied these structures using an optical microscope, X-ray diffraction analysis, and a reflective diffraction efficiency measurement.

7-A-2 Experimental

Irradiation system was same as described in Chapter 2. The structures in the inorganic materials on a glass substrate induced by the pulsed laser irradiation were observed by an optical interference microscope and an optical microscope and investigated by X-ray diffraction analysis for the characterization of the amorphous-crystalline phase. The measurement of reflective diffraction efficiency was carried out using an He-Ne laser (wavelength; 632.8 nm, maximum power; 10 mW) for the incident light beam.

The deposition methods of the amorphous ITO (In_2O_3+10 wt%SnO_2) and (In_2O_3+1 wt%TiO_2) thin films were DC magnetron sputtering with Ar, O_2, H_2O mixture (0.4Pa, Ar:O_2:H_2O=95:3:2) using a sintered oxide ceramic (In_2O_3+10 wt%SnO_2 and In_2O_3+1 wt%TiO_2) target at room temperature. Water vapor was taken from a water-filled bottle and its quantity was controlled by a needle pressure valve on the bottle. The target had a 6 inch diameter and the applied sputtering power was 2 W/cm^2. The substrate was rotated during sputtering to obtain a uniform layer on it. The thickness obtained was controlled by the sputtering time. Wet etching was done with a 3 %-15 % HCl aqueous solution.

7-A-3 Results and Discussion

Thin layers of amorphous ITO (In_2O_3+10 wt%SnO_2) and (In_2O_3+1 wt%TiO_2) were sputtered on a glass substrate under the conditions shown in Table 1.

Table. 1 Sputtering conditions for fabrication of (ITO) and ($In_2O_3+TiO_2$) thin layers on glass substrate.

	($In_2O_3+10wt\%SnO_2$)	($In_2O_3+1wt\%TiO_2$)
Sputtering power (W/cm^2)	2.0	2.0
Sputtering voltage (V)	448	418
Sputtering current (A)	0.79	0.85
Deposition rate (nm/s)	0.365	0.390

First, the laser pulses irradiated a (In_2O_3+1 wt%TiO_2) thin layer surface with approximately 100 nm –thickness sputtered on a glass substrate under the irradiation condition: irradiated energy, 312 nJ/pulse; sample scanning rate, 500 μm/s; objective lens, 10X; line interval (Λ), 20 μm; number of lines, 20 lines. Selective etching using a 3 %HCl solution was employed for the un-irradiated region. The relief grating structures on the sample before and after etching were observed using an optical interference microscope and the selective etching for un-irradiated region was confirmed as shown in Fig. 1.
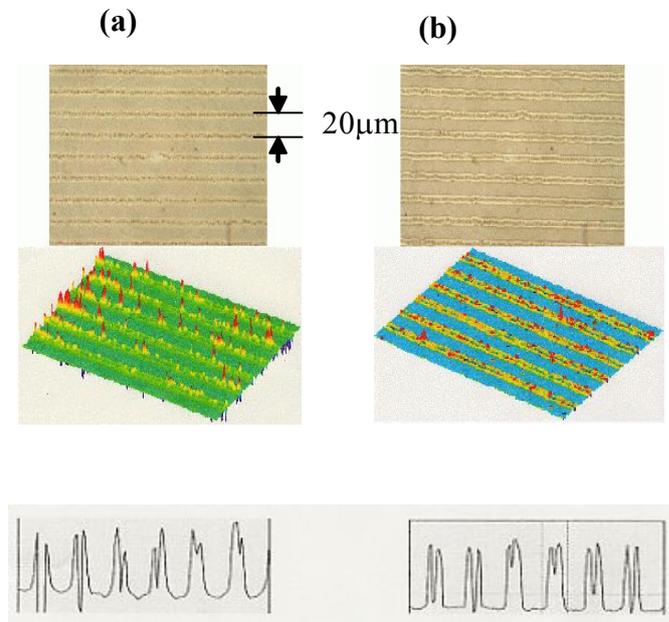
Fig. 1 Optical interference micrographs of relief grating structures induced by femtosecond laser pulses. (a) Irradiated non-etched sample. (b) Irradiated etched sample.

The amorphous-crystalline change was confirmed using a X-ray diffraction analysis in the condensed structures (line interval, 12 μm; number of lines, 40 lines; other irradiation conditions were the same as at the first experiment) induced by femtosecond laser pulse irradiation.
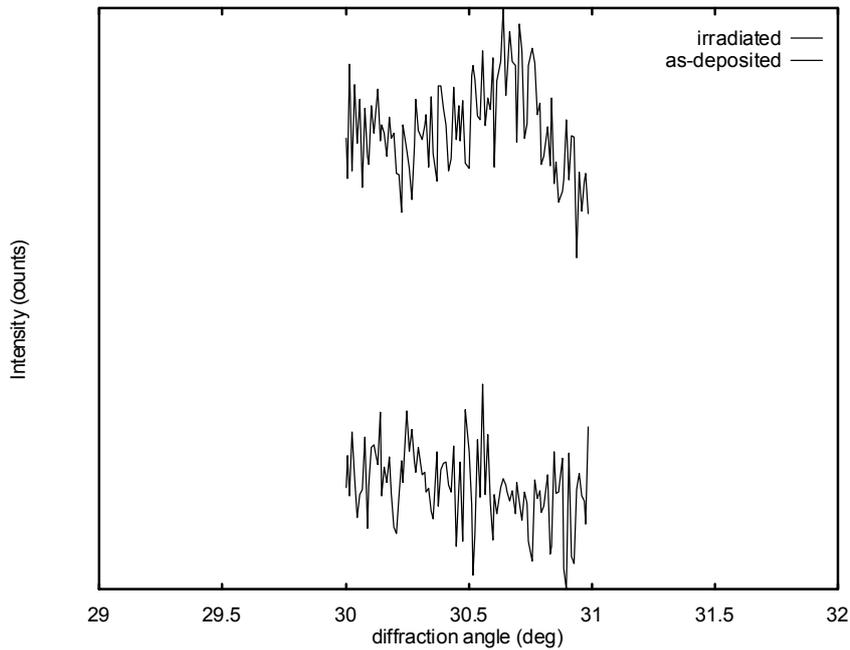
Fig. 2 X-ray diffraction patterns of (In_2O_3+1 wt%TiO_2) thin layers.
Dotted line: deposited un-irradiated sample. Solid line: irradiated sample.

As the area of the structure induced by the irradiation was only approximately 0.5 mm x 10 mm and the thickness was approximately 100 nm, the sample volume expected to be crystalline was too small to get enough diffraction strength, but we could obtain a subtle (222) diffraction peak near a 30.7 degree diffraction angle as shown in Fig. 2. Only amorphous background was observed for un-irradiated regions. Amorphous-to-crystalline phase change in mountain-like structures induced by femtosecond laser pulse irradiation was observed, but those mountain-like structures had two peaks with a cave-in at the center part as shown in Fig. 1. We need to optimize the irradiation condition to induce a more uniform structure such as a cone-shaped or rectangle one.

In the second set of experiments, laser pulses were focused onto or just above a (In_2O_3+1wt%TiO_2) thin layer surface with approximately 100 nm–thickness on a glass substrate under changing irradiation conditions. The standard irradiation conditions were as follows: irradiated energy, 300 nJ/pulse; sample scanning rate, 500 μm/s; objective lens, 10X; line interval, 20 μm; number of lines, 20 lines; focused position, onto the surface of layers; The variables in the irradiation conditions were the sample scanning rate and the focused position. These were varied as follows.

85

1) sample scanning rate: a) 250 µm/s, b) 500 µm/s, c) 750 µm/s (the focused position was on the surface of layer).
2) focused position: d) 50 µm above the surface of layer, e) 100 µm above the surface of layer, f) 10 µm below the surface of layer, that was approximately 10µm below the surface of the glass substrate (the sample scanning rate was 500 µm/s).

(a)   **(b)**   **(c)**

(d)   **(e)**   **(f)**
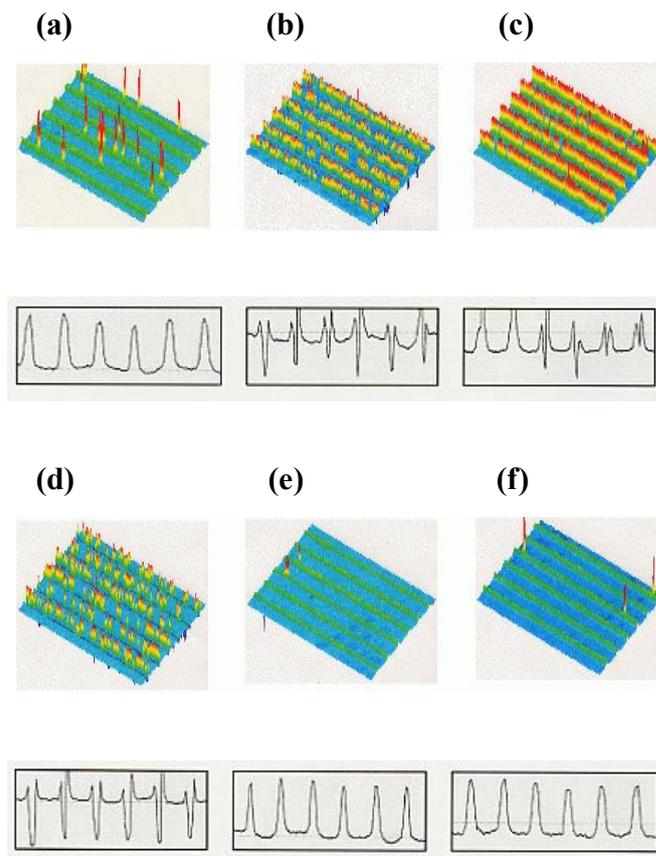
Fig.3 Optical interference micrographs of relief grating structures induced by femtosecond laser pulse under various irradiation conditions. Sample scanning rate;(a) 250 µm/s, (b) 500 µm/s, (c) 750 µm/s. (focused position was on the surface). Focused position; (d) 50 µm above the surface, (e) 100 µm above the surface, surface, and (f) 10 µm below the surface (scanning rate was 500 µm/s).

Figure 3 shows optical interference micrographs of relief grating structures induced by various irradiation conditions. Relief grating structures having nearly ideal cross-section patterns without cave-in are shown in a), e) and f) in Fig. 3. Those

favorable irradiation conditions were comparatively larger region irradiation and slower sample scanning rate so that more averaged and homogeneous energy would be obtained in the irradiated regions and the formation of a cave-in structure at the center of irradiated lines would be avoided. Those results were very interesting to the fabrication methodology of controlling relief grating structures on very thin inorganic layers.

Next, line irradiation was carried out onto (ITO) thin layer surface with approximately 1 μm–thickness on a glass substrate under the standard irradiation conditions as mentioned above. Apparent line shaped structures induced by the line irradiation were observed but the un-irradiated regions could not be selectively etched by the 3 %-15 % HCl solution. Several trials for amorphous-crystalline phase change detection were performed using a X-ray diffraction analysis, but any apparent difference between the irradiated and un-irradiated regions could not be observed. We concluded that sufficient amorphous-crystalline phase change could not be induced for the sample with 1 μm thickness because it was too thick and too heavily doped with SnO_2.
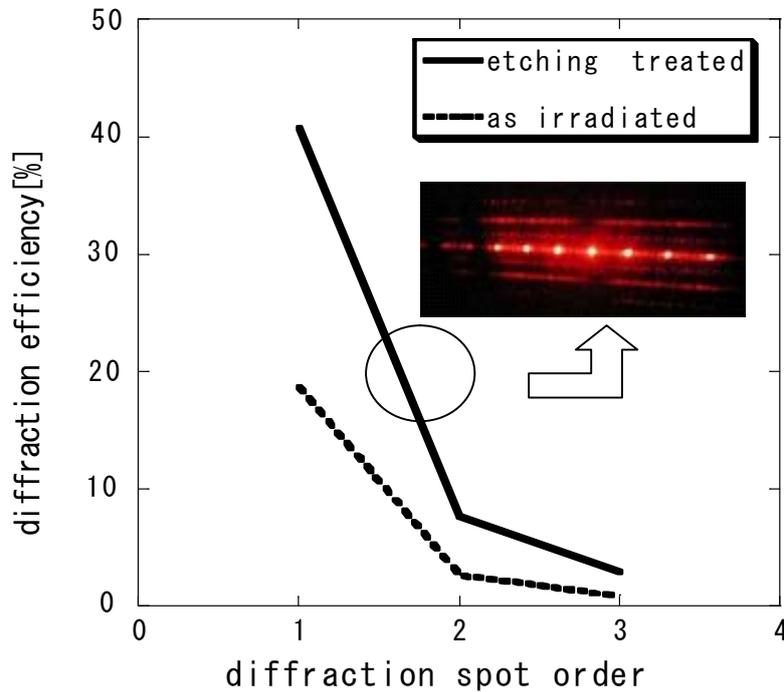
Fig. 4 Refractive diffraction efficiency vs diffraction spot order of Au coated relief grating. Solid line: etched sample. Dotted line: non-etched sample.

Finally, reflective diffraction efficiency from the relief grating structure was measured. A thin layer of gold with 60 nm thickness was deposited on the relief grating structure (line interval, 12 μm; number of lines, 40 lines) to enhance the reflective diffraction efficiency. First order diffraction efficiencies of approximately 40 % and 20 % were obtained for etched and non-etched samples (total reflectivity were 59 % and 67 %), respectively as shown in Fig. 4. Selective etching with a 3 % HCl solution was found to be more effective for fabricating good diffraction gratings.

7-A-4 Conclusion

Permanent relief grating structures were induced by the focused irradiation of NIR femtosecond laser pulses in 100 nm thin layers of amorphous inorganic (In_2O_3+1 wt%TiO_2). X-ray diffraction analysis showed amorphous-to-crystalline phase change by the irradiation of NIR femtosecond laser pulses and the formation of crystallized relief grating structures. The shapes of the crystallized relief structures could be varied by changing the irradiation scanning rate and the height of the focused point. A cone-shaped structure without cave-in was obtained by optimizing the irradiation conditions. A new method of fabricating relief grating structures on a thin inorganic layer was presented. Employment of selective wet etching on un-irradiated amorphous regions of the samples using a 3% HCl solution enhanced the crystalline relief grating patterns. The first order diffraction efficiencies of approximately 40 % and total reflectivity of 59 % were obtained with an etching treatment using a 3 % HCl solution and Au deposition with 60 nm thickness for irradiated (In_2O_3+1 wt%TiO_2) thin layer samples.

References and notes

(1) K. Miura, J. Qiu, H. Inoue, T. Mitsuyu, K. Hirao: Appl. Phys. Lett. **71** (1997) 3329.

(2) Y. Kondo, J. Qiu, T. Miura, K. Hirao, T. Yoko: Jpn. J. Appl. Phys. **38** (1999) L1146.

(3) T. Toma, Y. Furuya, W. Watanabe, K. Ito, J. Nishii, K. Hayashi: Opt. Rev. **7** (2000) 14.

(4) Y. Kondo, T. Suzuki, H. Inoue, K. Miura, K. Hirao: Jpn. J. Appl. Phys. **37** (1998) 94.

(5) K. Hirao, K. Miura: Jpn. J. Appl. Phys. **37** (1998) 2263.

(6) K. Miura, H. Inoue, J. Qiu, K. Hirao: Nuclear Instruments and Methods in Physics Research **B141** (1998) 726.

(7) B. C. Stuart, M. D. Feit, A. M. Rubenchik, B. W. Sore, M. D. Perry: Phys. Rev. Lett. **74** (1995) 2248.

(8) K. M. Davis, K. Miura, N. Sugimoto, K. Hirao: Opt. Lett. **21** (1996) 1729.

(9) E. N. Glezer, M. Milosavljevic, L. Huang, R. J. Finlay, T. H. Her, J. P. Callan, E. Mazur: Opt. Lett. **21** (1996) 2023.

(10) S. Ishibashi, Y. Higuchi, Y. Ota, K. Nakamura: J. Vac. Technol. A **8** (1990) 1399.

(11) S. Katayama, M. Horiike, K. Hirao, N. Tsutsumi: J. Polym. Sci. Part B **40** (2002) 537.

(12) S. Katayama, M. Horiike, K. Hirao, N. Tsutsumi: Jpn. J. Appl. Phys **41** (2002) 2155.

7-B Structures induced by irradiation of NIR femtosecond laser pulse in polysilane and polysilane layer coated polymer films

7-B-1 Introduction

In Chapter 7-A, Permanent relief grating structures were investigated by the focused irradiation of NIR femtosecond laser pulses in 100 nm thin layers of amorphous inorganic (In_2O_3+1 wt%TiO_2). In this previous chapter, structures of permanent relief grating were controllable by irradiation condition, such as scanning rate and irradiation height. It is very interesting that induced structures were controlled at the position of 10 μm-100 μm far from the focused point because structures induced by irradiation of NIR femtosecond laser pulse with high peak power have been reported to be confined locally in focused point. We also investigated an unique photo-sensitive effect of added dyes on the formation of structures in polymeric materials induced by irradiation of NIR laser pulse and confirmed that the absorption property and non-radiative efficiency of added dyes were responsible for the photo-sensitive effects[11]. We have reported that the induced structure in the P-(MMA/EA-BA) block copolymer show an aggregation of sub-micron scale deposit[12] and stripe-shaped layer structures with the assembled deposit formed the modulation of refraction index. Evaluate refractive index modulation of the ensemble of layers of these stripe-shaped structures were approximately 0.30 x 10^{-3} and these values are smaller than those of obtained for inorganic materials[13]. It is well-known that polysilane is a kind of polymer material in which higher refractive index modulation of over 1×10^{-1} is introduced by irradiation of UV laser in presence of oxygen. Extreme large modulation was responsible for change in chemical structures from Si-Si to Si-O-Si brought by photo-oxidation[14,15]. Polysilanes are σ conjugation materials and have an absorption peak at 300-350 nm regions which correspond to the transition from ground state to lowest singlet excited state. We have used NIR laser pulse with wavelength of 800 nm for the formation of the induced structures in transparent materials and 400 nm and 267 nm correspond to the wavelengths of two-photon and three-photon excitation, respectively. It is also well-known that polysilane is a polymer material which shows various unique properties, such as high refractive index, non-linear optical property, photo-conductivity, thermochromism and piezochromism. We are interested in the possibility of large refractive index modulation by multi-photon absorption in polysilane bulk and additive effect of polysilane layer on a polymer matrix by irradiation of NIR laser pulse.

In this Chapter, we investigate the structures induced in both polysilane and thin polysilane layer coated polymeric materials by irradiation of NIR femtosecond laser pulse, and study the refractive index modulation of induced structure in polysilane bulk

and a photo-sensitive effect of polysilane on the induced structure of polymeric materials with thin polysilane layer. We discuss the relation between the induced structures and multi-photon excitation by NIR femtosecond laser pulsing in polysilane.

7-B-2 Experimental

Irradiation system was same as described in Chapter 2. To measure the cross-section of the irradiated region of the sample film, the sample film was cut by a microtome. The cross-sections were observed by an optical microscope.
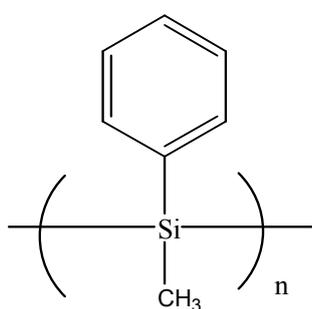
Poly (methyl phenyl silane)
(PMPS)
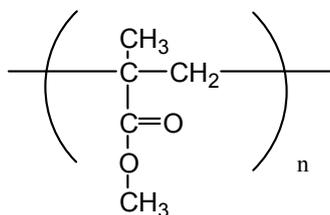
Poly (methyl methacrylate)
(PMMA)
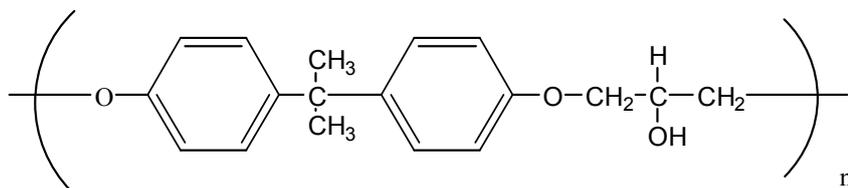
Thermoplastic bis-phenol A type epoxy
(Epoxy)

Fig. 1 Structural formulae of polymer samples used for laser irradiation.

Structural formulas of polymer samples used here are shown in Fig. 1. Commercially available Poly (methyl phenyl silane) (PMPS) (Osaka Gas Chemicals), poly (methyl methacrylate) (PMMA) (Mitsubishi Rayon) and thermoplastic bis-phenol A type epoxy (Epoxy) (Tohto Kasei) were used. Molecular weight of PMPS was 5600 (Mn) and PMPS bulk used for line irradiation was block sample as commercially obtained and/or casting film from tetrahydrofuran (THF) or toluene solution and we polished a surface for block sample by polishing paper (#800) in order to obtain smooth plane for incident beam of irradiation. PMMA and Epoxy were dissolved in ethyl acetate and THF, respectively to make 30 wt% solution for casting. Polymer solution was cast onto a glass substrate to prepare the film with approximately 500 μm in thickness. Thin PMPS film with approximately 4 μm in thickness was over-coated onto the PMMA and Epoxy films by spin-coating.

7-B-3 Results and Discussion

Figure 2 is optical micrographs of structures induced in PMPS block and PMPS cast film by irradiation of NIR femtosecond laser. Irradiation condition was as follows: irradiated depth, 50 μm (target depth); objective lens, X10; pulse energy, 55 nJ/pulse; sample scanning rate, 500 μm/s; line interval, 15-20 μm; number of lines, 10-20 lines.
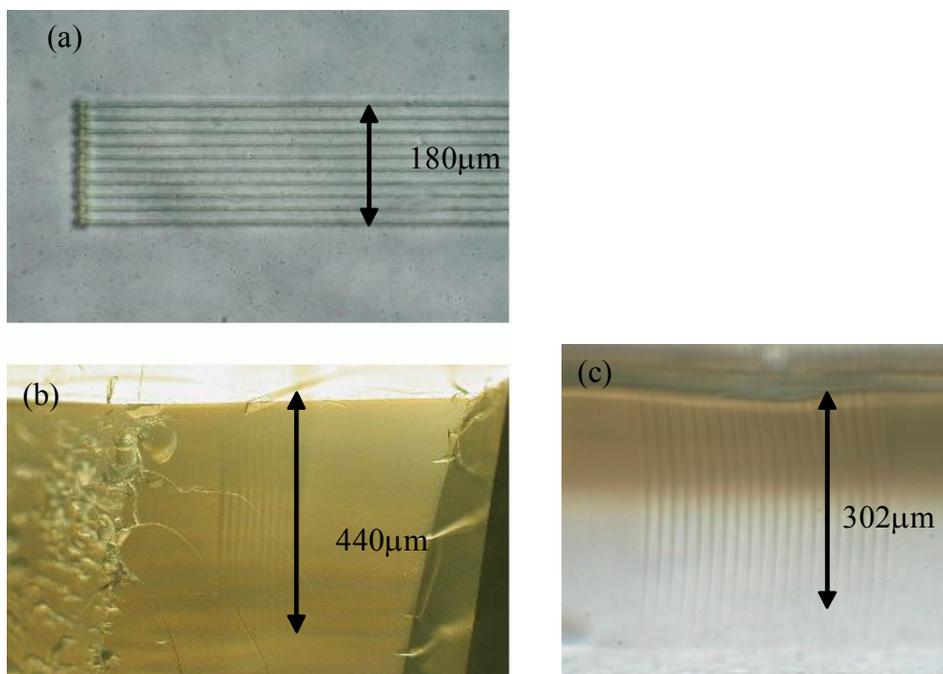
Fig. 2 Optical micrographs of structures induced in PMPS block and PMPS cast film. PMPS block: (a) front view. (b) cross-sectional view.
PMPS cast film: (c) cross-sectional view.

Laser irradiation induced stripe-shaped structures with approximately 440 μm in length for PMPS block and approximately 300 μm in length for PMPS cast films. We had already obtained the similar structure induced in inorganic glass by irradiation of NIR femtosecond laser[12] and P-(MMA/EA-BA) block copolymer.[12,13] These structures were formed from the focused point to the direction of laser propagation. The self-focused filaments in the irradiated direction of ultra-short laser pulse induced by high peak power might be responsible for the formation of these structures as already reported.[18-20] The length of the structures induced in PMPS bulk was longer than those in P-(MMA/EA-BA) and inorganic glass in which the line length was approximately 200 μm at best.[12,13]
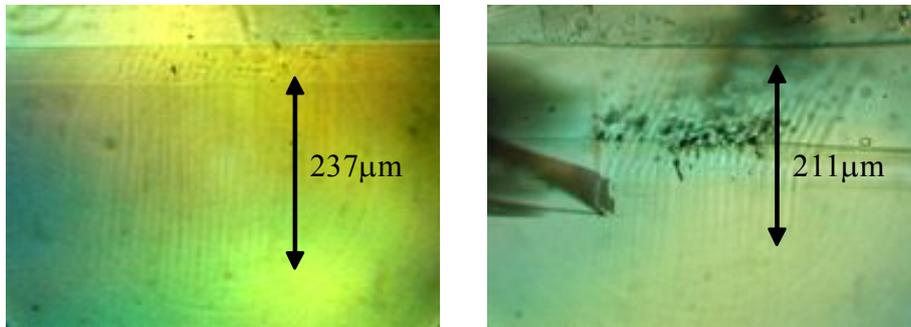
Fig. 3 Optical micrographs of structures induced in PMPS bulk by (a) single line irradiation and (b) superimposed line irradiation for three times.

Figure 3 shows optical micrographs of structures induced in PMPS bulk by single and superimposed line irradiation for three times. Fig. 3(a) is micrograph of the structures by single line irradiation and Fig. 3(b) is that by superimposed line irradiation for three times. Irradiation condition was as follows: irradiated depth, 50 μm (target depth); objective lens, X10; pulse energy, 55 nJ/pulse; sample scanning rate, 500 μm/s; line interval, 10 μm; number of lines, 20 lines. These induced structures showed Bragg-type transmission patterns and obtained diffraction parameters are as follows: Q value, (a) 5.6, (b) 5.0; diffraction efficiency, (a) 30%, (b) 29%; refractive modulation (Δn), (a) 6.0×10^{-4}, (b) 6.6×10^{-4}. The multiple irradiation does not give the significant increase of refractive index modulation in PMPS bulk, although that in P-(MMA/EA-BA) gave rise to the considerable increase of refractive index modulation.[13] We expected large

refractive index modulation of approximately 10^{-2} would be induced in PMPS bulk by NIR laser pulse. But actually obtained refractive modulation was $6\text{-}7 \times 10^{-4}$. The changes in Fourier transform infrared spectroscopy (FT-IR) before and after irradiation in PMPS bulk by NIR laser pulse and on the surface of PMPS bulk by a mercury UV light was investigated. In the case of the irradiation by the mercury UV light, Si-O absorption (1100 cm^{-1}) was increased and Si-Phenyl absorption (1480 cm^{-1}) was decreased with increasing the irradiation energy but in the case of the irradiation by NIR laser pulse, neither the increase of Si-O absorption nor the decrease of Si-Phenyl absorption were measured. These results might imply the induced refractive modulation was brought rather through the formation of self-focused filaments than photo-oxidation by multi-photon absorption.
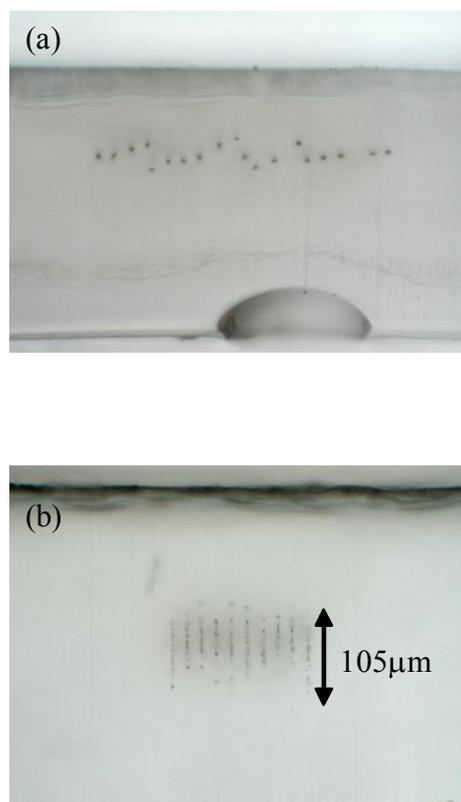
Fig. 4 Optical micrographs of structures induced in (a) Epoxy and (b) PMPS-coated Epoxy.

Figure 4 shows optical micrographs of structures induced in Epoxy (Fig. 4a) and PMPS-coated Epoxy (Fig. 4b) by NIR laser pulse irradiation.

Figure 5(a) shows optical micrograph of structures induced in PMPS-coated PMMA by NIR laser pulse irradiation and Fig. 5(b) is diffraction pattern from the structures. Irradiation condition was as follows: irradiated depth, 50 μm (target depth); objective lens, X10; pulse energy, 115 nJ/pulse; sample scanning rate, 500 μm/s; line interval, 20 μm; number of lines, 10 - 20 lines.
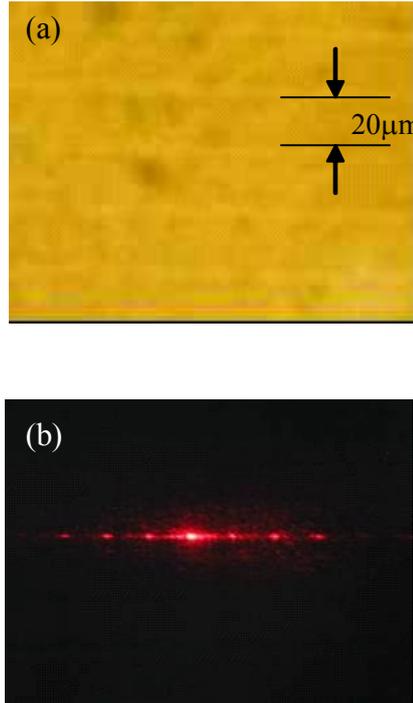
Fig. 5 (a) Optical micrograph of structures induced in PMPS-coated PMMA (front view). (b) Diffraction pattern from the structures.

Laser irradiation did not induce any stripe-shaped structures in uncoated PMMA and Epoxy films. On the contrary, both PMPS-coated PMMA and Epoxy films showed stripe-shaped structures after laser irradiation as shown in Fig. 4(b) and Fig. 5(a). The stripe-shaped structures in PMPS-coated PMMA did not have enough optical contrast on cross-sectional observation by optical microscope, therefore we only showed a front view micrograph in Fig. 5(a). As shown in Fig. 4 and Fig. 5, the thin PMPS-coated PMMA and Epoxy showed photo-sensitive effect on the formation of structure induced by NIR femtosecond laser pulses irradiation. In the case of the irradiation condition at target depth of 30 μm, same photo-sensitive effect was observed as the case at 50 μm but ablations of PMPS layer occurred at target depth of 0 μm (at the surface) and 10 μm.

We had already observed that the shapes of crystallized relief structures induced by irradiation of NIR laser pulse to amorphous inorganic (In_2O_3+1 wt%TiO_2) films were sensitive to the irradiation conditions (focused height and scanning rate of irradiation) and cone-shaped cross section structures were obtained by the optimized irradiation condition.[21] In this study and in the previous study[21], the region located approximately 30-100 μm from the focused spot even showed to be subjected to the influence of the irradiation. The power density at a distance of z from the focused spot is [sin (cz)/cz]^2 and the probabilities of two-photon absorption and three-photon absorption are [sin (cz)/cz]^4 and [sin (cz)/cz]^6, respectively. The over-coated PMPS has absorption peak wavelength at 300-350 nm and absorptions at 267 nm and at 400 nm which correspond to wavelengths of three-photon and two-photon excitation of irradiated NIR laser source, respectively. The existence of over-coated PMPS might change irradiation effect on the formation of induced structures as in ref.21. An ensemble of stripe-shaped structure induced in PMPS-coated PMMA showed the pseudo-Bragg type transmission pattern with diffraction efficiency of approximately 10 % and Q value of approximately 2 under optimal irradiation condition. This photo-sensitive effect showed a potential of writing a structure, such as a grating in optical polymeric devices, such as an optical polymeric fiber (OPF) which is made of PMMA and plastic cell for a display which is made of Epoxy and other transparent polymeric materials.

7-B-4 Conclusion

PMPS bulks showed longer stripe-shaped structures with approximately 200-400 μm length than we had ever observed in inorganic glass and other polymeric materials. Thin polysilane layers coated on both PMMA and Epoxy showed photo-sensitive effect on the formation of stripe-shaped structures in PMMA and Epoxy induced by irradiation of NIR femtosecond laser pulse. An ensemble of stripe-shaped structure acted as a diffraction grating. In this study and in our previous study,[21] even the region located approximately 30-100 μm from the focused spot is subjected to the influence of the irradiation and multi-photon absorption is responsible for these phenomena. This effect shows a potential of writing a structure in optical polymeric device such as an optical polymeric fiber (OPF).

References and notes

(1) W. J. Tomlinson, I. P. Kaminov, E. A. Chandross, R. L. Fork, W. T. Silfvast, Appl. Phys. Lett. **16** (1970) 486.

(2) K. Miura, J. Qiu, H. Inoue, T. Mitsuyu, K. Hirao, Appl. Phys. Lett. **71** (1997)

3329.

(3)   Y. Kondo, J. Qiu, T. Miura, K. Hirao, T. Yoko, Jpn. J. Appl. Phys. **38** (1999) L1146.

(4)   T. Toma, Y. Furuya, W. Watanabe, K. Ito, J. Nishii, K. Hayashi, Opt. Rev. **7** (2000) 14.

(5)   Y. Kondo, T. Suzuki, H. Inoue, K. Miura, K. Hirao, Jpn. J. Appl. Phys. **37** (1998) 94.

(6)   K. Hirao, K. Miura, Jpn. J. Appl. Phys. **37** (1998) 2263.

(7)   K. Miura, H. Inoue, J. Qiu, K. Hirao, Nuclear Instruments and Methods in Physics Research. **B141** (1998) 726.

(8)   B. C. Stuart, M. D. Feit, A. M. Rubenchick, B. W. Sore, M. D. Perry, Phys. Rev. Lett. **74** (1995) 2248.

(9)   K. M. Davis, K. Miura, N. Sugimoto, K. Hirao, Opt. Lett. **21** (1996) 1729.

(10) E. N. Glezer, M. Milosavljevic, L. Huang, R. J. Finlay, T. H. Her, J. P. Callan, Opt. Lett. **21** (1996) 2023.

(11) S. Katayama, M. Horiike, K. Hirao, N. Tsutsumi, J. Polym. Sci. Part B, Polym. Phys. **40** (2002) 2800.

(12) S. Katayama, M. Horiike, K. Hirao, N. Tsutsumi, J. Polym. Sci. Part B, Polym. Phys. **40** (2002) 537.

(13) S. Katayama, M. Horiike, K. Hirao, N. Tsutsumi, Jpn. J. Appl. Phys. **41** (2002) 2155.

(14) L. A. Hormak, T. W. Weidman, E. W. Kwock, J. Appl. Phys. **67** (1990) 2235.

(15) Y. Matsuura, K. Matsukawa, H. Inoue, Chem. Lett. (2001) 244.

(16) H. Kogelnik, Bell. Syst. Tech. J. **48** (1969) 2909.

(17) P. Yeh, "in Introduction to Photorefractive Nonlinear Optics", (Wiley Intersciece, New York, 1993) p. 61 – 65.

(18) R. R. Alfano, S. L. N. Shapiro, Phys. Rev. Lett. **24** (1970) 592.

(19) S. H. Cho, H. Kumagai, I. Yokota, K. Midorikawa, M. Obata, Jpn. J. Appl. Phys. **37** (1998) L737.

(20) K. Yamada, W. Watanabe, T. Toma, K. Itho, J. Nishii, Opt. Lett **26** (2001) 19.

(21) S. Katayama, M. Horiike, T. Nakamura, K. Hirao, N. Tsutsumi, Appl. Phys. Lett. **81** (2002) 832.

Chapter 8: Summary

The development of ultra-short laser pulses with high peak power has remarkably progressed past decade. Especially, a typical example of these ultra-short laser pulse has been a solid state NIR wavelength femtosecond laser pulse which has a feature of easy operation. Femtosecond laser pulse has another significant feature that the order of its time duration (10^{-15} second) is comparable to the time constant of electronic transition. This feature is very powerful tools for state analysis and for state control in ultra-short time scale. With the development of the NIR femtosecond laser pulse, it has become possible for many researchers to use these laser pulses as tools not only for measurement but also for manufacturing.

At the starting point of this thesis, there have been many studies of investigations on structures induced by irradiation of NIR femtosecond laser pulse in transparent inorganic materials. To the contrary, there have been a few reports on induced structure of polymer materials and still has remained to be investigated in detail how and what structures are induced by NIR femtosecond laser irradiation in polymer materials. Polymer materials are key materials widely used in various fields and intrinsic, unique properties different from other materials, therefore induced structures in polymer materials and comparison with these of other materials are interesting not only in industrial aspect but also in scientific aspect. From the viewpoint of this consideration, the author thinks that it is important and worth while to study on induced structures by NIR femtosecond laser irradiation in transparent polymer materials. In this thesis, the formation and analysis of induced structures in polymeric and amorphous materials by NIR femtosecond laser pulse irradiation were carried out.

In Chapter 1, the author described the general features of polymer materials, femtosecond laser pulse with high peak power. The author described 'multi-photon absorption processes' as a key process to the formation and analysis of induced structures. The author reviewed studies on structures induced in inorganic materials as well as in polymeric and organic materials by irradiation of NIR femtosecond laser pulse. The author reconfirmed the position and worth of this thesis.

In Chapter 2, the experimental set-up of used NIR laser pulse and the method of irradiation of NIR laser pulse (line irradiation) were described. Preparation of sample for irradiation, observation and identification of induced structures by irradiation were also shown. Evaluation methods of the performance of induced structure including diffraction measurement and micro-lens effect were described.

In Chapter 3, various polymer materials having different T_g's including p-(MMA/EA-BA) block copolymer prepared by new living radical polymerization were provided for line irradiation of NIR laser pulse. In the case of shallow depth irradiation, for example 30 μm in depth, volcano-like upheavals was observed on the surface of irradiated sample for higher T_g polymers, such as PES, PMMA, PC but caves and channels for lower T_g polymers, such as acrylic adhesive and olefin gel. The induced structures had significant relation to T_g for the irradiated polymers. Stripe-like aggregation consisted of sub-micron deposit was observed for irradiated p-(MMA/EA-BA) block copolymers which have both higher T_g and lower T_g in the material. These stripe-like aggregations changed their shapes from thin stripe to thick one, and to ellipse and finally voids and cracks appeared with increasing the irradiated pulse energy. The change in structure in irradiated copolymers had the same tendency as in the case of the inorganic materials in qualitative manner. But in quantitative manner, inorganic glass materials required 10 - 20 times much energy than polymer materials to induce the equivalent change. The other significant difference in stripe-like structures induced between p-(MMA/EA-BA) block copolymers and inorganic glass materials was that aggregation composed of sub-micron deposit was formed in polymer materials and not aggregation but uniform structure was formed in inorganic glass material. The analyses by AFM, and microspectrophotometric FT-IR revealed that sub-micron scale deposit might be re-produced structures after photo-decomposition or photo-crosslinking of polymer chain components.

In Chapter 4, one of the unique induced structures in polymer materials, that is, the stripe-like aggregation induced structure (grating structure) in p-(MMA/EA-BA) block copolymer, was investigated in more details. The author evaluated the performance of obtained grating structure using diffraction measurement. We confirmed that transmission diffraction occurred on the basis of the linear relation of $\sin\theta$ vs. $1/\Lambda$. Linear relation between diffraction spot intensity vs. photo-cross-linker content for each order diffraction (for the condition of $\Lambda = 15\,\mu m$ $N_G = 40$) was observed. The Raman-Nath type and Bragg type transmission diffraction patterns with diffraction efficiencies of approximately $1 - 13$ % and Q value of approximately 0.1 - 9 were obtained and the refractive index change were calculated as approximately $0.20 - 3.0 \times 10^{-3}$. Optimized condition obtained using Robust design (Taguchi method) gave perfect Bragg type diffraction pattern with Q value of approximately 9 and refractive index change of 0.30×10^{-3}. Furthermore, refractive index change can be cumulative by

multiple superimposed lines irradiation as in the case of inorganic glass materials. Superimposed lines irradiation of 3 times produced the refractive index change in the order of 10^{-3}, but the value of 10^{-3} is still smaller than that of inorganic glass materials.

In Chapter 5, grating structures induced in dye-doped polymer materials, PMMA, Epoxy and P-(MMA/EA-BA) block copolymer, were investigated. PMMA and P-(MMA/EA-BA) block copolymer showed a dye additive effect in which dyes having absorption at 400 nm (two-photon absorption of irradiated femtosecond laser pulse) and lower fluorescence quantum yield favored for the formation of thicker grating structures. To the contrary, Epoxy did not show the dye additive effect. The mechanism of the dye additive effect phenomenon for PMMA and P-(MMA/EA-BA) block copolymer was discussed on the basis of two-photon excitation (absorption) by dye at 400 nm and the following non-radiative transition process of the absorbed energy to polymer matrix which lead to the photo-degradation and photo-cross-linking of PMMA. The author measured the transmission diffraction property of the grating structures induced by the irradiation of femtosecond laser pulse and confirmed that they are useful to be a transmission diffraction grating. Obtained results would be useful for new methodology of short-pulse laser irradiation for the production of polymeric optical device and for the control and the protection of photo-chemical damage in polymer materials by laser irradiation.

In Chapter 6, the other one of the unique induced structures in polymer materials, that is, the upheaval induced structures in high T_g, was investigated in more details.

In Chapter 6-A, upheaval structures on the surface of various polymers with high T_g induced by the line irradiation of NIR femtosecond laser pulse in the polymer bulk was investigated. Bell-shaped upheaval structures were obtained in PC and PEI, but ABSM copolymers and AS copolymers gave the upheaval structures with flattop. It was demonstrated that the periodic bell-shaped upheaval structure obtained in PC acts as micro-lens but ABSM copolymers and AS copolymers did not show micro-lens effect. Replication of the periodic bell-shaped upheaval structure in PC was carried out by electroforming (non-electrolytic plating of Ni and the following electrolytic plating of Ni) and potting AS copolymer of approximately 30wt% THF solution into the electroformed mother mold as like the LIGA process. The replicated upheaval structure made of AS copolymer also showed micro-lens effect. We propose here a novel methodology for the micro-scale polymeric optical-device like micro-lens array by means of laser molding in polymeric materials using femtosecond laser pulse and

additional mass-production using pseudo-LIGA process.

In Chapter 6-B, the formation of periodic bell-shaped upheaval structure on the surface of PC bulk induced by NIR femtosecond laser pulse irradiation was investigated in detail by the observation using various microscopes. The upheaval structure was not formed under the condition of deeper target depth and lower irradiation energy. At a constant target depth of 50 μm, induced structures on the surface were changed with the increase of irradiation energy from small periodic bell-shaped upheaval structure to large periodic bell shaped upheaval structure and the author confirmed continuous band shaped structure not having clear upheaval structure on the surface with intermediate irradiation energy. The periodic upheaval structures on the surface were confirmed to be upheld by voids and cracks in the observation of SEM micrographs and also confirmed to be connected to induced structure with transmitted contrast in the optical micrographs which diffused from the focused points. Differential interference contrast images through laser scanning micrographs were rod-like and/or elliptic and showed a low NA effect. On the basis of obtained results of experiments, consideration of multi-photon absorption probability and viscoelastic property of polymeric material, the author supposed the mechanism of the formation of upheaval structures on PC in which induced structures in PC are significantly related to the formation of upheaval structures. For the formation of periodic bell-shaped upheaval structure on PC, it is necessary that induced structure with refractive index modulation formed in PC bulk by multi-photon absorption are to be discrete in the X axis and anisotropic thermal gradient induced by diffusion of focused energy allows mass transfer of voids and crack and reactive product from the focused point to the surface.

In Chapter 7, structures induced in amorphous inorganic materials by irradiation of NIR femtosecond laser pulse were investigated. The author confirmed two interesting phenomena; the first one is that the control of induced structures is possible even at the position of 30-100 μm far from focused point of NIR femtosecond laser pulse irradiation. The second one is thin layer of polysilane on polymer bulks shows additive (photo-sensitive) effect on the formation of induced structures in polymer bulks just as dyes doped in polymer bulks described in Chapter 5.

In Chapter 7-A, permanent relief grating structures were induced by the focused irradiation of NIR femtosecond laser pulses in 100 nm thin layers of amorphous inorganic (In_2O_3+1 wt%TiO_2). X-ray diffraction analysis showed amorphous-to-crystalline phase change by the irradiation of NIR femtosecond laser pulses and the formation of crystallized relief grating structures. The shape of the

crystallized relief structures was able to be varied by changing the irradiation scanning rate and the height of the focused point. A cone-shaped structure without cave-in was obtained by optimizing the irradiation conditions. A new method of fabricating relief grating structures on a thin inorganic layer was presented. Employment of selective wet etching on un-irradiated amorphous regions of the samples using a 3% HCl solution enhanced the crystalline relief grating patterns.

In Chapter 7-B, poly-methyl phenyl silane (PMPS) bulks showed longer stripe-shaped structures with approximately 200-400 μm in length than we had ever observed in inorganic glass and other polymeric materials. Values of refractive index modulation evaluated by transmission diffraction method were at most 0.6×10^{-3} and the author could not obtain large value comparable to that of inorganic glass materials. Thin polysilane layers coated on both PMMA and Epoxy showed photo-sensitive effect on the formation of stripe-shaped structures in PMMA and Epoxy induced by irradiation of NIR femtosecond laser pulse. An ensemble of stripe-shaped structure acted as a diffraction grating. In this study and in our previous study, even the region located approximately 30-100 μm from the focused spot is subjected to the influence of the irradiation and multi-photon absorption is responsible for these phenomena. This effect shows a potential of writing a structure in optical polymeric device such as an optical polymeric fiber (OPF).

Integrating the results and discussion throughout this thesis and comparing with preceding studies on induced structures in inorganic glass materials can draw conclusions at the present stage of the study are shown as follows:

First, for polymer materials, required irradiation energy for the formation of the induced structures is approximately 1/10-1/100 times as small as that for inorganic glass materials.

Second, for polymer materials, two unique induced structures which have not been observed for inorganic glass materials were founded; the first one is upheaval structure on the surface of polymer materials with high T_g's. The second one is grating structure with sub-micron scale deposit in p-(MMA/EA-BA) block copolymers.

Third, dyes and polysilane which have absorption in the range of wavelength at two-photon excitation (400 nm) of irradiation NIR femtosecond laser pulse show additive effect and photosensitive effect on the formation of polymer bulks in which dye was doped and/or on which polysilane was set.

Fourth, even the region located approximately 30-100 μm from the focused spot is subjected to the influence of NIR femtosecond laser pulse irradiation.

List of Publications

Chapter 3   "Structures Induced by Irradiation of Femto-Second Laser Pulse in Polymeric Materials."
Shigeru Katayama, Mika Horiike, Kazuyuki Hirao and Naoto Tsutsumi.
J. Polym. Sci. Part B: Polym Phys. **40** (2002) 537-544.

Chapter 4   "Diffraction Measurement of Grating Structure Induced by Irradiation of Femtosecond Laser Pulse in Acrylate Block Copolymers."
Shigeru Katayama, Mika Horiike, Kazuyuki Hirao and Naoto Tsutsumi.
Jpn. J. Appl. Phys. **41** (2002) 2155-2162.

Chapter 5   "Structure Induced by Irradiation of Femtosecond Laser Pulse in Dyed Polymeric Materials"
Shigeru Katayama, Mika Horiike, Kazuyuki Hirao and Naoto Tsutsumi.
J. Polym. Sci. Part B: Polym Phys. **41** (2002) 2800-2806.

Chapter 6

Chapter 6-A   "Laser Molding in Polymeric Materials Using Femto-second Laser Pulse and Replication via Electroforming"
Shigeru Katayama, Mika Horiike, Masakatsu Urairi, Kazuyuki Hirao and Naoto Tsutsumi.
Opt. Rev. **10** (2003) 196-201.

Chapter 6-B   "Periodic Bell-shaped Upheaval Structure on Surface of Polycarbonate by Irradiation of Femto-second Laser Pulse."
Shigeru Katayama, Mika Horiike, Kazuyuki Hirao and Naoto Tsutsumi.
Jpn. J. Appl. Phys.**42**(2003)6926-6930

Chapter 7

Chapter 7-A   "Femtosecond laser induced crystallization and permanent relief grating structures in amorphous inorganic ($In_2O_3＋1wt％$ TiO_2) films.
Shigeru Katayama, Mika Horiike, Toshitaka Nakamura, Kazuyuki Hirao and Naoto Tsutsumi.
Appl. Phys. Lett. **81** (2002) 832-834.

Chapter 7-B   "Structures induced in polysilane and thin polysilane layer coated polymer films by irradiation of femto-second laser pulse"

Shigeru Katayama, Mika Horiike, Masakatsu Urairi, Kazuyuki Hirao and Naoto Tsutsumi.

Chem. Phys. Lett. **373** (2003) 140-145.

Others

1. Oral publications

  1) ' Induced structure in polymer by irradiation of femtosecond laser pulses'

  M. Horiike, S. Katayama, N. Tsutsumi, K. Hirao

  Symposium of Photon Craft International Cooperative Research Project (Japan Science and Technology Corporation :JST). Oct. 19, 2002.

  2) 'Structures induced by irradiation of femtosecond laser pulse in polymeric materials'

  S. Katayama, M. Horiike, N. Tsutsumi

  17th Symposium on Optical and Electrical Properties of Organic Materials. Jun. 12, 2003.

  Fiber Preprints, Japan, **58** No.2 (Symposia) (2003) 102.

2. Japanese patent submitted

  There are approximately 40 Japanese patents submitted by S. Katayama, M. Horiike *et al* as inventors including submitted patent No. 2000-253189 (2000.8.23).

Acknowledgements

Nagaokakyo,
July 2003

Shigeru Katayama